論文 / 著書情報
Article / Book Information

題目(和文)	高価陽イオンを含んだ溶融塩化物中のイオン移動度
Title(English)	Ionic mobilities in molten chiorides containing multivalent cations
著者(和文)	松浦治明
Author(English)	HARUAKI MATSUURA
出典(和文)	学位:博士(理学), 学位授与機関:東京工業大学, 報告番号:乙第3081号, 授与年月日:1997年9月30日, 学位の種別:論文博士, 審査員:
Citation(English)	Degree:Doctor of Science, Conferring organization: Tokyo Institute of Technology, Report number:乙第3081号, Conferred date:1997/9/30, Degree Type:Thesis doctor, Examiner:
学位種別(和文)	博士論文
Type(English)	Doctoral Thesis

Doctor Thesis

Ionic mobilities in molten chlorides containing multivalent cations

Department of Electronic Chemistry, Tokyo Institute of Technology

by Haruaki Matsuura

May 6, 1997

To my wife,

Noriko

Contents

Chapter 1.

Introduction

Molten salts - ionic melts have properties of high electrical and thermal conductivity[1]. According to these characters, ionic melts are used for solvents of chemical reactions and of thermal fluid. Historically, molten salt technology has been developed mainly by electrowinning of Al. Nowadays, many metals including alkali, alkaline-earth, rare earth, as well as U are deposited by an electrorefining method. Molten salt electrochemistry is still being developed, for example, in electroplating for changing the character of metal surface or codepositing valuable alloys. Molten salt fuel cells has been constructed almost on an industrial level.

Molten salts technology has also been applied to nuclear technology also by its high stability against radiation. For example, molten LiF-BeF_2 was studied in detail as a fusion blanket or a molten salt breeder reactor at Oak Ridge National Laboratory. Molten LiCl-KCl containing U and other elements was investigated for pyrochemical treatment of the nuclear metallic fuel containing high-radioactive materials (Integral Fast Reactor concept) at Argonne National Laboratory. After the cold war the situation for research field of nuclear energy has changed in the world. It is not needed to say much that, nowadays, Japan is most advanced in researching nuclear technology, especially in molten salt chemistry field.

A number of studies of transport phenomena in molten salt systems have been carried out by various investigators through measurements of ionic mobilities, transport numbers, diffusion coefficients, electrical conductivities, etc. The experimental results have been discussed in connection with mass transport and the structure of the ionic melts. From a viewpoint of applicability to technological aspects, it is necessary to

study transport properties especially in mixture systems. Molten salt mixtures are more applicable for practical use than the corresponding pure melts because of their lower melting points. Moreover, research on mixture systems is more informative than that of pure melts, which allows us to select conditions such as materials, temperatures and concentrations. Many publications have appeared and experimental data have been summarized in various tables[2].

Ionic mobilities are useful for obtaining information about the charge, ionic size and extent of solvation of the ions, and mechanisms of ionic conductance in the melts. The problems of electro-osmotic flow, the choice of the reference frame, and ionic structure models have not yet been solved completely. There is a serious difficulty in defining the absolute mobilities of individual ions in a molten salt, since it does not contain fixed particles which could serve as a coordinate reference. Then, Klemm[3] has proposed to define an internal mobility, which is defined with reference to the mobility to one definite ion of the system; for example, the reference could be the mobility of a common anion. On the other hand, Chemla has employed the external mobility, which is measured relative to the walls of the vessel containing the melt. Chemla[4] observed that, when the walls are made of stable inorganic compounds, the external moblities are quite consistent with the corresponding values of self-diffusion coefficients. Discussions on ionic mobilities have been reviewed by some authors. Here we will summarize shortly the literature concerning ionic mobilities in melts.

Ionic mobilities in molten salts have been measured with various experimental techniques; that is, the Klemm method (column method)[5], the Hittorf method (disc method)[4], the zone electromigration method (layer method)[6], and the electromotive force method (emf method)[7]. These methods are explained in the review article[3]. In some cases agreement of data between different methods is satisfactory but in other

cases discrepancy is evident. Among these methods, the internal transport numbers may be measured most accurately and precisely by the Klemm method. As the Klemm method was invented for the purpose of isotope separation[5],[8], even such a small difference in mobilities as in the isotopic ions can be determined accurately and precisely. Some of the advantages of this method are as follows:

(1) The high accuracy for the measurement of internal mobilities can be obtained. With this method, a gradient in concentration is build up along a column by a combination of electric transport and diffusion. Even for the small difference of ionic mobilities, the change in the chemical composition around the anode becomes relatively large, which will make the data accurate. The interference of diffusion can be avoided.

(2) For additive mixtures, the internal mobilities even of a species of low concentration can be measured accurately and precisely.

(3) An accurate control and measurements of temperature are possible and a wide experimental temperature range can be covered.

(4) Internal cation mobilities can be measured at any concentration.

(5) The method is relatively insensitive to small amounts of impurity.

However, with this method external transport numbers or external mobilities cannot be obtained.

The Hittorf method is inferior to the Klemm method in accuracy and precision, because:

(1) the initial composition remains unchanged only in the region of a disc in the former, while it remains in an extended range in a column in the latter;

(2) The concentration change is generally small in the former, while it is large in the latter.

For the zone electromigration, radio isotopes or enriched stable isotopes have to be used. This method may be technically difficult to employ at higher temperatures.

The emf method is also inferior to the Klemm method for the following reasons[9],[10]

(1) Activities have to be measured independently which inevitably involves considerable errors;

(2) Emf's are, in general, more sensitive to impurities than mobilities;

(3) At low concentration of a given ion, the error in ε (relative difference in internal mobilities) is enlarged;

(4) The emf methods can be applied only for additive binary systems and not even for additive ternary systems.

The patterns of isotherms of the internal mobilities in molten binary systems consisting of two monovalent cations and a common anion may be classified into two types as shown in Fig. 1.1: the first one (Type Ia, Ib, Ic, and Id) is that mobilities of both cations decrease with increasing mole fraction of the larger cations. Binary nitrate, carbonate and chloride systems seem to belong to this type; the other (Type II) is that with increasing mole fraction of the larger cation, mobilities of the larger cation increase whereas those of the smaller cation decrease. Binary sulfate, fluoride and hydroxide systems may belong to this type.[11]

The Chemla effect has been found in binary monovalent mixtures with a common anion; the mobilities of the larger cation are greater than those of the smaller one in a certain range of temperature and composition[12],[13],[14],[15]. For example, we will explain by the results of molten (Li, K)Cl mixture[16] as shown in Fig. 1.2. The Chemla crossing point is the point where the isotherms of two cation mobilities as a function of the mole fraction cross each other. At a higher concentration of LiCl, Li^+ is more

mobile and at a lower concentration, K^+ is more mobile, and therefore, from the anode side the concentration gradually shifts to that of the Chemla crossing point. In the 1960's two interpretations were presented to explain the Chemla effect; one is based on an anion polarization model[17], the other is based on complexed or associated ion formation[4],[13],[18],[19],[20],[21],[22],[23]. However, neither is able to account for the Chemla effect satisfactorily. For example, the polarization model was not explainable the type II of the Chemla effect mentioned above. This could not explain either that the Chemla crossing point shifts toward a higher concentration range of the smaller cation with increasing temperature. Complex species are not likely to be predominate ones in electric transport processes.

Binary alkali nitrate systems have been systematically investigated[11]. The isotherms of the internal mobilities are shown in Fig. 1.3. Figure 1.3 shows that, as the relative difference in two cationic sizes is greater, the difference in the slopes of the isotherms of the two cations becomes greater, and hence the crossing point appears more clearly. This figure reveals also that with increasing temperature the crossing point shifts toward higher concentration of a smaller cation. Further insight of the isotherms has revealed that, when the Coulombic term is expected to be the dominant factor for determining mobility, the internal mobility of a cation is well expressed by:

$$u = [A / (V_m - V_0)] \exp(-E / RT) \qquad (1.1)$$

where A, V_0 and E are constants independent of the second cation.

In addition to the Coulombic attraction effect expressed by equation (1.1), the *free space effect*[24] occurs when the free space is particularly small for a relatively large ion. The free space is defined as the molar volume minus the volume occupied by "ion cores". It should be mentioned that the free space effect and the Coulombic attraction effect occur in the opposite direction as a function of molar volume. In other words, a

maximum of internal mobility exists as a function of molar volume.

If the internal mobility of a cation of interest becomes appreciably greater than expected from equation (1.1) by being affected by the second cation, this is due to the *agitation effect*[25]. As the cause of the agitation effect, the small mass and/or the pair potential profile should be considered. When the motion of the second cations is active owing to its small mass, the motion of the common anion will also become active, which will result in accelerating the internal mobility of the cation of interest. The agitation effect caused by the small mass has been substantiated by molecular dynamics simulation. Usually, the agitation effect, if any, is not pronounced.

By contrast, if the internal mobility of a cation of interest becomes smaller affected by foreign cations, this is named the *tranquilization effect*[26]. The tranquilization effect occurs explicitly in the case that the interaction of the second cation with a common anion is very strong. It should be mentioned that, if the second cation is multivalent, the tranquilization effect becomes clear for the internal mobility of a monovalent cation.

Okada *et al.*, have interpreted the Chemla effect mainly in terms of the self-exchange velocity (SEV)[11),(27], and we shall now summarize this interpretation briefly. The SEV, which can be calculated from a molecular dynamics (MD) simulation, refers to a separating motion of neighboring cations and anions. The calculated internal mobilities in pure LiCl and in a mixture (x_{Li}=0.10)[28] were obtained from the same MD run as that for the SEV using an equation[29] based on the linear response theory. The results of these MD simulation have been used previously for a study of the collective dynamics of the ions[30]. In these MD simulation, rigid ion models[31),(32] were used for the pair potentials. The detailed MD procedures are reported elsewhere[28]. Thus, the Chemla effect is reproduced in the SEV's.

Compared with molten nitrate systems, there are not so many works for chloride systems because of its high corrosion to cell materials and its high vapor pressure. In Table 1.1, a list of investigations is given, in which internal or external transport numbers of monovalent cations in additive binary chloride systems have been measured in a wide concentration range, and therefore the corresponding mobilities are derived. In the chloride systems, equation (1.1) holds, although V_0 considerably depends on temperature. The quantitative meaning of A, V_0 and E is not rigorous for the moment[33]. V is the molar volume of the mixture. V_0 is a modification factor due to the finite dimension of the particles. Thus, equation (1.1) indicates that the second cation effects on the internal mobility of the cation of interest through determining the number density of the common anion.

It is interesting to know whether the mobilities are expressed by such equation also in the system containing multivalent cations. The internal mobility ratios of binary molten systems containing multivalent cations have so far been measured for the systems given in Table 1.2. In all the systems, the mobilities of divalent cations are smaller than that of monovalent ones, and no Chemla effect has been observed. Divalent cations have stronger interaction with anions than monovalent ones have, and therefore mobilities of divalent cations could be smaller.

The relationship between the structure and properties of molten rare earth chlorides have studied systematically by Mochinaga *et al.*, which is summarized in Table 1.3. According to their review articles[34],[35],[36], there is some connection between networking structure and equivalent conductivity, that is high networking structure is related to low conductivity. We have more precisely explored the mechanism of conductance about each constituting cations by measuring internal mobilities in the mixture.

We have carried out the present experiments for the following purposes;

a) scientific aspects: an investigation of the conductance mechanism containing multivalent cation in multi-multivalent chloride systems (chapter 3) and in mono-multivalent chloride systems (chapter 4),

b) technological aspects: a study on applicability of the electromigration method for nuclear waste treatment process[37](chapter 5).

Table 1.1 Binary mono-monovalent cations chloride systems

Two cations		Method	Reference
1	2		
Li	Na	K	(38)
Li	K	H	(17)
		E	(22)
		K	(39)
		K	(40)
		K	(16)
Li	Rb	K	(16)
Li	Cs	E	(22)
		K	(41),(42)
Na	K	E	(22)
		E	(43)
		K	(38)
Na	Cs	E	(22)
Li	Ag	E	(44)
Na	Ag	E	(45)
Ag	K	E	(45),(46)
Ag	Rb	E	(45)
Ag	Cs	E	(45),(46)

E:emf method, H:Hittorf method, K: Klemm method, Z: Zone electromigration method

Table 1.2 Binary systems containing multivalent cations

System	Cation 1	Cation 2	Method	Reference
Nitrate	Li	Ca	Z	(47)
			K	(48)
	Li	Sr	K	(48)
	Li	Ba	K	(48)
	Na	Ca	-	(49)
			K	(48)
	Na	Sr	K	(48)
	Na	Ba	K	(48)
	K	Ca	K	(50)
	K	Sr	K	(51)
	K	Ba	K	(51)
Chloride	Li	Ca	E	(52)
	Li	Sr	E	(53)
	Li	Ba	E	(54)
	Li	Cd(II)	E	(55)
	Li	Pb(II)	B	(56)
			E	(43)
			K	(57)
	Na	Ca	E	(52)
	Na	Sr	E	(53)
	Na	Ba	E	(54)
	K	Ca	E	(52)

(Table 1.2 continued)

	K	Sr	E	(53)
	K	Ba	E	(54)
	K	Pb(II)	E	(43)
	K	Mg	E	(43)
	Rb	Ca	E	(52)
	Rb	Sr	E	(58)
	Rb	Ba	E	(58)
	Cs	Ca	E	(59)
	Cs	Sr	E	(58)
	Cs	Ba	E	(58)
			E	(60)
Bromide	Li	Ca	E	(61)
	Na	Ca	E	(62)
	Na	Sr	E	(62)
	Na	Ba	E	(62)
	K	Ca	E	(62)
	K	Sr	E	(62)
	K	Ba	E	(62)
	Rb	Ca	E	(61)
	Cs	Ca	E	(61)

E:emf method, H:Hittorf method, K: Klemm method, Z: Zone electromigration method

Table 1.3 Structure and properties of molten rare earth chlorides

Elements	Phase diagram	Molar volume	Conductivity	Refractive Index
Y	(63)	(63),(64)	(65)	(66),(67)
La	(68)	(69),(70)	(71)	(72)
Ce				
Pr	(73)	(64)	(74)	(75)
Nd		(64)	(76)	
Sm		(77)	(77)	
Eu				
Gd	(78)	(79)	(80)	(79)
Tb				
Dy	(81)	(82)		(66),(67)
Ho				
Er		(83)	(83)	
Tm				
Yb				
Lu				

(Table 1.3 continued)

Elements	X-ray Diffraction	Raman Spectroscopy
Y		
La		
Ce	(84),(85),(86)	(84)
Pr		
Nd		
Sm		
Eu		
Gd		(87)
Tb		
Dy	(88),(89)	(88)
Ho		
Er	(86),(90)	
Tm		
Yb		
Lu		

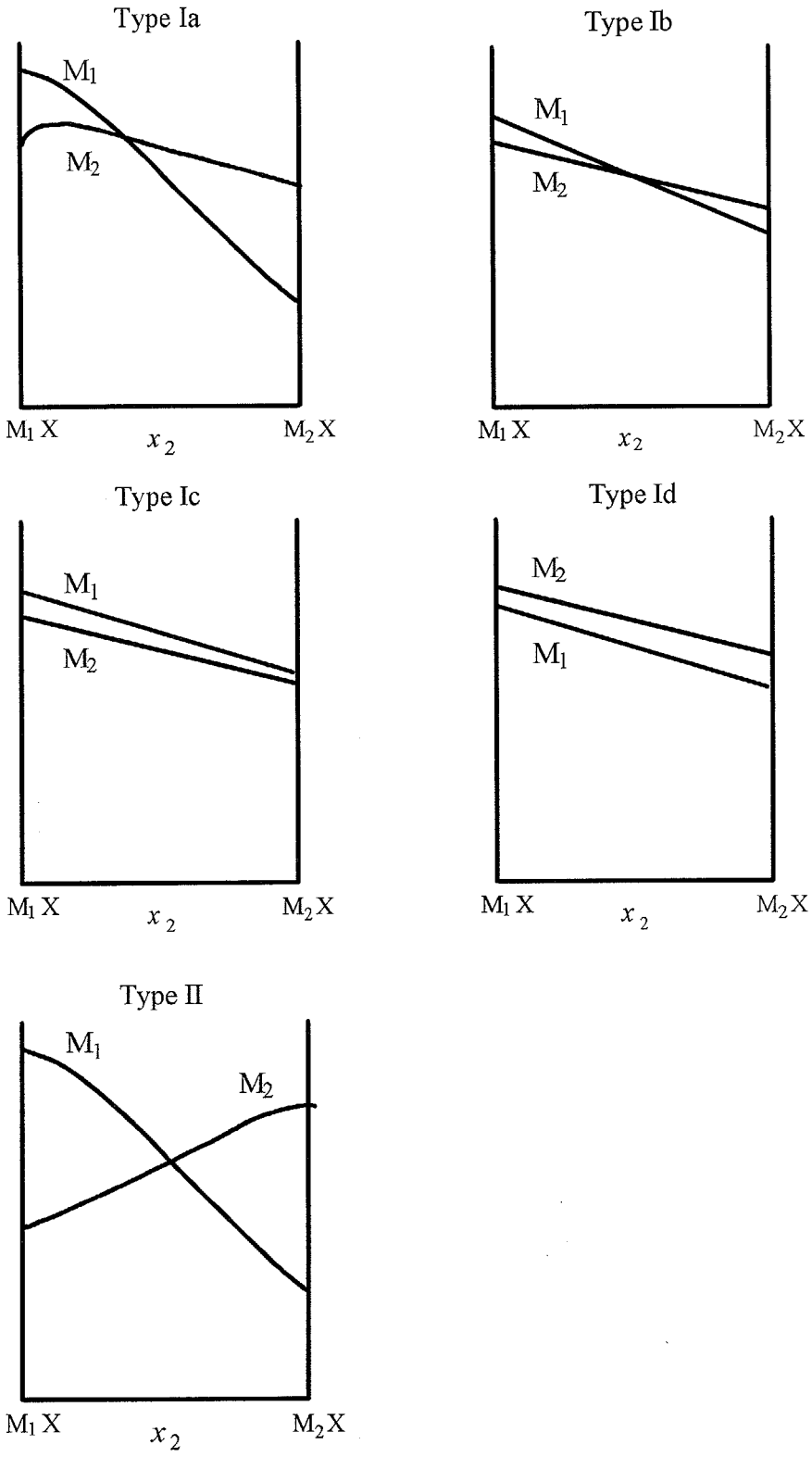

Fig. 1.1 The isotherm patterns of internal mobilities *vs* mole fraction of M_2X in systems $(M_1, M_2)X$, where M_1 and M_2 are the smaller and larger monovalent cations, respectively, and X is a common anion.

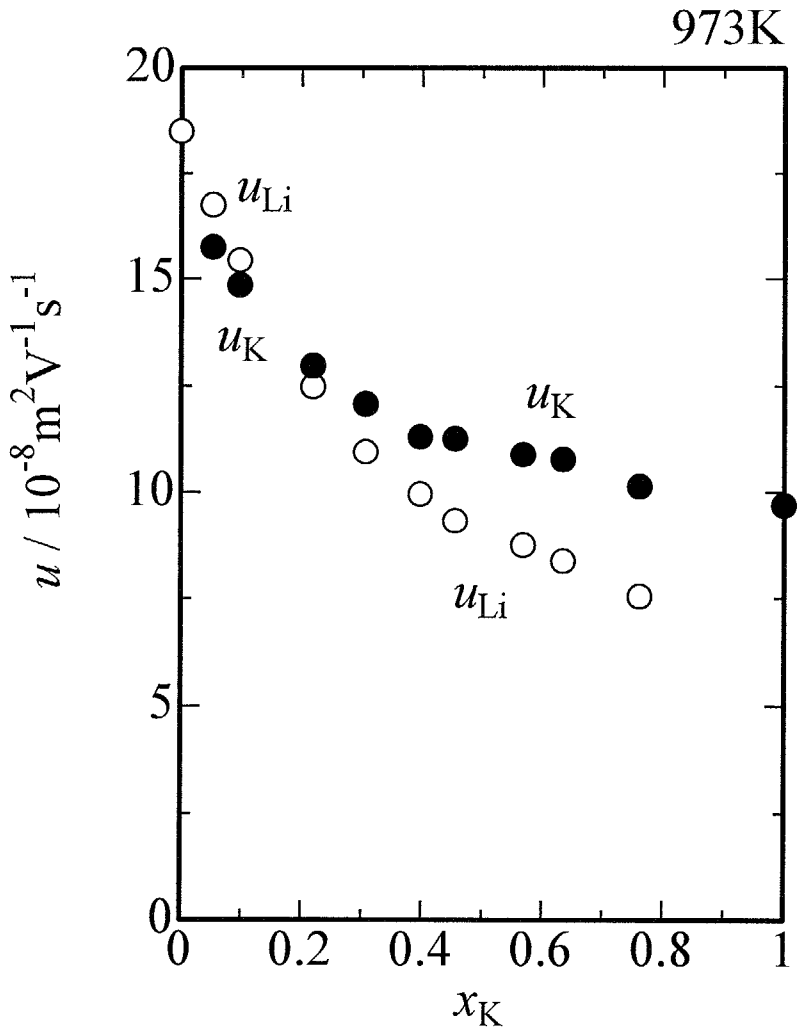

Fig. 1.2 The isotherm of internal mobilities in the system (Li, K)Cl at 673K[16].

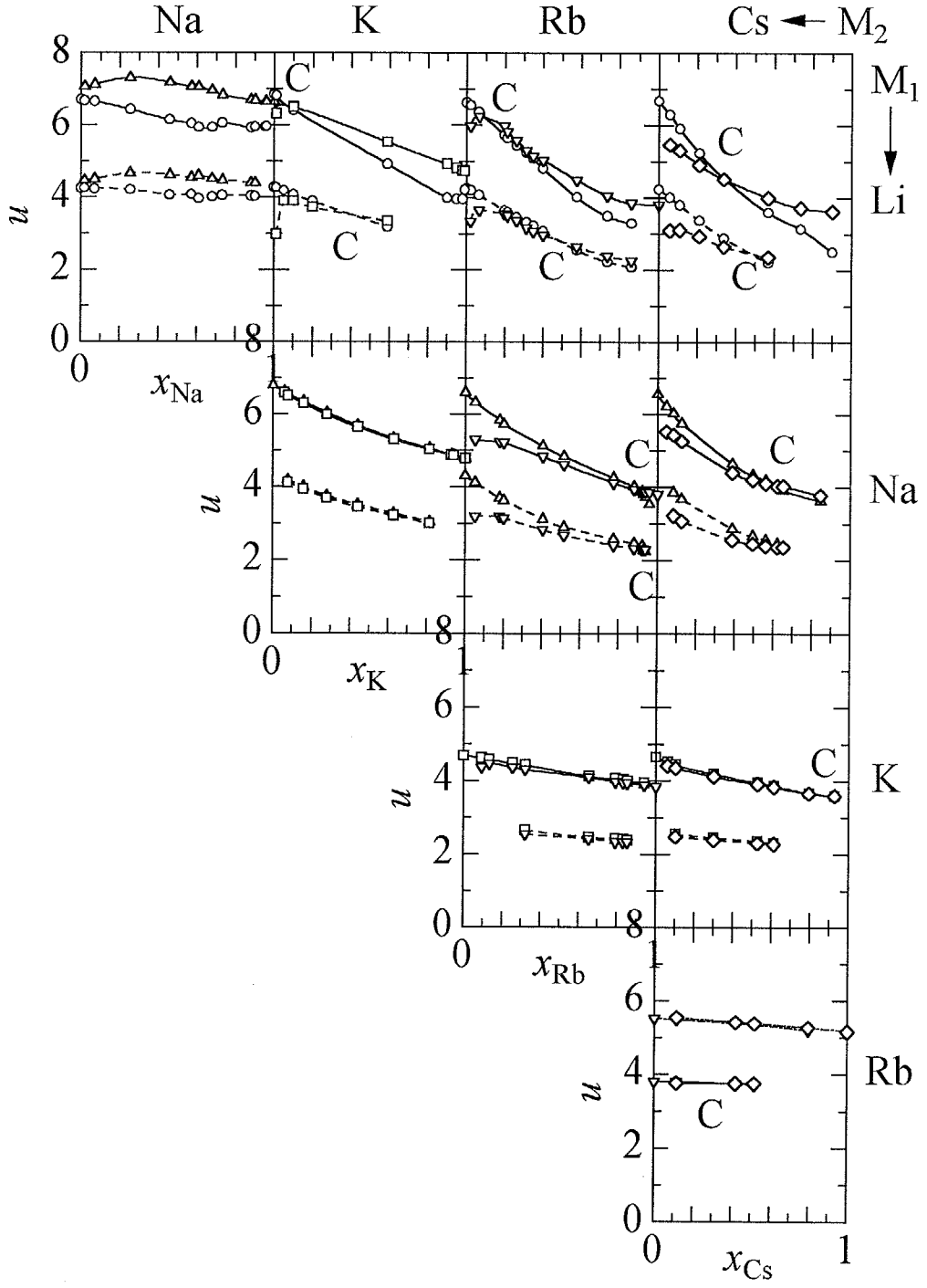

Fig. 1.3 The isotherms of internal mobilities measured by the Klemm method in binary alkali nitrates at 573K and 673K, except (Rb, Cs)NO_3 at 673K and 773K. For comparison these results easily, data shown in each isotherm was recalculated from original papers[15],[25],[91],[92],[93],[94],[95],[96] in this figure, which is rearranged from the figure shown in [11].

References

[1] "Yoyuen Netsu-gijutsu no Kiso(The fundamentals of molten salts and thermal technologies)" ed by The Society of Molten Salt Thermal Technology, Agne (1993) [in Japanese]

[2] Molten Salts: Volume 4, Part 2, Chlorides and Mixtures, Electrical Conductance, Density, Viscosity, and Surface Tension Data
G. J. Janz, R. P. T. Tomkins, C. B. Allen, J. R. Downey, Jr., G. L. Gardner, U. Krebs and S. K. Singer, *J. Phys. Chem. Ref. Data*, **4**, 871-1178 (1975)

[3] *Advances in Molten Salt Chemistry, Vol. 6*
A. Klemm, Ed. by G. Mamantov, C. B. Mamantov and J. Braunstein, p. 1. Elsevier, Amsterdam (1987)

[4] Mobilité Électrique des Ions Na^+ et K^+ Dans les Systèmes KNO_3-$NaNO_3$ Fondus
F. Lantelme and M. Chemla, *Bull. Soc. Chim. Fr.* 2200-2203 (1963)[in French]

[5] Anreicherung der schweren Isotope von Li und K durch elcktrolytische Ionenwanderung in geschmolzenen Chloriden
A. Klemm, H. Hintenberger and P. Hoernes, *Z. Naturforsch.*, **2a**, 245-249 (1947)[in German]

[6] Concetration d'isotopes par électromigration sur amiante imprégnée de sels fondus
M. Chemla and A. Bonnin, *C. R. Acad. Sci.*, **241**, 1288-1291 (1955)[in French]

[7] Überführungserscheinungen in Salzschmelzen
K. E. Schwarz-Köln, *Z. Electrochem.*, **47**, 144-147 (1941)[in German]

[8] Anreichrung des shweren Silberisotops durch Ionenwanderung in Silberjodid
A. Klemm, *Naturwissenshaften*, **32**, 69-70 (1944).[in German]

[9] Internal Cation Mobilities in Molten (Na, Ag)NO_3 Remeasured by the Column Method
K. Ichioka, I. Okada and A. Klemm, *Z. Naturforsch.*, **44a**, 747-750 (1989)

[10] Internal Cation Mobilities in Molten (Li, Ag)NO_3 and (K, Ag)NO_3 Remeasured by the Klemm Method
I. Okada and K. Ichioka, *Z. Naturforsch.*, **47a**, 781-787 (1992)

[11] Ionic Mobilities of Monovalent Cations in Molten Salt Mixtures
M. Chemla and I. Okada, *Electrochim. Acta.*, **35**, 1761-1776 (1990)

[12] M. Chemla, Commissariat à l'Énergie Atomique, Brevet D'Invention, France, No. 1216418 (1960)

[13] Électromigration en contre-courant dans des mélanges d'halogénures fondus
J. Périé and M. Chemla, *C.r. Acad. Sci.*, **250**, 3986-3988 (1960)[in French]

[14] Séparation d'Isotopes par Électromigration en Contre-Courant Dans des Systèmes d'Halogénures Fondus
J. Périé, M. Chemla and M. Gignoux, *Bull. Soc. Chim. Fr.* 1249-1256 (1961)[in French]

[15] Internal Cation Mobilities in the Molten Systems (Li-Rb)NO_3 and (Li-Cs)NO_3
I. Okada, R. Takagi and K. Kawamura, *Z. Naturforsch.*, **34a**, 498-503 (1979)

[16] H. Horinouchi and I. Okada, to be published

[17] Relative Cation Mobilities in Potassium Chloride-Lithium Chloride Melts
C. T. Moynihan and R. W. Laity, *J. Phys. Chem.* **68**, 3312-3317 (1964)

[18] Mobilité Électrique et Diffusion des Ions Li^+, K^+ et Na^+ Dans les Systèmes KNO_3-$LiNO_3$ Fondus
F. Lantelme and M. Chemla, *Electrochimica Acta.* **10**, 663-671 (1965)[in French]

[19] Propriétés de Transport de l'Ion NO_3^- Dans des Mélanges de Nitratés Alcalins Fondus
F. Lantelme and M. Chemla, *Electrochimica Acta.* **11**, 1023-1033 (1966)[in French]

[20] Diffusion and ionic transport in molten alkali metal halides
M. Chemla, F. Lantelme and O. P. Mehta, *J. Chim. Phys. Physicochim. Biol.(Oct. Num. Spec.)*, 136-143 (1969)[in French]

[21] Conductibilité Électrique des Systèmes LiBr-KBr Fondus
O. P. Mehta, F. Lantelme and M. Chemla, *Electrochim. Acta.* **14**, 505-513 (1969)[in French]

[22] Diffusion Potentials and Transport Numbers in Molten Alkali Chlorides and their Binary Mixtures
M. V. Smirnov, K. A. Aleksandrov and V. A. Khokhlov, *Electrochim. Acta*, **22**, 543-550 (1977)
[23] Structure and Diffusion in Mixtures of Ionic Liquids
F. Lantelme and P. Turq, *Mol. Phys.* **38**, 1003-1014 (1979)
[24] Internal Cation Mobilities in the Molten Ternary System (Li, Na, K)Cl of the Eutectic Composition
A. Endoh and I. Okada, *Z. Naturforsch.*, **43a**, 638-642 (1988)
[25] Internal Mobilities in Molten Systems (Na-K)NO_3 and (K-Cs)NO_3
C. Yang, R. Takagi and I. Okada, *Z. Naturforsch.*, **38a**, 135-141 (1983).
[26] MD-Simulation of Molten LiCl; Self-Exchange Velocities of Li-Isotopes near Cl^--Ions
I. Okada, *Z. Naturforsch.*, **39a**, 880-887 (1984)
[27] A Molecular Dynamics Simulation of Molten (Li-Rb)Cl Implying the Chemla Effect of Mobilities
I. Okada, R. Takagi and K. Kawamura, *Z. Naturforsch.*, **35a**, 493-499 (1980)
[28] I. Okada, S. Okazaki and Y. Miyamoto, to be published
[29] Molten Salt Ionic Mobilities in Terms of Group Velocity Correlation Functions
A. Klemm, *Z. Naturforsch.*, **32a**, 927-929 (1977)
[30] Molecular-Dynamics Study of the Dynamic Structure Factors of Molten LiCl and LiCl-CsCl
S. Okazaki, Y. Miyamoto and I. Okada, *Phys. Rev. B*, **45**, 2055-2062 (1992)
[31] Ionic Sizes and Born Repulsive Parameters in the NaCl-Type Alkali Halides - II
M. P. Tosi and F. G. Fumi, *J. Phys. Chem. Solids*, **25**, 45-52 (1964)
[32] Structure of Molten Alkali Chlorides I. A Molecular Dynamics Study
M. Dixon and M. J. Gillan, *Philos. Mag. B*, **43**, 1099-1112 (1981)
[33] Local Structure and Okada's Empirical Relation for the Internal Mobility of Cations in Molten Alkali Nitrates
J. Habasaki, *Z. Naturforsch.*, **44a**, 595-596 (1989)
[34] Molten Salts of Rare Earth Chlorides
J. Mochinaga and K. Igarashi, *Kidorui*, **15**, 13-23 (1989)[in Japanese]
[35] Structure and Property of Molten Salts
J. Mochinaga, *Yoyuen*, **35**, 47-64 (1992)[in Japanese]
[36] Structure, Equivalent Conductivity and Molar Volume of Molten Salts
J. Mochinaga, Y. Iwadate and K. Fukushima, *J. Fac. Eng. Chiba Univ.*, **45**, 1-10 (1993)[in Japanese]
[37] Enrichment of Lanthanum in Its Dilute Molten Salt Solution
M. Iwasaki and R. Takagi, *J. Nucl. Sci. Technol.*, **31**, 751-753 (1994).
[38] Internal Cation Mobilities in the Molten Binary Systems (Li, Na)Cl and (Na, K)Cl
C. -C. Yang and B. -J. Lee, *Z. Naturforsch.*, **48a**, 1223-1228 (1993)
[39] Determination of Internal Cation Mobilities in the Molten System (Li-K)Cl at 723 K
R. Takagi, H. Shimotake and K. J. Jensen, *J. Electrochem. Soc.*, **131**, 1280-1283 (1984)
[40] Internal Cation Mobilities and their Isotope Effects in the Molten System (Li, K)Cl
A. Lundén and I. Okada, *Z. Naturforsch.*, **41a**,1034-1040 (1986)
[41] The Chemla Effect in Molten (Li, Cs)Cl Electromigration and MD Simulation
I. Okada, S. Okazaki, H. Horinouchi and Y. Miyamoto, *Mat. Sci. Forum*, **73-75**, 175-182 (1991)
[42] The Chemla effect in the mobilities in the molten binary system of lithium chloride and caesium chloride
I. Okada and H. Horinouchi, *J. Electroanal. Chem.*, **396**, 547-552 (1995)
[43] Transference Numbers and Ionic Mobilities from Electromotive Force Measurements on Molten Salt Mixures
W. K. Behl and J. J. Egan, *J. Phys. Chem.* **71**, 1764-1769 (1967)
[44] Fused Salt Concentration Cells with Transference. Tranport Numbers of Molten (Li, Ag)Cl and Molten Alkali Jodide and Silver Jodide Mistures

J. Richter, E. Kirschbaum and H. Valenta, *Z. Naturforsch.*, **38a**, 880-884 (1983)

[45] Fused Salt Concentration Cells with Transference Transport Numbers of Molten Alkali Chloride and Silver Chloride Mixtures
R. Conradt, J. Richter and H. Wettich, *Z. Naturforsch.*, **38a**, 128-134 (1983)

[46] Electric Conductivities of Binary Molten (K, Ag)Cl, (Cs, Ag)Cl, (K, Ag)Br, (Na, Ag)I, and (Ca, Ag)I Mixtures
H. -P. Boßmann, A. Hildebrandt and J. Richter, *Z. Naturforsch.*, **41a**, 1129-1136 (1986)

[47] Electrical Mobilities of Lithium-6, Calciium-45, and Nitrate Ions in Liquid Mixtures of Lithium Nitrate and Calcium Nitrate
Jan C. T. Kwak, J. A. A. Ketelaar, P. P. E. Maenaut and A. J. H. Boerboom, *J. Phys. Chem.*, **74**, 3449- 3451 (1970)

[48] A Dynamic Dissociation Model for Internal Mobilities in Molten Alkali and Alkaline Earth Nitrate Mixtures
T. Koura, H. Matsuura and I. Okada, *J. Mol. Liquids*, **73/74**, 195-208 (1997)

[49] Electromigration of Sodium and Calcium in Molten Mixtures of Their Nitrates
V. P. Shvedov, I. A. Ivanov and I. M. Barbashinov, *Soviet Electrochem.*, **2**, 1021-1022 (1966)

[50] Internal Cation Mobilities in the Molten Binary System KNO_3-$Ca(NO_3)_2$
J. Habasaki, C. Yang and I. Okada, *Z. Naturforsch.*, **42a**, 695-699 (1987)

[51] Internal Cation Mobilities in the Molten Binary Systems KNO_3-$Sr(NO_3)_2$ and KNO_3-$Ba(NO_3)_2$
C. Yang, J. Habasaki, O. Odawara and I. Okada, *Z. Naturforsch.*, **42a**, 1021-1023 (1987)

[52] On the structure of charge-unsymmetrical salt melts of alkaline earth and alkali metal chlorides
H. -H. Emons, G. Bräutigam and H. Vogt, *Z. anorg. allg. Chem.* **394**, 279-289 (1972) [in German]

[53] EMF Measurements in Binary Unsymmetrical Salt Melts of Strontium Chloride and Alkali Chlorides
H. -H. Emons, G. Bräutigam and H. Wader, *Z. anorg. allg. Chem.* **403**, 97-106 (1974)[in German]

[54] EMF Measurements in Binary Chargeunsymmetrical Salt Melts of Barium- and Alkali Chlorides
H. -H. Emons, G. Bräutigam and R. Scheunpflug, *Z. anorg. allg. Chem.* **411**, 118-124 (1972)[in German]

[55] Thermodynamic Properties, Transference Numbers, and Ionic Mobilities in Molten Lithium Chloride-Cadmium Chloride Mixtures from EMF Measurements
W. K. Behl, *J. Electrochem. Soc.*, **121**, 959-962 (1974)

[56] Überführungsmessungen zur Bestimmung der Beweglichkeiten von ^6Li, ^7Li und Pb in geschmolzenen LiCl-$PbCl_2$ Gemischen
A. Klemm and E. U. Monse, *Z. Naturforsch.*, **12a**, 319 (1957)[in German]

[57] Internal Mobilities in Molten (Li, Pb(II))Cl as Remeasured by the Klemm Method
H. Haibara and I. Okada, *Z. Naturforsch.*, **45a**, 827-831 (1990)

[58] Transporteigenschaften geschmolzener binärer Saltzmischungen vom Typ MCl-M'Cl_2 (M=Rb, Cs; M'=Sr, Ba)
G. Bräutigam and H. -H. Emons, *Z. Phys. Chem. (Lpt)* **261**, 425-432 (1980)[inGerman]

[59] Physikalisch-Chemische Eigenschaften von Schmelzgemischen aus Calciumchlorid und Cäsiumchlorid
H. -H. Emons and G. Bräutigam, *Rev. Roum. Chim.*, **21**, 223-228 (1976) [in German]

[60] Charge Transport in Molten Mixtures of Cesium and Barium Chloride
V. A. Khokhlov, M. V. Smirnov and K. A. Aleksandrov, *Soviet Electrochem.*, **21**, 57-61 (1985)

[61] Electrical transport properties of molten alkali metal bromide- alkaline-earth bromide binary mixtures
H. -H. Emons, W. Voigt, G. Bräutigam and M. Bösel, *Ext.Abstr. Meet. -Int. Soc. Electrochem.*, **30**, 264-265 (1979): unpublished data

[62] Electrical Transport Properties of Molten Alkali Bromide-Alkaline Earth Bromide Binary Mixtures

W. Voigt, H. -H. Emons, G. Bräutigam and M. Bösel, *Z. anorg. allg. Chem.*, **443**, 169-174 (1978)[in German]

[63] Phase Diagrams of YCl_3-KCl, YCl_3-NaCl and YCl_3-KCl・NaCl Systems, and Densities of Their Molten Mixtures
J. Mochinaga and K. Irisawa, *Bull. Chem. Soc. Jpn.*, **47**, 364-367 (1974)

[64] Molar Volume Equations of Several Molten Binary Systems (Y, Pr, Nd)
J. Mochinaga, K. Igarashi, H. Kuroda and H. Iwasaki, *Bull. Chem. Soc. Jpn.*, **49**, 2625-2626 (1976)

[65] Electrical conductivity of molten YCl_3-NaCl, YCl_3-KCl and YCl_3-$CaCl_2$ systems
J. Mochinaga, K. Fukushima, Y, Iwadate, H. Kuroda and T. Kawashima, *J. Alloy. Comp.*, **193**, 33-35 (1993)

[66] Refractive Indices, Molar Refractivities and Electronic Polarizabilities of YCl_3-NaCl, and $DyCl_3$-NaCl Mixture Systems in the Molten State
J. Mochinaga and Y. Iwadate, *Denki Kagaku*, **47**, 345-354 (1979)

[67] Refractive Indices of $DyCl_3$-KCl, YCl_3-KCl and Pure $MgCl_2$ and $CaCl_2$ Melts
Y. Iwadate, K. Igarashi and J. Mochinaga, *Denki Kagaku*, **48**, 97-103 (1980)

[68] Phase Diagram of the System $LaCl_3$-$CaCl_2$-NaCl
K. Igarashi, H. Ohtani and J. Mochinaga, *Z. Naturforsch.*, **42a**, 1421-1424 (1987)

[69] Molar Volume of Molten Binary $CaCl_2$-NaCl, $LaCl_3$-NaCl and $LaCl_3$-$CaCl_2$ and Ternary $LaCl_3$-$CaCl_2$-NaCl Systems
K. Igarashi, Y. Iwadate, H. Ohno and J. Mochinaga, *Z. Naturforsch.*, **40a**, 520-524 (1985)

[70] Molar Volume and Surface Tension of Molten $LaCl_3$-KCl Mixtures
K. Igarashi and J. Mochinaga, *Z. Naturforsch.*, **42a**, 690-694 (1987)

[71] Electrical Conductivity of Molten $LaCl_3$-NaCl, $LaCl_3$-KCl and $LaCl_3$-$CaCl_2$
K. Fukushima, Y. Iwadate, Y. Andou, T. Kawashima and J. Mochinaga, *Z. Naturforsch.*, **46a**, 1055-1059 (1991)

[72] Refractive Index of Molten $LaCl_3$-KCl, $LaCl_3$-NaCl and $LaCl_3$-$CaCl_2$ Mixtures
K. Igarashi, Y. Iwadate, J. Mochinaga and K. Kawamura, *Z. Naturforsch.*, **39a**, 754-758 (1984)

[73] Phase Diagram of Ternary $PrCl_3$-$CaCl_2$-NaCl System
T. Hattori, H. Ikezawa, R. Hirano and J. Mochinaga, *Nihon Kagaku Kaishi*, 952-955 (1982)[in Japanese]

[74] Electrical Conductivity of Molten Charge-Asymmetric Salts
---$PrCl_3$-NaCl, $PrCl_3$-KCl and $PrCl_3$-$CaCl_2$ Systems
Y. Iwadate, K. Igarashi, J. Mochinaga and T. Adachi, *J. Electrochem. Soc.*, **133**, 1162-1166 (1986)

[75] Refractive Index of Molten $PrCl_3$-NaCl and $PrCl_3$-KCl Mixture
Y. Iwadate, K. Kikuchi, K. Igarashi and J. Mochinaga, *Z. Naturforsch.*, **37a**, 1284-1288 (1982)

[76] Electrical Conductivity of Molten $NdCl_3$-KCl, $NdCl_3$-NaCl and $NdCl_3$-$CaCl_2$ Solutions
J. Mochinaga, Y. Iwadate and K. Igarashi, *J. Electrochem. Soc.*, **138**, 3588-3592 (1991)

[77] Molar Volume Variation and Ionic Conduction in Molten $SmCl_3$-NaCl, $SmCl_3$-KCl, and $SmCl_3$-$CaCl_2$ Systems
K. Fukushima, S. Koseki, K. Wakabayashi, S. Yamane and Y. Iwadate, submitted to *J. Alloy. Comp.*

[78] Phase Diagram of Binary $GdCl_3$-NaCl and $GdCl_3$-$CaCl_2$ System
T. Hattori, Y. Iwadate, K. Igarashi and J. Mochinaga, *Denki Kagaku*, **56**, 783-784 (1988)

[79] Refractive Index and Molar Volume of Molten Binary $GdCl_3$-NaCl, $GdCl_3$-KCl Systems
Y. Sasaki, K. Igarashi and J. Mochinaga, *Denki Kagaku*, **50**, 226-231 (1982)

[80] Ionic Conductivity of Molten $GdCl_3$-NaCl and $GdCl_3$-KCl Systems
K. Fukushima, M. Hayakawa and Y. Iwadate, *J. Alloy. Comp.*, **245**, 66-69 (1996)

[81] Phase Diagram of Ternary $DyCl_3$-KCl-NaCl System
J. Mochinaga, H. Ohtani and K. Igarashi, *Denki Kagaku*, **49**, 19-21 (1981)

[82] Densities and Molar Volumes of Molten Rare-Earth Chlorides: $PrCl_3$, $NdCl_3$, $GdCl_3$ and $DyCl_3$

K. Cho, K. Irisawa, J. Mochinaga and T. Kuroda, *Electrochim. Acta*, **17**, 1821-1827 (1972)
[83] Molar Volume Variation and Ionic Conduction in Molten $ErCl_3$-NaCl and $ErCl_3$-KCl systems
K. Fukushima, T. Ikumi, J. Mochinaga, R. Takagi, M. Gaune-Escard and Y. Iwadate, *J. Alloy. Comp.*, **229**, 274-279 (1995)
[84] Melt Structure of Lanthanide Trichlorides Analyzed by X-ray Diffraction and Raman Spectroscopy Part One: $CeCl_3$
Y. Iwadate, K. Fukushima, K. Igarashi and J. Mochinaga, *J. Fac. Eng. Chiba Univ.*, **44**, 31-35 (1992)
[85] X-ray Diffraction and Raman Spectroscopic Study on the Short-Range Structure of Molten $CeCl_3$
J. Mochinaga, M. Ikeda, K. Igarashi, K. Fukushima and Y. Iwadate, *J. Alloys. Comp.*, **193**, 36-37 (1993)
[86] Melting Behaviour in Hexagonal $CeCl_3$ and Monoclinic $ErCl_3$ Crystals
Y. Iwadate, N. Okako, Y. Koyama, H. Kubo and K. Fukushima, *J. Mol. Liquids*, **65/66**, 369-372 (1995)
[87] Raman Spectra of Molten Cl_3-KCl and $GdCl_3$-NaCl
A. Matsuoka, K. Fukushima, K. Igarashi, Y. Iwadate and J. Mochinaga, *Nippon Kagaku Kaishi*, 471-474 (1993)[in Japanese]
[88] Short Range Structures of Several Rare Earth Chloride Melts
J. Mochinaga, Y. Iwadate and K. Fukushima, *Mat. Sci. Forum*, **73-75**, 147-152 (1991)
[89] Structure of Molten $DyCl_3$ and Equimolecular $DyCl_3$-NaCl
J. Mochinaga, Y. Miyagi, K. Igarashi, K. Fukushima and Y. Iwadate, *Nippon Kagaku Kaishi*, 459-464 (1993) [in Japanese]
[90] X-Ray Diffraction Study on the Local Structure of Molten $ErCl_3$
Y. Iwadate, T. Iida, K. Fukushima, J. Mochinaga and M. Gaune-Escard, *Z. Narurforsch.* **49a**, 811-814 (1994)
[91] Internal Mobilities in (Na-Rb)NO_3 Melts
I. Okada, R. Takagi and K. Kawamura, *Z. Naturforsch.*, **36a**, 381-384 (1981)
[92] Internal Cation Mobilities in the Molten Systems (Li-Na)NO_3 and (Na-Cs)NO_3
C. -C. Yang, R. Takagi and I. Okada, *Z. Naturforsch.*, **35a**, 1186-1191 (1980)
[93] The Internal Mobilities of the Molten Binary System (Rb-Cs)NO_3
R. Takagi, K. Kawamura and I. Okada, *Z. Naturforsch.*, **39a**, 759-763 (1984)
[94] Internal Cation Mobilities and Their Isotope Effects in the Molten System (Li, K)NO_3
A. Lundén, J. Habasaki and I. Okada, *Z. Naturforsch.*, **42a**, 683-689 (1987)
[95] Cation Mobilities Including Isotope Effects for Electromigration in Molten Mixures of Potassium and Rubidium Nitrate
A. Ekhed and A. Lundén, *Z. Naturforsch.*, **34a**, 1207-1211 (1978)
[96] Molten Salts: Volume 4, Part 1, Nitrates and Mixtures, Electrical Conductance, Density, Viscosity, and Surface Tension Data
G. J. Janz, U. Krebs, H. F. Seigenthaler and R. P. T. Tomkins, *J. Phys. Chem. Ref. Data*, **1**, 581 (1972)

Chapter 2.

Countercurrent electromigration

2.1 Principle

For explaining the principle, a schematic diagram for the electromigration is shown in Fig. 2.1. When the electrical field is applied between anode and cathode, cations migrate toward the cathode. The migration mobilities of each cation, u_1 and u_2 depend on cationic radii, valences, polarizabilities, molar volumes, and so on. During migration, there occurs a back flow for cations, which is caused by osmotic force keeping the liquid level constant. This flow is called a countercurrent flow, u_c, which is equal to all kinds of species. Due to this countercurrent flow, a cation with lower mobility is enriched toward the anode.

2.2 Derivation of mass balance equation

Let us assume a mixture consisting of cations 1 and 2 and a common anion 3.

In a separation tube the flows J_i per cross sectional area in the direction from the anode to cathode is expressed by,

$$J_1 = (v_1 - v_c)c_1 - D_1 \nabla c_1 \tag{2.1}$$

$$J_2 = (v_2 - v_c)c_2 - D_2 \nabla c_2 \tag{2.2}$$

$$J_3 = (-v_3 - v_c)c_3 - D_3 \nabla c_3 \tag{2.3}$$

where J_i is the net flow of each component i, v_i: the scalar component of the external velocity, v_c: the velocity of countercurrent flow with reference to the wall, D_i: the effective diffusion coefficient, c_i: equivalent concentration.

In the right-hand of Eq. (2.1), $v_1 c_1$, $v_c c_1$ and $D_1 \nabla c_1$ represent the migration flow, the countercurrent flow and the diffusion flow. The convection flow can be neglected in

the migration tube.

In a plane B where the concentration does not change during electromigration, the diffusion flow is neglected.

$$J_1 = (v_1 - v_c)c_1 \tag{2.4}$$

$$J_2 = (v_2 - v_c)c_2 \tag{2.5}$$

$$J_3 = (-v_3 - v_c)c_3 \tag{2.6}$$

From the electrical neutrality

$$c_1 + c_2 - c_3 = 0 \tag{2.7}$$

The electrical current density I_d at the plane B is

$$I_d = I / S = F(J_1 + J_2 - J_3) \tag{2.8}$$

where S is the cross sectional area at the place B, F Faraday constant and the constant current I is assumed for simplicity.

ε is defined as

$$\varepsilon = \frac{(v_1 - v_2)(c_1 + c_2)}{\{(v_1 + v_3)c_1 + (v_2 + v_3)c_2\}} \tag{2.9}$$

From Eqs. (2.4), (2.5), (2.6), (2.7) and (2.8)

$$I_d / F = J_1 + J_2 - J_3 = v_1c_1 + v_2c_2 + v_3c_3 = (v_1 + v_3)c_1 + (v_2 + v_3)c_2 \tag{2.10}$$

From Eqs. (2.9) and (2.10)

$$v_1 + v_3 = \left(\frac{I_d}{c_3F}\right)\left\{1 + \left(\frac{c_2}{c_3}\right)\varepsilon\right\} \tag{2.11}$$

$$v_2 + v_3 = \left(\frac{I_d}{c_3F}\right)\left\{1 - \left(\frac{c_1}{c_3}\right)\varepsilon\right\} \tag{2.12}$$

Dividing both sides of Eqs. (2.11) and (2.12) by voltage per unit length E at the place B gives u_1 and u_2, internal mobilities of 1 and 2, respectively;

$$u_1 = \left(\frac{I_d}{c_3 EF}\right)\{1 + x_2\varepsilon\} \tag{2.13}$$

$$u_2 = \left(\frac{I_d}{c_3 EF}\right)\{1 - x_1\varepsilon\} \tag{2.14}$$

where x_1 and x_2 are equivalent fractions of 1 and 2, respectively, at the place B, that is before electromigration; $x_1 + x_2 = 1$.

Since electrical conductivity of the mixture at the place B, $\kappa = I_d / E$ and equivalent volume of the mixture at the place B, $V_m = 1/c_3$

$$u_1 = \left(\frac{\kappa V_m}{F}\right)\{1 + x_2\varepsilon\} \tag{2.15}$$

$$u_2 = \left(\frac{\kappa V_m}{F}\right)\{1 - x_1\varepsilon\} \tag{2.16}$$

In countercurrent electromigration of molten salts, there is generally no volume flow along the separation tube, in other words, such a condition can be fulfilled and therefore across the plane B

$$J_1 V_{13} + J_2 V_{23} = 0 \tag{2.17}$$

where V_{13} and V_{23} are equivalent volumes of pure melts 13 and 23, respectively. The additivity of the molar volume is assumed, which is found to be generally the case.

$$v_c(t) = (v_1 c_1 V_{13} + v_2 c_2 V_{23}) / (c_1 V_{13} + c_2 V_{23}) \tag{2.18}$$

$v_c(t)$ could be a function of t, but actually independent of t, as far as $v_1(t)$ and $v_2(t)$ are independent of t.

If the volume between A and B is V, the equivalent quantity of 13 there, $N_1(t)$ is

$$N_1(t) = c_1 V - \int_0^t J_1(t) S dt = c_1 V - (v_1 - v_2) c_1 c_2 V_{23} S t / (c_1 V_{13} + c_2 V_{23}) \tag{2.19}$$

Similarly, the equivalent quantity of 23, $N_2(t)$ is

$$N_2(t) = c_2V - \int_0^t J_2(t)Sdt = c_2V - (v_2 - v_1)c_1c_2V_{13}St / (c_1V_{13} + c_2V_{23}) \tag{2.20}$$

From Eqs. (2.19) and (2.20),

$$v_1 - v_2 = -\left(\frac{1}{St}\right)\left\{\frac{N_1(t)}{c_1} - \frac{N_2(t)}{c_2}\right\} \tag{2.21}$$

It follows from Eqs. (2.10) and (2.21) that

$$\frac{(v_1 - v_2)}{\{(v_1 + v_3)x_1 + (v_2 + v_3)x_2\}} = -\left(\frac{F}{It}\right)\left\{\frac{N_1(t)}{x_1} - \frac{N_2(t)}{x_2}\right\} \tag{2.22}$$

Therefore,

$$\varepsilon = \frac{(u_1 - u_2)}{(x_1u_1 + x_2u_2)} = -\left(\frac{F}{Q}\right)\left\{\frac{N_1(t)}{x_1} - \frac{N_2(t)}{x_2}\right\} \tag{2.23}$$

Equation (2.23) was derived by Klemm[1] and by Ljubimov and Lundén[2].

Even if $J_1V_{13} + J_2V_{23} = \alpha \neq 0$ in Eq. (2.17), Eq (2.23) is the same, because the term corresponding to α vanishes when the equation corresponding to Eq. (2.19) is subtracted by that of Eq. (2.20).

The standard deviation of ε is represented as follows,

$$\sigma_\varepsilon = \sqrt{\left(\frac{\partial\varepsilon}{\partial x_1}\right)^2\sigma_{x_1}^2 + \left(\frac{\partial\varepsilon}{\partial x_2}\right)^2\sigma_{x_2}^2 + \sum_{i=1}\left(\frac{\partial\varepsilon}{\partial N_{1i}}\right)^2\sigma_{N_{1i}}^2 + \sum_{i=1}\left(\frac{\partial\varepsilon}{\partial N_{2i}}\right)^2\sigma_{N_{2i}}^2}$$

$$= \sqrt{\left(\frac{F}{Q}\right)^2\left(\frac{\sum N_{1i}}{x_1^2}\right)^2\sigma_{x_1}^2 + \left(\frac{F}{Q}\right)^2\left(\frac{\sum N_{2i}}{x_2^2}\right)^2\sigma_{x_2}^2 + \sum_{i=1}\left(\frac{F}{Q}\right)^2\left(\frac{1}{x_1}\right)^2\sigma_{N_{1i}}^2 + \sum_{i=1}\left(\frac{F}{Q}\right)^2\left(\frac{1}{x_2}\right)^2\sigma_{N_{2i}}^2}$$

$$= \left(\frac{F}{Q}\right)\sqrt{\left(\frac{\sum N_{1i}}{x_1^2}\right)^2\sigma_{x_1}^2 + \left(\frac{\sum N_{2i}}{x_2^2}\right)^2\sigma_{x_2}^2 + \left(\frac{1}{x_1}\right)^2\sum_{i=1}\sigma_{N_{1i}}^2 + \left(\frac{1}{x_2}\right)^2\sum_{i=1}\sigma_{N_{2i}}^2}$$

Therefore, standard deviations of internal mobilities σ_{u_1} and σ_{u_2}, respectively

$$\sigma_{u_1} = \sqrt{\left(\frac{\partial u_1}{\partial x_2}\right)^2 \sigma_{x_2}^2 + \left(\frac{\partial u_1}{\partial \varepsilon}\right)^2 \sigma_\varepsilon^2}$$

$$= \sqrt{\left(\frac{\kappa V_m}{F}\right)^2 \varepsilon^2 \sigma_{x_2}^2 + \left(\frac{\kappa V_m}{F}\right)^2 x_2^2 \sigma_\varepsilon^2}$$

$$= \left(\frac{\kappa V_m}{F}\right) \sqrt{\varepsilon^2 \sigma_{x_2}^2 + x_2^2 \sigma_\varepsilon^2}$$

$$\sigma_{u_2} = \sqrt{\left(\frac{\partial u_2}{\partial x_1}\right)^2 \sigma_{x_1}^2 + \left(\frac{\partial u_2}{\partial \varepsilon}\right)^2 \sigma_\varepsilon^2}$$

$$= \sqrt{\left(\frac{\kappa V_m}{F}\right)^2 \varepsilon^2 \sigma_{x_1}^2 + \left(\frac{\kappa V_m}{F}\right)^2 x_1^2 \sigma_\varepsilon^2}$$

$$= \left(\frac{\kappa V_m}{F}\right) \sqrt{\varepsilon^2 \sigma_{x_1}^2 + x_1^2 \sigma_\varepsilon^2}$$

2.3 Experimental procedure

For employing electromigration in molten chloride systems, we should introduce Cl_2 gas into the cathode to prevent from depositing of Li metal[3],[4]. However, in this construction, chlorine gas, which is poisonous, has to be used. Therefore, Haibara and Okada[5] revised the cell. Molten $PbCl_2$ was used around the cathode and reduced to Pb metal in order to prevent the Li reduction. As this type of the cell seems to be more easily to manage than the former, the experiment was performed by the electromigration cell, which is shown in Fig. 2.2.

The container for the salt bath, I, and the cathode compartment, G, were made of alumina(Nikkato Corp., SSA-S grade). The melt bath, D, which contained a mixture of LiCl-KCl of the eutectic composition was kept in a large container. In the cathode compartment, molten $PbCl_2$, F, was loaded for reduction of Pb^{2+} instead of the reduction of bath components. The main container was covered with a graphite cap, O. The cathode compartment had a hole of 5mm ϕ as a melt channel which was packed

with quartz wool. Both cathode and anode, A, were made of a super fine graphite rod (5mm ϕ).(Toyo Carbon Co., Ltd.) The cathode rod was covered by alumina ceramics, C, for protection from corrosion. Migration tubes, M, were made of quartz glass. The upper part of the migration tube had an outlet for Cl_2 gas, P. The lower part of the migration tube was packed with alumina powder, L, (100 μ m ϕ)(Nishio Chemical Ind.) in order to prevent convection of the melt in the migration tube (4mm ϕ). Quartz wool was packed at the bottom, J, and at the end of the anode in contact with the melt, N. Temperature was kept constant with a temperature controller(Shimaden Co., Ltd. DSL) and measured by a Chromel-Alumel thermocouple, K, during migration.

Since the melts should be kept under Ar gas atmosphere for preventing rare earth chlorides from oxidation and LiCl from hydration, we have performed all migration in an Ar-flow environment. The sample melt of a given composition was well mixed in another quartz vessel. The sample melt was introduced into the migration tube through the bottom by sucking with a handy pump(Shinku Kiko PS-05). The migration tube with sample melt was quickly moved and set into the migration cell. A constant DC current supplier(Kikusui Electronics. Corp. PAD 500-0.6A) fed electric currents less than 0.2A. Transported charge was measured by a Cu coulometer. After several thousand Coulombs of charge was transported, the migration tube was taken out from the bath and the salt was quenched quickly. The tube was cleaned outside and cut into several pieces of 7～8 mm length also in the glove box. The salt in each fraction was dissolved to diluted hydrochloric acid for analyzing the amount of each cation.

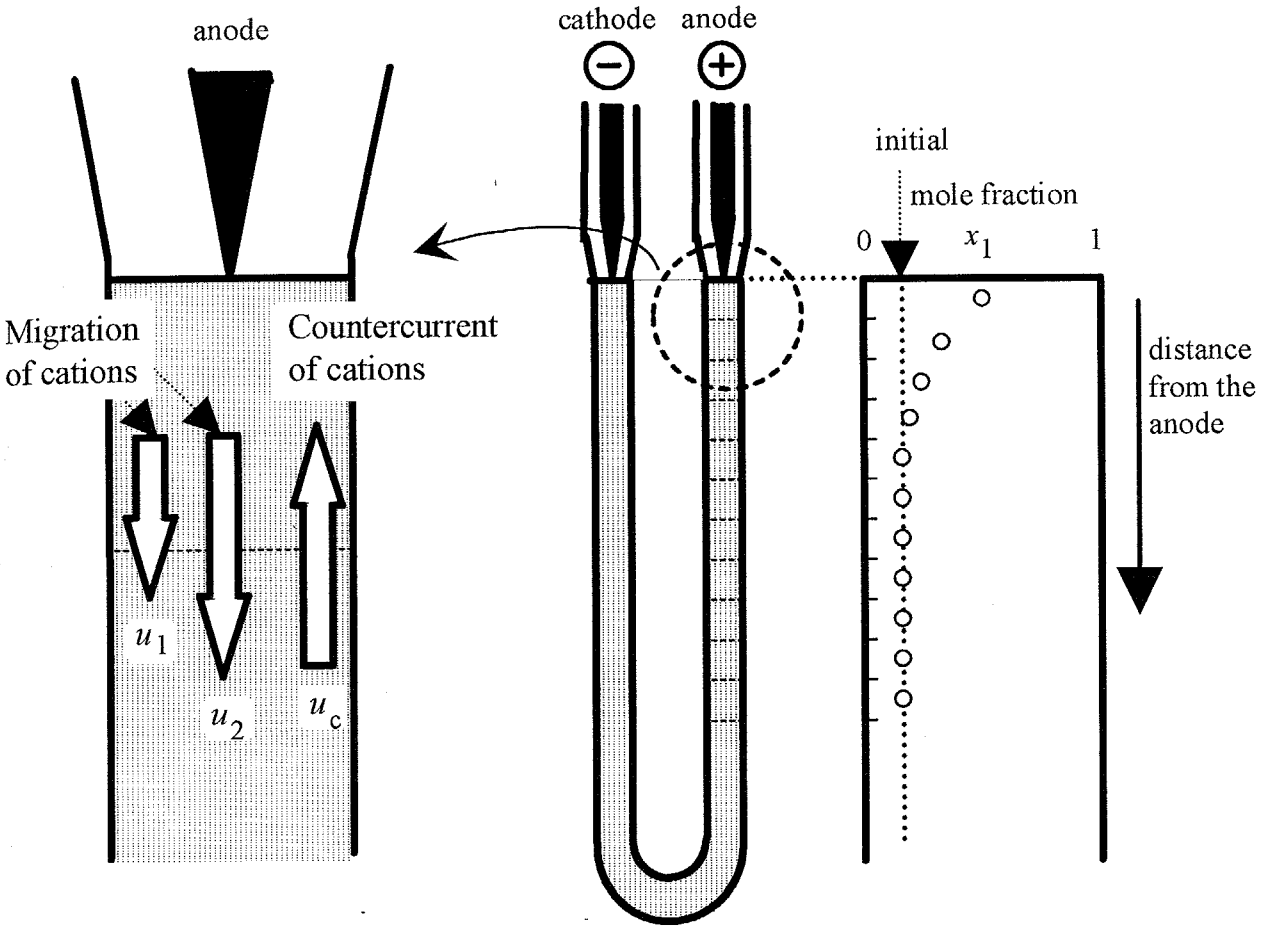

Fig. 2.1 Schematic diagram for countercurrent electromigration

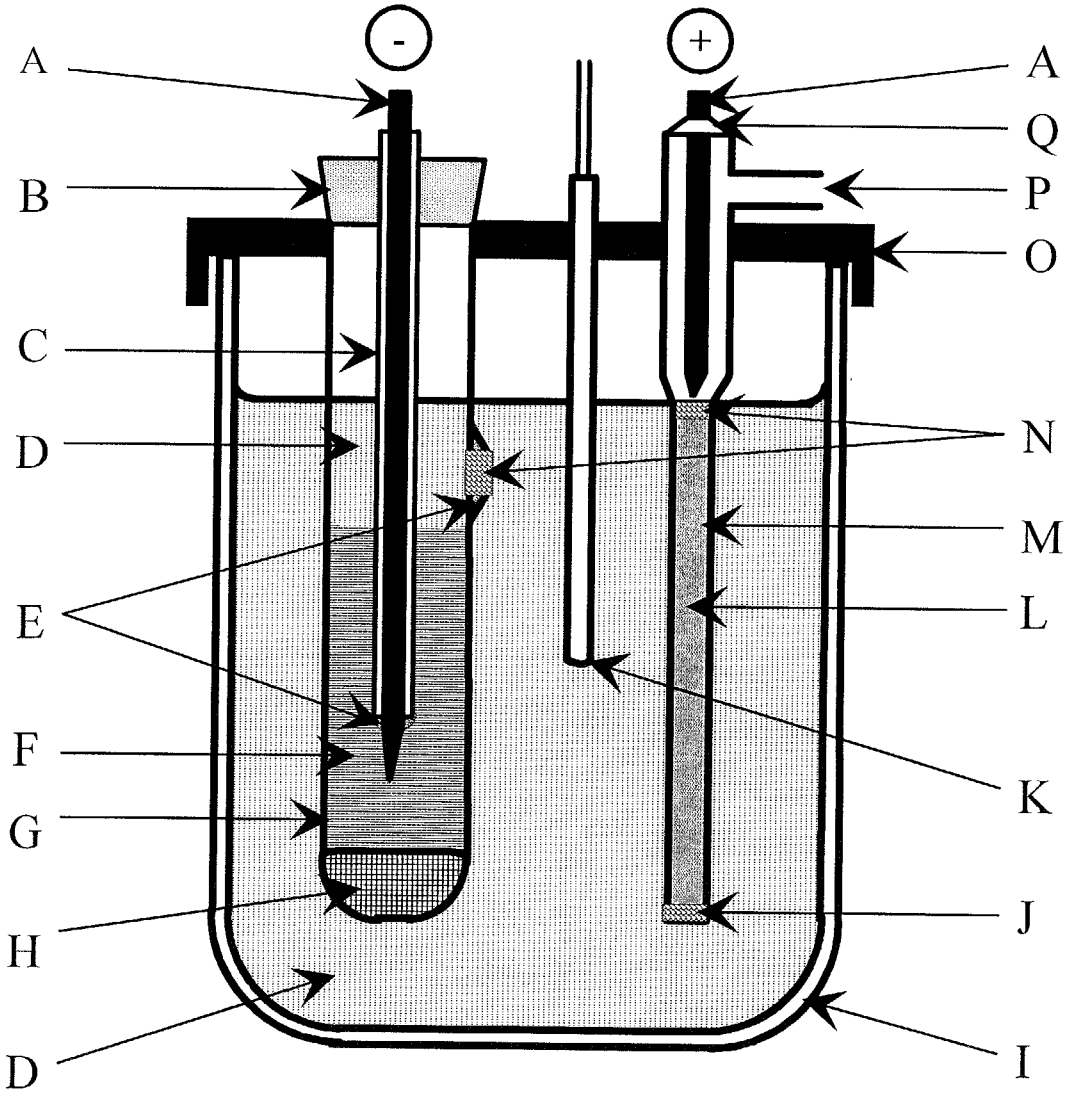

Fig. 2.2 Cell for countercurrent electromigration

A: graphite electrode; B: Silicone-Teflon stopper; C: alumina sheath; D: molten salt bath (LiCl-KCl eutectic); E: alumina cement; F: molten $PbCl_2$; G: anode compartment; H: molten Pb metal; I: large container; J: quartz filter; K: thermocouple; L: alumina powder; M: migration tube; N: quartz wool; O: carbon cap; P: Cl_2 gas outlet; Q: Teflon sealtape;

References

---

[1] Die Phänomenologie zweier Verfahren zur Isotopentrennung
A. Klemm, *Z. Naturforsch.*, **1**, 252-257 (1946).[in German]
[2] Electromigration in Molten and Solid Binary Sulfate Mixtures: Relative Cation Mobilities and Transport Numbers
V. Ljubimov and A. Lundén, *Z. Naturforsch.*, **21a**, 1592-1600 (1966).
[3] Internal Cation Mobilities and their Isotope Effects in the Molten System (Li, K)Cl
A. Lundén and I. Okada, *Z. Naturforsch.*, **41a**, 1034-1040 (1986)
[4] Internal Cation Mobilities in the Molten Ternary System (Li, Na, K)Cl of the Eutectic Composition
A. Endoh and I. Okada, *Z. Natruforsch.*, **43a,** 638-642 (1988)
[5] Internal Mobilities in Molten (Li, Pb(II))Cl as Remeasured by the Klemm Method
T. Haibara and I. Okada, *Z. Naturforsch.*, **45a**, 827-831 (1990)

Chapter 3.

Internal cation mobilities in molten multivalent-multivalent cation chloride systems

3.1 Background

Chemla and Okada have reviewed internal mobilities of various monovalent cations in binary molten systems with a common anion[1]. They state that, when the Coulombic attraction between cation and anion is expected to be the dominant factor for the electrical conductance, the internal mobilities are well expressed by

$$u = [A / (V - V_0)]\exp(-E / RT) \qquad (3.1)$$

where V is the molar volume and A, E, and V_0 are parameters characteristic of the considered cation and nearly independent of the cocation. Equation (3.1) holds, for instance, for the molten binary chlorides (Li, M)Cl (M=Na[2], K[3], Rb[3], and Cs[4],[5]) and (Na, K)Cl[2]. In the binary monovalent cation systems the Chemla effect usually occurs[1], which has been interpreted in terms of the self-exchange velocity[6].

We expected that the data of the internal mobilities would yield a hint about the electrically-conducting species in melts consisting of multivalent cations. To my knowledge, mobilities was not measured in additive binary divalent cation systems, while internal mobilities have been studied in binary alkali-alkaline earth nitrates[7],[8],[9] and halides[10],[11]. Thus, the main aim of our study was to measure the internal cation mobilities in the binary divalent cation system $(Ca, Ba)_{(1/2)}Cl$ and to obtain insight into the electrical conductance in divalent cation chloride melts.

Moreover, the mobility data of these mixtures of rare earth elements provide useful information on a separation of rare earth elements by the contercurrent electromigration methods. Mobilities in molten mixture systems with trivalent cations

and a common anion have not yet been published. In this chapter, I have also measured the internal mobilities in two molten binary systems of trivalent rare earth element ions, $(Y, La)_{(1/3)}Cl$ and $(Y, Dy)_{(1/3)}Cl$. Some properties of pure $Y_{(1/3)}Cl$, $La_{(1/3)}Cl$ and $Dy_{(1/3)}Cl$ related to the mobilities are summarized in Table 3.1. The ionic radius of Y^{3+} is distinctly smaller than that of La^{3+}, and similar to that of Dy^{3+}.

The structure of the pure melts of $CaCl_2$ and $BaCl_2$ has been previously studied by neutron diffraction[12),(13)], X-ray diffraction[14),(15)] and Raman spectroscopy[16]. Based on the hole model, Bockris *et al.* assumed that the main positively charged entities in alkaline earth chloride melts would be MCl^+ complexes[17]. This assumption was, however, doubted later[18]. It has been argued[13] that even for $ZnCl_2$ melts in which the species are polymerized the electrically-conducting species are not be such ones as $ZnCl^+$ or $ZnCl_3^-$.

Structural properties of the pure rare earth chloride melts have been studied by neutron diffraction[19], X-ray diffraction[20),(21)] and Raman spectroscopy[22),(23)]. The Y^{3+} or Dy^{3+} containing species existing in such chloride melts are conjectured by X-ray diffraction and neutron diffraction to be six-coordinated $[RCl_6]^{3-}$, where R is the rare earth atom. If the main electrically-conducting species is an anionic one such as $[RCl_6]^{3-}$, the lighter isotope of R should be enriched at the anode, because the lighter species migrates faster toward the anode.

For elucidating the main electrically-conducting species in rare earth chlorides, I have measured the isotope effect for melts of trivalent cation systems. The isotope effect on internal cation mobilities in countercurrent electromigration has been studied in a variety of molten salts[10], though no data on the isotope effect for melts of trivalent cation systems have been reported. The countercurrent electromigration method can give accurate and precise data even for very small difference in the internal mobilities,

for example, between two isotopes. One of the aim of the work described in this chapter was to learn by measuring the isotope effect in electromigration whether the electrically-conducting species containing rare earth elements, was cationic or anionic. Molten $DyCl_3$ was chosen mainly, because the melting point is not too high (991 K) and partly because Dy has 7 stable isotopes; ^{156}Dy: 0.06%, ^{158}Dy: 0.10%, ^{160}Dy: 2.43%, ^{161}Dy: 18.9%, ^{162}Dy: 25.5%, ^{163}Dy: 24.9%, ^{164}Dy: 28.2%. The abundance ratios of the first two isotopes are quite low, and measurements were thus obtained with the other 5 isotopes.

3.2 Experimental

3.2.1 Reagent

$CaCl_2$ and $BaCl_2$ (Kanto Chemical Company, Inc.) of reagent grade were used without further purification. The salts were vacuum dried overnight at ca. 450 K. Anhydrous chemicals YCl_3, $LaCl_3$ and $DyCl_3$ were prepared by the chemical reaction of the oxides(Mitsui Mining Smelting Company, Ltd.) with excess NH_4Cl (Kanto Chemical Company, Inc.), and purified by sublimation at 1273 K under a reduced pressure to remove gases (NH_3, HCl), residual NH_4Cl and oxichloride impurities. The apparatus for the purification is shown in Fig. 3.1, which has been described in detail[24].

3.2.2 Conventional ac technique

The conductance cell used is shown in Fig. 3.2. The cell was made of quartz, the inner diameter and length of the capillary being ca. 2 mm and ca. 10 cm, respectively. Before measuring conductivity of the melt at each concentration, the conductance cell was calibrated with pure NaCl melt[25]. The cell constant was evaluated to be 142.87 cm^{-1}. Various molar ratios were prepared by mixing the pure salts in accurately weighed quantities in a glove box filled with dry N_2.

A conventional ac technique was applied to obtain the polarization-free resistance of the melt by varying the input frequency from 1.0 to 10 kHz. The experimental temperature for each sample melt was varied by ca. 900 to 1200 K. The apparatus used for the measurement has been described in detail[26].

3.2.3 Countercurrent electromigration

For the experiments in $(Ca, Ba)_{(1/2)}Cl$ and $(Y, La)_{(1/3)}Cl$, the concentrations and temperatures shown in Figs. 3.3 and 3.4 were chosen in view of the phase diagrams[27],[28]. The phase diagram of $(Y, Dy)_{(1/3)}Cl$ was not available in literature.

After sufficient mixing at a desired composition, the mixture was melted in a small quartz vessel under an Ar gas flow. The electromigration cell was shown in chapter 2; The diameter of diaphragm part of the separation tube was 4mm. The temperature was kept at the preset value within $\pm$ 2 K during electromigration with a temperature controller. The transported charge after each run was measured by a Cu coulometer and a commercially available coulometer (Hokuto Denko HF201) in a series of measuring internal mobilities and isotope effects, respectively. The contents of alkaline earth elements and rare earth elements in each fragment were determined by an ion chromatographic analyzer (IC 500 Yokogawa Hokushin Electric. Co, Ltd.) and by an inductively coupled plasma (ICP) spectrometer (ICPS-5 Shimadzu Corporation), respectively. For measuring the isotope effect, the isotope ratios of Dy were measured by a mass spectrometer (Finnigan Mat 261).

3.3 Results

3.3.1 Electrical conductivity

The polarization-free resistance (R_{inf}) of the melt was estimated by linear extrapolation of the measured resistances (R_{meas}) to infinite frequency by an empirical relation[29),(30)], as shown in Fig. 3.5.

$$R_{meas} = R_{inf} + C\omega^{-1/2} \qquad (3.2)$$

where ω and C are the frequency and a fitting parameter, respectively. The temperature dependence on the conductivity of each concentration in (Y, La)$_{(1/3)}$Cl and (Y, Dy)$_{(1/3)}$Cl systems are shown in Figs. 3.6 and 3.7, respectively. The measured values were fitted to a linear function of temperature, and the calculated parameters are given in Table 3.2. The conductivity isotherms at 1073 K in (Y, La)$_{(1/3)}$Cl and (Y, Dy)$_{(1/3)}$Cl are shown in Figs. 3.8 and 3.9, respectively.

Conductivity data in molten (Ca, Ba)$_{(1/2)}$Cl have already been measured by Kochinashvili and Barzakovskii, which are shown in Fig. 3.10[31].

3.3.2 Internal mobilities

The relative differences in the internal mobilities of cations 1 and 2, ε, are defined as

$$\varepsilon = (u_1 - u_2) / u_c \tag{3.3}$$

where u_c is the average cationic internal mobility of the mixture, u_c is related to the conductivity κ, and the molar volume V_m of the mixture given by

$$u_c = \kappa V_m / F \tag{3.4}$$

where F is the Faraday constant and the molar unit is defined as $M_{(1/Z)}Cl$(M: cation, Z: cationic charge).

The ε values were calculated by an equation based on the material balance[32),(33)]

$$\varepsilon = -(F / Q)(N_1 / x_1 - N_2 / x_2) \tag{3.5}$$

where Q is the transported charge, N_M s are the quantities in mole of $(1/Z)M^{Z+}$ in the separation tube on the anode side of the position where the chemical composition has remained unchanged during electromigration, and x_1 and x_2 are the mole fractions of cations 1 and 2, respectively, before electromigration (x_1+x_2=1).

The ε values in $(Ca, Ba)_{(1/2)}Cl$ system and in both $(Y, La)_{(1/3)}Cl$ and $(Y, Dy)_{(1/3)}Cl$ systems are given in Tables 3.3 and 3.4, respectively, together with the main experimental conditions.

The internal mobilities of M_1^{Z+} and M_2^{Z+} are obtained from

$$u_1 = (\kappa V_m / F)(1 + x_2 \varepsilon) \tag{3.6}$$

$$u_2 = (\kappa V_m / F)(1 - x_1 \varepsilon) \tag{3.7}$$

As the density data of the mixtures were not available, we assumed additivity of the molar volumes of the relevant pure melts[27)]. In Tables 3.5 and 3.6 the calculated u_1 and u_2 are also given together with the molar volume and the conductivity.

The isotherms of the internal mobilities in the systems $(Ca, Ba)_{(1/2)}Cl$, $(Y, La)_{(1/3)}Cl$

and $(Y, Dy)_{(1/3)}Cl$ at 1073 K are shown in Figs. 3.11, 3.12 and 3.13, respectively.

3.3.3 Isotope effect

The results of five runs are summarized, together with the main experimental conditions, in Table 3.7.

For one of these experiments, the distribution of the Dy isotopes in the separation tube after electromigration is shown in Fig. 3.14. Figure 3.14 shows that the isotopes are more enriched in the 2nd fraction than in the 1st one, because the salt in the 1st fraction also contained unelectromigrated material. Otherwise, the heavier isotopes were enriched toward the anode, which means that the lighter isotopes migrated toward the cathode.

Relative differences in the internal mobility of Dy isotopes of mass numbers, M=160, 161, 163 and 164, with reference to that of M=162, ε_M, have been calculated from eqn. (68) in ref. [32]

$$\varepsilon_M = -(F/Q)\sum n_i (x_i^M / x_0^M - x_i^{162} / x_0^{162}), \qquad (3.8)$$

where n_i is the molar quantity of $Dy_{(1/3)}Cl$ in the i-th fraction, x_0 is the isotope abundance ratio before electromigration, x_i is the ratio in the i-th fraction after electromigration; F is the Faraday constant, and Q the transported charge. The summation was taken from fraction 1 to the fraction where the original isotope ratio did not change during electromigration. The calculated ε_M's are shown in Fig. 3.15.

3.4 Discussion

3.4.1 Molten (Ca, Ba)$_{(1/2)}$Cl system

Figure 3.11 shows that, although u_{Ca} in pure $Ca_{(1/2)}Cl$ is greater than u_{Ba} in pure $Ba_{(1/2)}Cl$; u_{Ca} is smaller than u_{Ba} in all the investigated conditions. However, it is conjectured from the isotherms in Fig. 3.11 that at sufficiently low x_{Ba} particularly at low temperature (below the melting point) the smaller cation would be more mobile than the larger one. These features resemble those for the system (Li, Na)Cl[2]. This resemblance is presumably caused by the fact that among the interactions between alkali and chloride ions the ones between Li and Cl and between Na and Cl are particularly strong and that their relative difference is comparable to that for Ca and Cl vs. Ba and Cl.

Both mobilities decrease with increasing concentration of the larger cation. This decrease is steeper for the smaller cation. This rule for the present system is quite the same as that for the binary alkali halides[2],[3] and nitrates[1]. From Figs. 3.3 and 3.11, the Chemla crossing point is not expected to appear in the liquid state range of the present system.

Both u_{Ca} and u_{Ba} are plotted for 1073 K against the molar volume of the mixture in Figure 3.16. With increasing molar volume, both u_{Ca} and u_{Ba} decrease. This tendency is also the same as that found for the alkali chlorides and nitrates[1],[2],[3].

We have conjectured that in molten alkali chlorides the electrically-conducting species are monoatomic alkali and chloride ions[4] because (i) the internal mobilities in (Li, Cs)Cl calculated based on the linear response theory[34] for the MD trajectories are strictly proportional to the self-exchange velocities, that is the separating velocity of neighboring cation-anion pairs, and (ii) the free space effect[1], which is usually found for systems containing polyatomic species, is not found experimentally for such systems as (Li, Cs)Cl.

In the present system, u_{Ba} smoothly increases with increasing concentration of $Ca_{(1/2)}Cl$ also in its high concentration range. This indicates that the free space effect does not occur, which suggests that polyatomic species are not involved as the current-carrying species. Thus, since the above-mentioned general rules for the mobility isotherms in alkali chlorides hold also for the present system, one is led to believe that the electrically-conducting species in the alkaline-earth chlorides are also monoatomic.

The reciprocal of u_{Ca} and u_{Ba} is plotted against the molar volume in Figure 3.17. These lines seem to lie on straight lines, as expected from (3.1). The parameters for (3.1) are given in Table 3.8. Figure 3.17 also suggests that the Chemla crossing point would shift toward higher concentrations of the smaller cations with increasing temperature. This trend is similar to that found in alkali chlorides and nitrates[1),(2),(3)].

u_{Ca} and u_{Ba} are compared with u_{Na} and u_K[(2)] at 1073 K in Figs. 3.18 and 3.19, respectively. The ionic radii of Ca^{2+} and Ba^{2+} are similar to those of Na^+ and K^+, respectively; the ionic radii of the 6-coordination state are 100 pm for Ca^{2+}, 102 pm for Na^+, 135 pm for Ba^{2+} and 138 pm for K^+[(35)]. The mobilities of the divalent cations are considerably smaller than those of the monovalent cations. This can be interpreted qualitatively in terms of the cation-anion interactions. Since the coulombic interaction of the divalent cation with Cl^- is considerably stronger than that of the monovalent cations. Although the self-exchange velocities have not been computed for the alkaline-earth chloride systems, one can assume that the self-exchange velocities for the alkaline-earth ions are by about factor of 3 smaller than those for the alkali ions of smaller sizes. This also suggests that electrically-conducting species are the monoatomic ions in the present system. The fact that the isotope effect on the internal mobilities of pure $Ca_{(1/2)}Cl$ and $Ba_{(1/2)}Cl$[(36)] is not extremely small compared to that of alkali halides also supports this assumption.

3.4.2 Molten (Y, La)$_{(1/3)}$Cl and (Y, Dy)$_{(1/3)}$Cl systems

Figure 3.12 shows that u_{La} is greater than u_Y in all the investgated conditions i.e., the larger cation La^{3+} is more mobile than the smaller one, Y^{3+}. A Chemla crossing point does not appear. This feature resembles those for the systems (Li, Na)Cl[2] and (Ca, Ba)$_{(1/2)}$Cl. In all those cases the coulombic interactions between the cations and chloride ions are strong, since in (Li, Na)Cl the cation-anion distance is relatively small and in (Ca, Ba)$_{(1/2)}$Cl and (Y, La)$_{(1/3)}$Cl, the cations are multivalent.

It has been found the internal mobilities are approximately proportional to the self-exchange velocities (SEV), which are defined as the separating velocities of neighboring unlike ion pairs[37] and may be calculated by molecular dynamics simulation. All the following apparently anomalous phenomena concerning electric conductance of molten salts can be qualitatively reproduced by considering the SEVs: the Chemla effect[1],[5],[6],[38], a maximun of electrical conductivity as a function of temperature[39], a maximum electrical conductivity of some salts such as LiCl and LiBr as a fuction of pressure[40], and an increase in the isotope effect of mobilities with temperature[6],[41].

To show how the SEVs of two cations change in accordance with number density of common anions and how the change depends on the cationic "size", the potentials felt by Li^+ and K^+ ions collinearly located between two Cl^- ions can be schematically depicted. In an example, in Fig. 3.20, two Cl^--Cl^- distances of 580 and 670 pm are given which approximately correspond to Cl^--Cl^- distances at 1000 K for melts of the fictive NaCl-type crystalline structure, of pure LiCl and KCl, respectively, using the Tosi-Fumi potentials[42]. As the concentration of the larger cation increases, the average distance between neighboring Cl^- ions usually increases, and the cations become less favorable to move away from the referenced Cl^- ion toward the other. The magnitude of the decrease in the SEV is greater for the smaller sized cation than for the larger one, as can

be seen in Fig. 3.20.

The main factors infuencing internal mobilities of monovalent cation molten salts[1] have previously been considered to be: (*i*) ionic radius and charge, (*ii*) distance between like ions, i.e., molar volume, (*iii*) ionic mass, and (*iv*) kinetic energy, i.e., temperature. Factor (*i*) determines the repulsive and attractive parts of cation-anion potentials. In other words, this factor determines the shape of the pair potential shown in Fig. 3.20. Factor (*ii*): Mixing of two salts having a common anion corresponds to a change in the average distance between two anions, as shown by comparison of two Cl^--Cl^- distances in Fig. 3.20. The effect (*iii*) of the mass is small, but if all other factors are equal, the ion having a smaller mass has always higher mobility, as is discussed later. Figure 3.20 reveals that the potential profiles felt by the cations change considerably in accordance with the Cl^--Cl^- distances as well as with the pair potentials. Therefore, at a given temperature, the magnitude of the SEV is mainly determined by a combination of factors (*i*) and (*ii*).

The (Y, La)$_{(1/3)}$Cl system is interesting in that the molar volume of $Y_{(1/3)}Cl$ is greater than that of $La_{(1/3)}Cl$, whereas the ionic radius of Y^{3+} ion is smaller than that of La^{3+} ion, as given in Table 3.6. Figure 3.12 shows that, with increasing x_{La}, that is with decreasing molar volume, the internal mobilities of both Y^{3+} and La^{3+} increase. The behavior is generally found for binary monovalent[1] and divalent cation systems with a common anion. The magnitude of the increase is, however, greater for the larger cation, La^{3+}, than for the smaller one, Y^{3+}, a tendency that has not been found in other systems studied. The reason is not entirely clear; a considerable difference in the short-range order around the two cations may be ralated to the difference in the crystal structure, and thus, in the volume change on melting, as given in Table 3.6.

In Fig. 3.21, the internal cation mobilities of the present system are plotted

against the molar volume in comparison with those of typical monovalent and divalent cation systems. The mobilities become smaller in going from monovalent to trivalent cations, presumably because the cation-anion coulombic interaction becomes stronger. The magnitude of the decrease in the mobilities as a function of the molar volume is in the order: trivalent > divalent ~ monovalent. As the coulombic potential surfaces between unlike ions have steeper gradients with increasing cation valence, it is reasonable that the increase in molar volume corresponding to increase in the Cl^--Cl^- distance influences the SEV more in going from monovalent to trivalent cation systems. The fact that the decreasing magnitude is relatively moderate in these divalent cation chlorides may be related to the fact, found by neutron diffraction[13] that the nearest Cl^--Cl^- distance does not change greatly in going from $CaCl_2$ to $BaCl_2$. The average Cl^--Cl^- distance strongly affects the SEV, as presumed also from Fig. 3.20.

The u_Y for $(Y, Dy)_{(1/3)}Cl$ is appreciably greater than u_{Dy} in the investigated range. When these pure salts are compared, the cationic radii, the molar volumes, and the conductivities are much the same, but the cationic masses are quite different. Thus, the effect of the difference in mass may overcome the small difference in the ionic radii, where the latter effect presumably favors $Dy_{(1/3)}Cl$ having a slightly larger cationic radius (see Table 3.6). The value of the mass effect[32] μ, defined as the ratio of the relative mobility difference, ε, to the relative mass difference, has been calculated and is given in Table 3.9.

The precision of the concentration ratio of the two rare earth elements obtained from independent measurements by ICP is inevitably not so good as that of the isotope ratio measured by mass spectrometry. Nevertheless, it may be concluded that the values of the mass effect of the two cationic species in the $(Y, Dy)_{(1/3)}Cl$ are not so different from those for the Dy isotopes of pure $Dy_{(1/3)}Cl$ and are not extremely small

when compared with those of alkali or alkaline-earth ions in their halides (*e.g.*, $-\mu = 0.071$ in KCl and 0.051 in $CaCl_2$[10] where the main electrically conducting cationic species are conjectured to be the nonassociated cations[43]). The lifetime of such nonassociated species is, however, as short as ~ 0.5×10^{-13}s[6],[41]. The predominant species containing a lighter rare earth isotope (or element) migrates toward the cathode faster than that containing a heavier one. These experimental findings suggest that the main electrically conducting cationic species is nonassociated trivalent M^{3+} ions. Structural studies have suggested that trivalent rare earth cations in chloride melts exist as octahedral units $[MCl_6]^{3-}$ [19],[23]. Thus, the electrically conducting species is not the same as that of species found by Raman spectroscopy, neutron diffraction, and so on. It has been suggested by Saboungi *et al.*[19] that the network of the unit is loose on a much longer time scale. If we assume that the unit is also partially loose on a much shorter time scale, even where the proportion of such a loose cation-anion pair is small, this could be clarified by calculating the distribution of the SEV for each pair. In fact, our assumption does not contradict the information yielded by neutron diffraction, because neutron diffraction supplies information on space-averaged as well as time-averaged structure.

The molar volume of $Y_{(1/3)}Cl$ is slightly larger than that of $Dy_{(1/3)}Cl$, whereas the cationic radius of the former is smaller than that of the latter. Even in this mixture system, the general rule holds that, with decreasing molar volume, the mobilities increase and that the increasing magnitude is greater for the smaller size cation[1].

The general factors (*i*) - (*iv*) given above for monovalent cations seem to hold also for the present III-III valent cation mixture systems. It would be impossible, however, to predict *a priori* from the ionic radii alone which of two cations in a charge-symmetric binary system is more mobile under given conditions. For example, comparison of the

potential profiles for Li^+ and K^+, shown in Fig. 3.20, cannot predict which SEV of the two cations is greater. Calculation of the SEV may be helpful for further microscopic insight into the internal mobilities in the present system.

3.4.3 Isotope effect

Figure 3.15 as well as Fig. 3.14 demonstrates that the species containing the lighter Dy isotopes migrates toward the cathode and is therefore cationic.

The mass effect, μ, defined as ε_M divided by the relative mass difference[32], has been calculated. The calculated values of μ are averaged for the $4\varepsilon_M$'s (M=160,161,163 and 164) at each electromigration, and given in Table 3.7. It seems that $|\mu|$ slightly increases with increasing temperature in the investigated range as in most of other salts[10],[44],[45], though the tendency is not so clear here, because of the experimental errors.

The mass effects of cations in various pure chloride melts so far studied[10] are plotted against the mass of the cations in Fig. 3.22. Empirical equations were presented for the mass effect of the cations in molten monovalent and divalent cation halides[46]:

$$\mu = -0.15/(1+M/2.1M_-) \tag{3.9a}$$

$$\mu = -0.079/(1+M/2.1M_-) \tag{3.9b}$$

where M- is the mass of the halide ion, that is 35.5 in the present case. For some divalent cations such as alkaline earth and Pb(II) ions eq.(3.9b) holds and for others eq. (3.9a) does. With increasing mass of the cation, the mass effect seems generally to decrease. This decrease is partly due to the decrease in the external transport number for the heavier cation. The relative difference in internal cation mobilities ε_c^i is related to the relative difference in external cation mobilities ε_c^e by

$$\varepsilon_c^i = t_c^e \varepsilon_c^e \tag{3.10}$$

where t_c^e is the external cation transport number. Equation (3.10) implies that the isotope effect on the internal cation mobilties ε_c^i is smaller with decreasing external cation transport number. However, it should be also kept in mind that external

transport numbers have been measured only for limited salts and are influenced by the nature of the external solid materials to some extent. External transport numbers of external mobilities cannot be measured by countercurrent electromigration. Convenient methods for measuring external transport numbers of pure molten salts are not available at present.

The electrically-conducting species in alkali halide melts such as LiCl and CsCl are conjectured from molecular dynamics simulation to be monovalent alkali metal ions and chloride ions[43]. The mass effect of the Dy is not particularly small as compared with those of other monovalent or divalent cations as seen from Fig. 3.22. The calculated values from the empirical relations (3.9a) and (3.9b) (eq. (3.9)) are -0.047 and -0.025, respectively; the present experimental value -0.032 is between these two and not so different from these. Thus, the main electrically-conducting species in $DyCl_3$ melt are also conjectured to be trivalent cations, Dy^{3+}, and therefore chloride ions Cl^-. However, the lifetime of such electrically-conducting species as Dy^{3+} is assumed to be short and of a ps order. This needs to be clarified by molecular dynamics simulation.

Similar situation was found for molten zinc chloride; whereas the existing species, from spectroscopy and diffraction studies, appear to be chains of chloride tetrahedra about Zn cations[47),(48)], the electrically-conducting species are Zn^{2+} and chloride ions, as is shown by the isotope effect[49].

Table 3.1 Some properties of pure $Y_{(1/3)}Cl$, $La_{(1/3)}Cl$ and $Dy_{(1/3)}Cl$.

Rare earth chloride	$Y_{(1/3)}Cl$	$La_{(1/3)}Cl$	$Dy_{(1/3)}Cl$
Atomic number of cation	39	57	66
Atomic weight of cation	88.9095	138.9055	162.50
Cationic radius, pm	90.0[50]	103.2[50]	91.2[50]
Crystal structure type	$AlCl_3$[51]	UCl_3[51]	$AlCl_3$[51]
Coodination number of cation in the crystal solid	6	9	6
Coodination number of cation in the melt	~6[19],[23]	~6[22]	~6[20],[21]
Melting point, K	987[52]	1150[52]	928[52]
Charge in molar volume on melting, %	0.45[52]	19.4[52]	0.32[52]
Molar volume at 1073 K, 10^{-6} m^3 mol^{-1}	25.46[52]	25.00[52]	25.36[52]
Conductivity at 1073 K, S m^{-1}	51.2	110.7[53]	56.2

Table 3.2 Parameters of electric conductivity; $\kappa = -A + BT$.

(a) $(Y, La)_{(1/3)}Cl$

x_{La}	A(S m^{-1})	B(S m^{-1} K^{-1})	Standard deviation (S m^{-1})
0	162.1	0.1988	0.1
0.102	160.8	0.2030	0.3
0.207	154.8	0.2048	0.2
0.493	146.6	0.2122	0.2
0.601	178.5	0.2460	0.1

(b) $(Y, Dy)_{(1/3)}Cl$

x_{Dy}	A(S m^{-1})	B(S m^{-1} K^{-1})	Standard deviation (S m^{-1})
0.251	161.5	0.2004	0.1
0.501	155.4	0.1958	0.1
0.784	142.8	0.1848	0.2
0.901	145.4	0.1876	0.3
1	143.7	0.1863	0.2

Table 3.3

Experimental conditions and ε in the molten system (Ca, Ba)$_{(1/2)}$Cl at 973 K (a) and 1073 K (b).

Run No.	x_{Ba}	Q(C)	ε
(a)			
1	0.255±0.001	1124.1	-0.029±0.005
2	0.257±0.001	920.4	-0.034±0.004
3	0.320±0.002	2602.2	-0.034±0.002
4	0.323±0.001	1533.3	-0.035±0.004
5	0.347±0.000	1310.0	-0.042±0.008
6	0.365±0.001	1806.9	-0.044±0.005
7	0.366±0.000	1311.4	-0.025±0.000
8	0.418±0.001	2576.3	-0.035±0.001
9	0.437±0.001	2258.1	-0.035±0.001
10	0.450±0.001	1111.1	-0.060±0.008
11	0.509±0.002	1382.3	-0.044±0.002
(b)			
1	0.033±0.001	2231.8	-0.041±0.003
2	0.033±0.002	1530.6	-0.050±0.002
3	0.055±0.001	2213.8	-0.037±0.001
4	0.099±0.000	1337.3	-0.045±0.002
5	0.106±0.001	1555.2	-0.043±0.001
6	0.134±0.001	2033.4	-0.047±0.002
7	0.164±0.001	2203.6	-0.051±0.003
8	0.184±0.001	803.9	-0.046±0.003

(Table 3.3 continued)

9	0.339±0.000	1602.8	-0.055±0.002
10	0.445±0.000	1158.0	-0.051±0.001
11	0.614±0.001	1010.3	-0.053±0.002

Table 3.4

Experimental conditions and ε in the molten systems $(Y, La)_{(1/3)}Cl$ (a) and $(Y, Dy)_{(1/3)}Cl$ (b) at1073 K.

(a)$(Y, La)_{(1/3)}Cl$

Run No.	x_{La}	Q(C)	ε
a-1	0.104±0.008	1746	-0.169±0.019
a-2	0.231±0.006	1729	-0.192±0.006
a-3	0.276±0.011	1443	-0.211±0.013
a-4	0.387±0.008	1428	-0.268±0.018
a-5	0.512±0.004	1124	-0.206±0.014
a-6	0.608±0.008	3011	-0.196±0.006

(b)$(Y, Dy)_{(1/3)}Cl$

Run No.	x_{Dy}	Q(C)	ε
b-1	0.150±0.004	3236	0.040±0.003
b-2	0.277±0.001	1233	0.095±0.004
b-3	0.546±0.004	2536	0.046±0.003
b-4	0.556±0.003	2270	0.077±0.003
b-5	0.773±0.005	2065	0.078±0.003

Table 3.5 Internal mobilities of Ca^{2+} and Ba^{2+} in the molten system $(Ca, Ba)_{(1/2)}Cl$ at 973 K (a) and 1073 K (b).

Run No.	x_{Ba}	$\kappa \cdot 10^2$ (S m^{-1})	$V_m \cdot 10^6$ (m^3 mol^{-1})	$u_{Ba} \cdot 10^8$ (m^2 V^{-1} s^{-1})	$u_{Ca} \cdot 10^8$ (m^2 V^{-1} s^{-1})
(a)					
1	0.255	1.44	27.46	4.20±0.08	4.08±0.01
2	0.257	1.44	27.48	4.21±0.07	4.09±0.01
3	0.320	1.41	27.78	4.16±0.04	4.02±0.01
4	0.323	1.41	27.79	4.16±0.06	4.02±0.01
5	0.347	1.40	27.91	4.16±0.08	3.99±0.02
6	0.365	1.39	28.00	4.15±0.07	3.98±0.01
7	0.366	1.39	28.00	4.11±0.02	4.00±0.00
8	0.418	1.37	28.25	4.10±0.03	3.96±0.01
9	0.437	1.36	28.34	4.08±0.02	3.95±0.01
10	0.450	1.36	28.41	4.13±0.07	3.89±0.02
11	0.509	1.34	28.69	4.06±0.03	3.89±0.01
(b)					
1	0.033	1.92	26.93	5.56±0.08	5.34±0.00
2	0.033	1.92	26.93	5.61±0.08	5.34±0.00
3	0.055	1.90	27.04	5.51±0.07	5.32±0.00
4	0.099	1.87	27.26	5.50±0.08	5.27±0.00
5	0.106	1.87	27.29	5.48±0.06	5.26±0.00
6	0.134	1.85	27.43	5.47±0.08	5.23±0.01
7	0.164	1.83	27.58	5.46±0.08	5.19±0.01
8	0.184	1.82	27.68	5.42±0.08	5.18±0.00

(Table 3.5 continued)

9	0.339	1.74	28.44	5.30±0.05	5.02±0.01
10	0.445	1.69	28.96	5.21±0.04	4.95±0.01
11	0.614	1.62	29.80	5.10±0.03	4.84±0.02

Table 3.6 Internal mobilities in the molten systems $(Y, La)_{(1/3)}Cl$ (a) and $(Y, Dy)_{(1/3)}Cl$ (b) at1073 K.

(a)$(Y, La)_{(1/3)}Cl$

Run No.	x_{La}	κ (S m^{-1})	$V_m \cdot 10^6$ (m^3 mol^{-1})	$u_Y \cdot 10^8$ (m^2 V^{-1} s^{-1})	$u_{La} \cdot 10^8$ (m^2 V^{-1} s^{-1})
	0	51.2	25.46	1.35	
a-1	0.104	57.8	25.42	1.50±0.00	1.75±0.03
a-2	0.231	65.2	25.36	1.64±0.00	1.97±0.01
a-3	0.276	67.8	25.34	1.68±0.01	2.05±0.02
a-4	0.387	73.9	25.28	1.74±0.01	2.25±0.02
a-5	0.512	81.7	25.22	1.91±0.01	2.35±0.01
a-6	0.608	87.3	25.18	2.01±0.01	2.45±0.01
	1	(111)[a]	(25.00)[a]		2.88

[a]Extrapolated values with respect to temperature[53].

(b)$(Y, Dy)_{(1/3)}Cl$

Run No.	x_{Dy}	κ (S m^{-1})	$V_m \cdot 10^6$ (m^3 mol^{-1})	$u_Y \cdot 10^8$ (m^2 V^{-1} s^{-1})	$u_{Dy} \cdot 10^8$ (m^2 V^{-1} s^{-1})
b-1	0.150	52.3	25.45	1.39±0.00	1.33±0.00
b-2	0.277	52.9	25.43	1.43±0.00	1.30±0.00
b-3	0.546	54.2	25.41	1.46±0.00	1.40±0.00
b-4	0.556	54.2	25.40	1.49±0.00	1.38±0.00
b-5	0.773	55.2	25.38	1.54±0.00	1.43±0.00
	1	56.2	25.36		1.48

The sign ± represents the standard deviation.

Table 3.7 Main experimental conditions and the results of electromigration.

Run No.		1	2	3	4	5
Electric current (mA)		300	100	200	200	200
Voltage (V)		180~210	60~75	80~110	190~200	200~220
Duration (hr)		22	64	40	43	26
Transported charge (C)		22740	22757	28014	29812	18235
Temperature (K)		1073±3	973±3	973±2	1023±2	1043±2
Separation tube						
length (mm)		152	150	100+30+20[a)]	200	200
int. diam. (mm)		4	4	4+8+4[a)]	4	4
$\varepsilon \cdot 10^4$	M=160	3.3±0.2	3.5±0.3	3.2±0.8	2.9±0.2	4.1±0.1
	161	2.2±0.2	2.3±0.4	2.1±0.7	2.2±0.2	2.0±0.1
	163	-1.9±0.2	-2.0±0.3	-2.0±0.6	-1.8±0.1	-1.9±0.1
	164	-3.9±0.1	-5.1±0.4	-5.2±0.3	-3.5±0.2	-3.8±0.1
$-\mu$		0.030	0.035	0.034	0.029	0.032

[a)]From the anode side, the tube was made of three parts fused together, of 4, 8, and 4 mm internal diameters and 100, 30, and 20 mm in length, respectively.

Table 3.8 Parameters for u in Eq. (3.1) in the molten $(Ca, Ba)_{(1/2)}Cl$.

Cation	A	E	V_0
	(10^{-12} m^5 V^{-1} s^{-1} mol^{-1})	(kJ mol^{-1})	(10^{-6} m^3 mol^{-1})
Ca	1.22	19.1	-0.961(973 K)
			-0.837(1073 K)
Ba	1.36	18.4	-5.769(973 K)
			-4.121(1073 K)

Table 3.9 Values of mass effect μ in the molten binary system at various compositions at 1073 K.

Run no	b-1	b-2	b-3	b-4	b-5	*
x_{Dy}	0.150	0.277	0.546	0.556	0.773	1
$-\mu$	0.017	0.16	0.079	0.13	0.13	0.032

*Measured for the Dy isotopes in pure $Dy_{(1/3)}Cl$ melt.

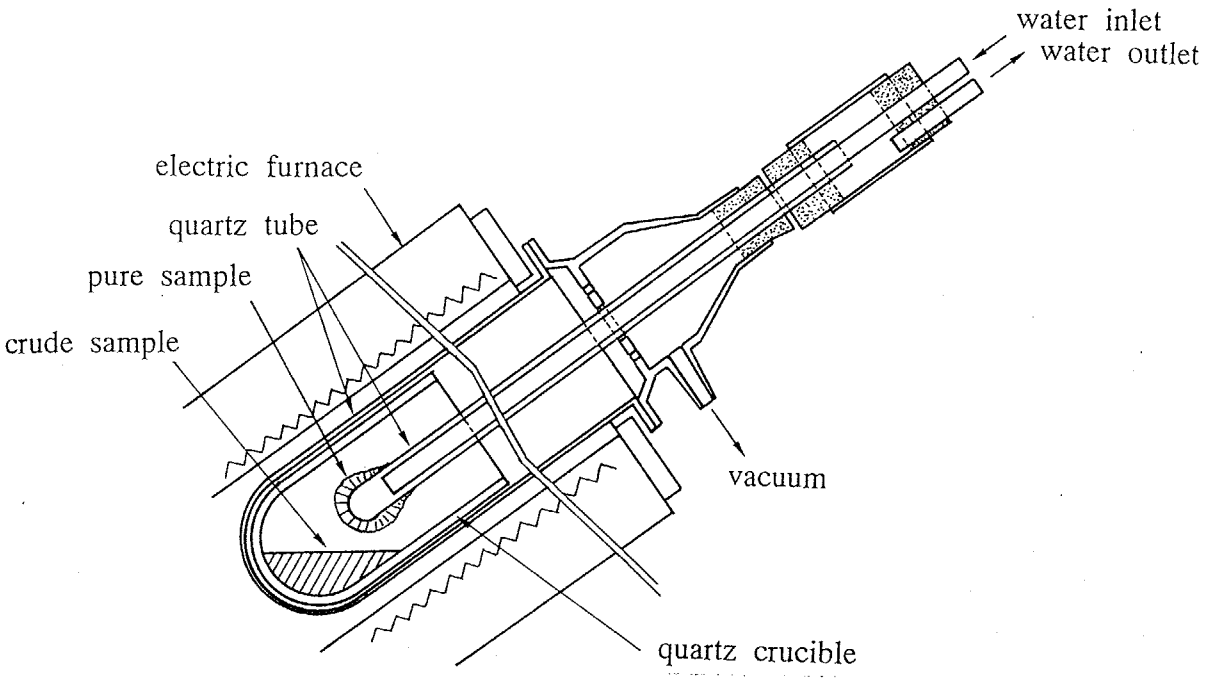

Fig. 3.1 Apparatus for sublimation of rare earth chlorides.

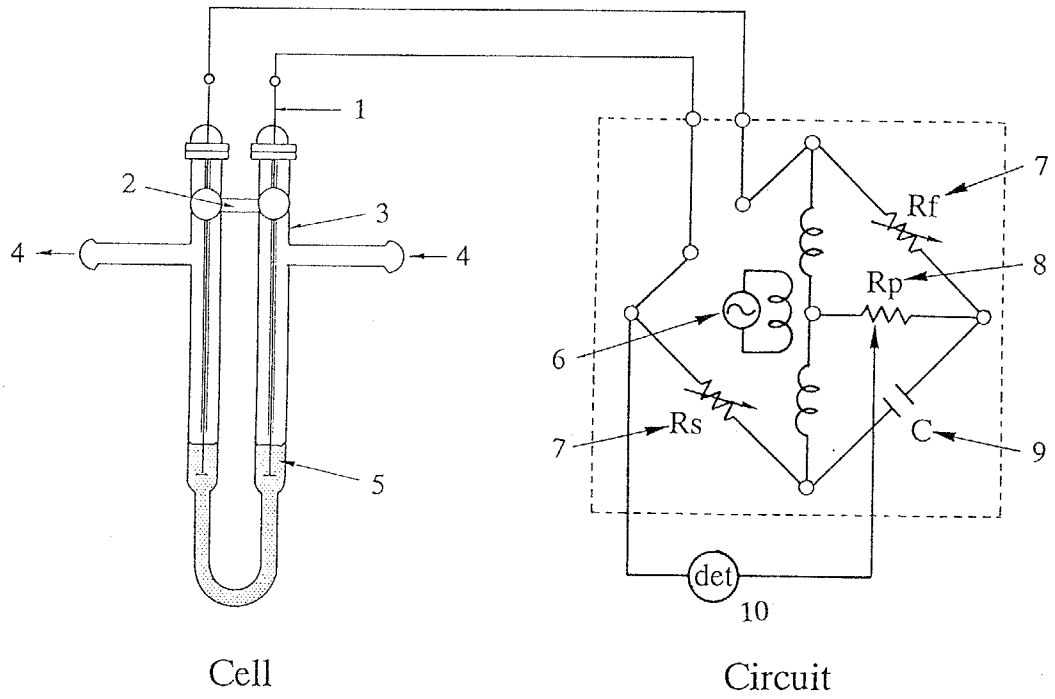

Fig. 3.2 Schematic diagram for the electric conductivity measurement: the cell and circuit. 1, Pt electrode; 2, gas bypath; 3, U-shaped quartz cell; 4, Ar gas; 5, sample melt; 6, function generator; 7, variable resistor; 8, resistor; 9, capacitor; 10, synchroscope for zero detection.

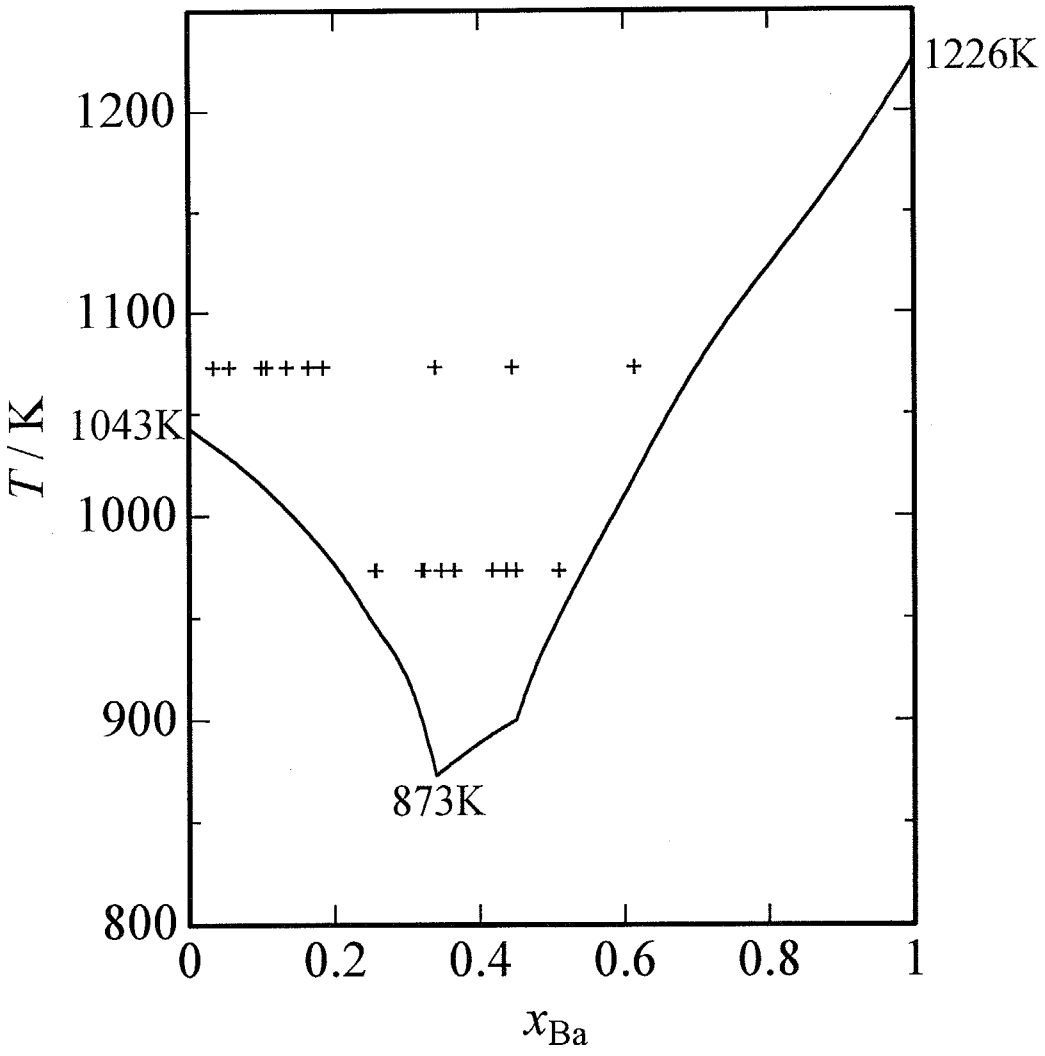

Fig. 3.3 Concentration and temperature ranges of the measurements of ε for the system $(Ca, Ba)_{(1/2)}Cl$[27].

+: measured points.

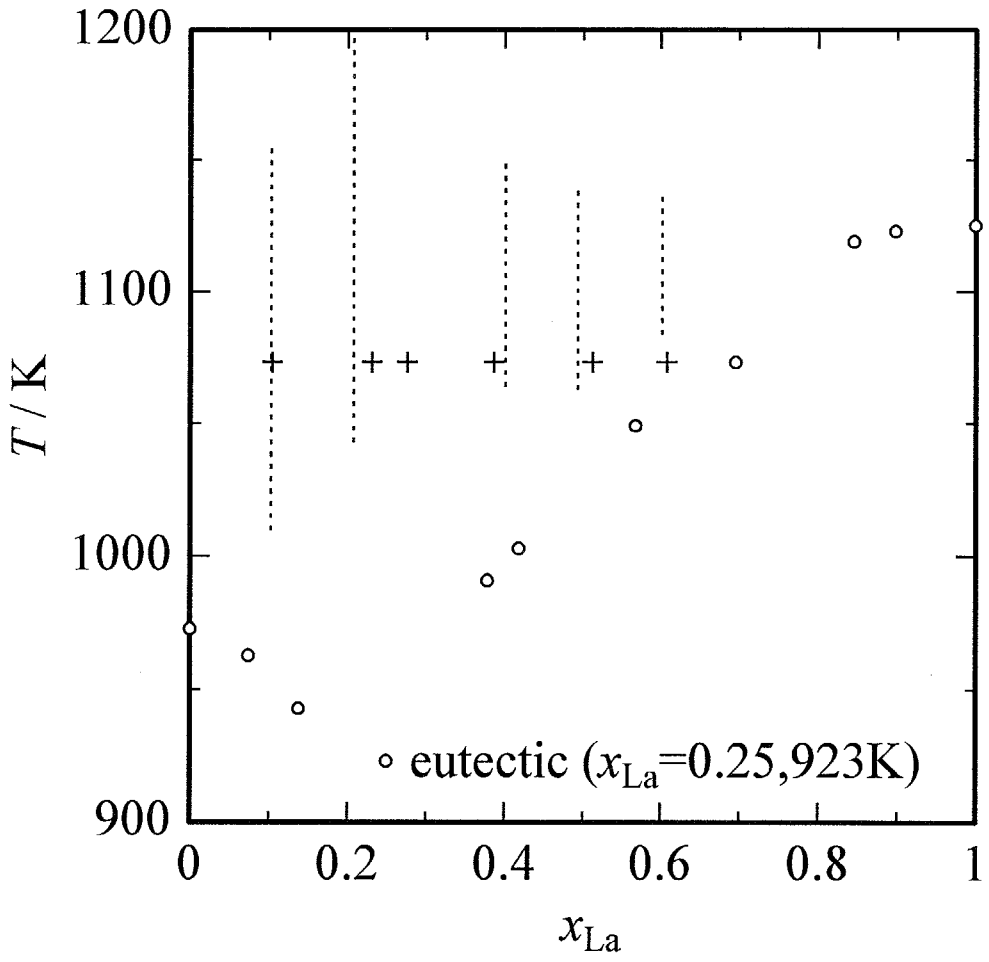

Fig. 3.4 Concentration and temperature ranges of the measurements of ε for the system $(Y, La)_{(1/3)}Cl$[28].

+: measured points.

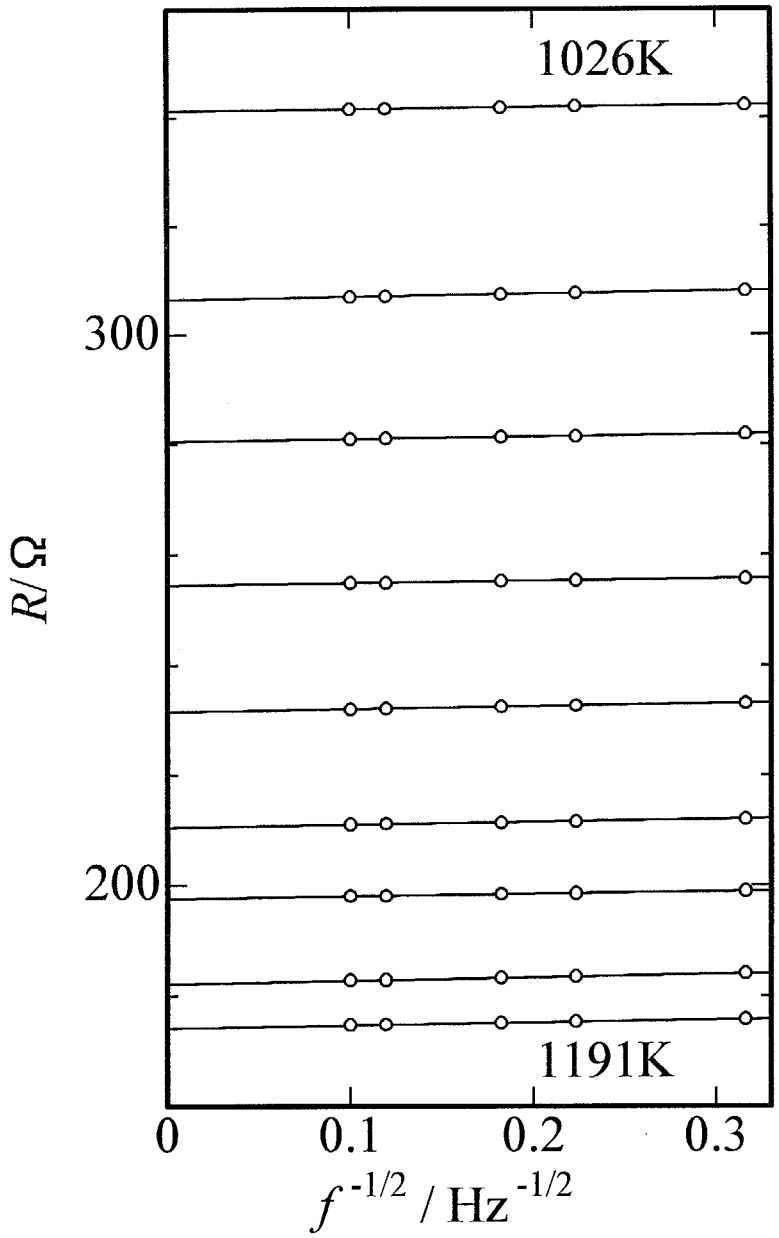

Fig. 3.5 Frequency dependence of resistance measured.

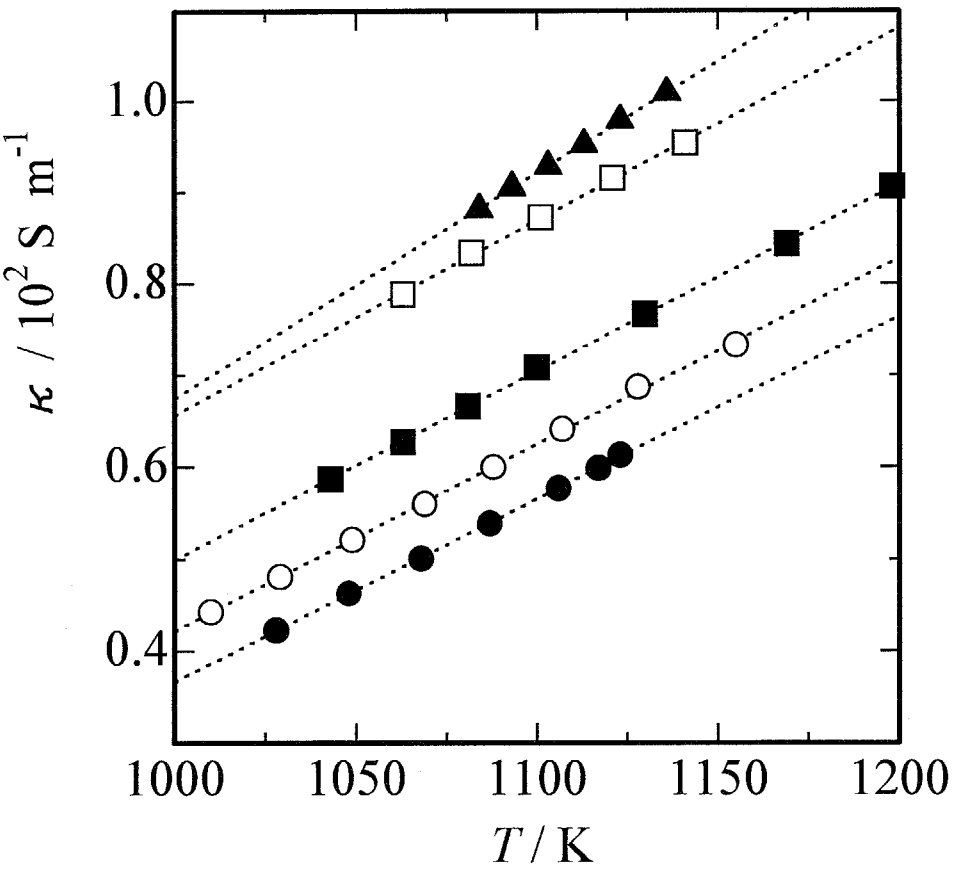

Fig. 3.6 Temperature dependence of electric conductivities in the molten system (Y, La)$_{(1/3)}$Cl

●: pure $Y_{(1/3)}Cl$; ○: x_{La}=0.102; ■: x_{La}=0.207; □: x_{La}=0.493; ▲: x_{La}=0.601.

The dotted lines are drawn by the equation with the parameters in Table 3.2.

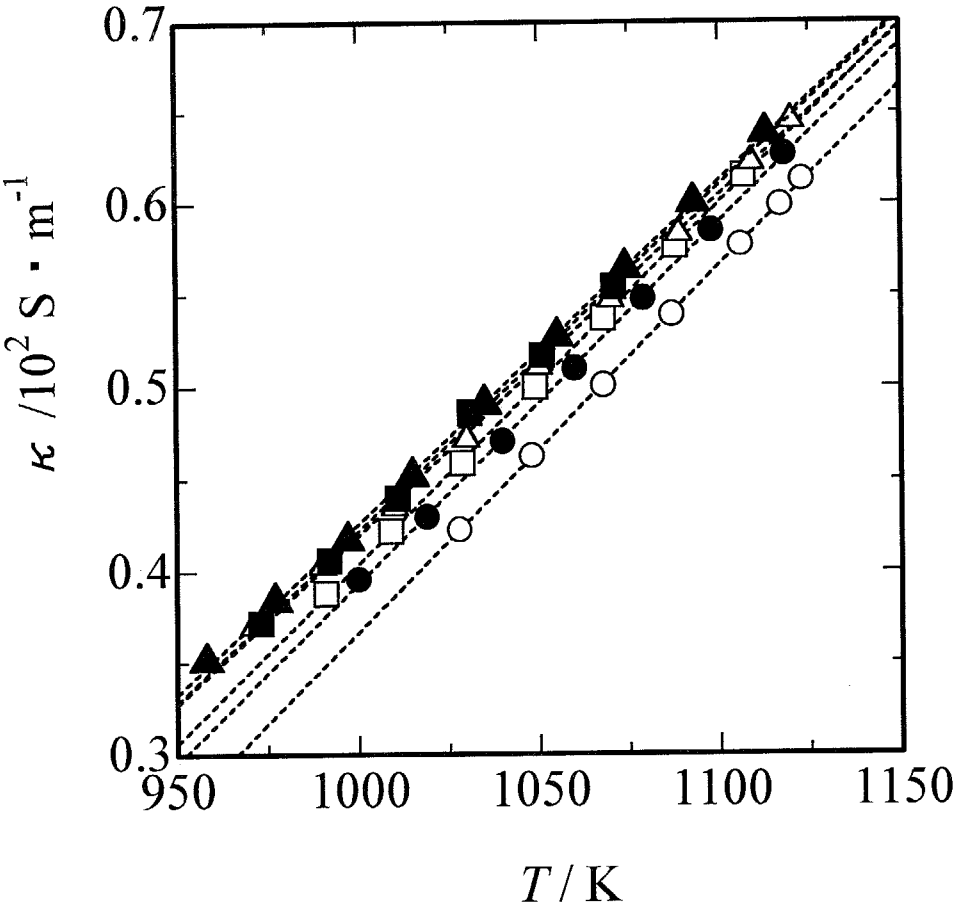

Fig. 3.7 Temperature dependence of electric conductivities in the molten system (Y, Dy)$_{(1/3)}$Cl

●: pure $Y_{(1/3)}Cl$; ○: x_{Dy}=0.251; ■: x_{Dy}=0.501; □: x_{Dy}=0.784; ▲: x_{Dy}=0.901; △: pure $Dy_{(1/3)}Cl$.

The dotted lines are drawn by the equation with the parameters in Table 3.2.

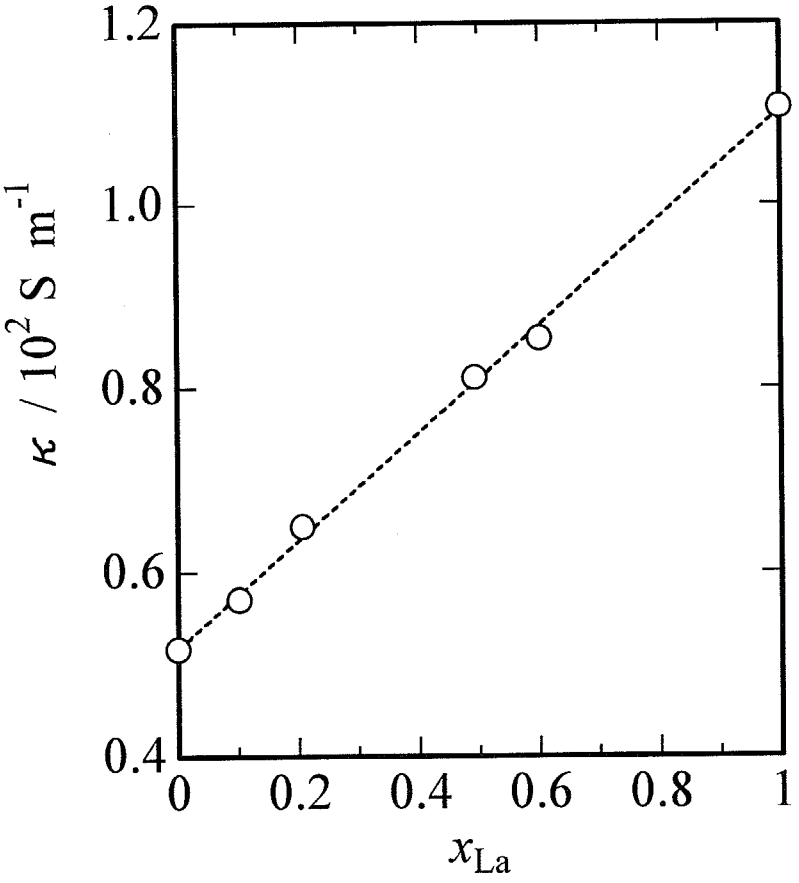

Fig. 3.8 Isotherms of the electric conductivity at 1073 K in the molten system (Y, La)$_{(1/3)}$Cl. The value for pure La$_{(1/3)}$Cl shown in parentheses is extrapolated from that for the melt[53] with respect to temperature. The dashed line is drawn by a least squares fit: $\kappa / \mathrm{S\ m^{-1}} = 51.7 + 58.5 x_{\mathrm{La}}$.

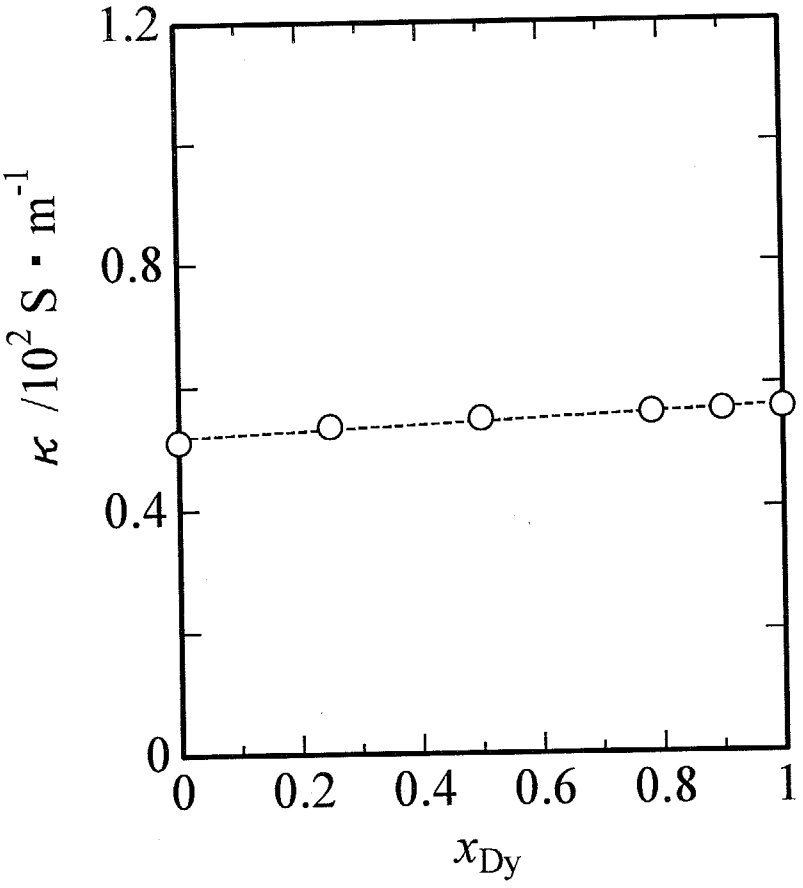

Fig. 3.9 Isotherms of the electric conductivity at 1073 K in the molten system (Y, Dy)$_{(1/3)}$Cl. The dashed line is drawn by a least squares fit: $\kappa / \mathrm{S\ m^{-1}} = 51.8 + 4.64 x_{\mathrm{Dy}}$.

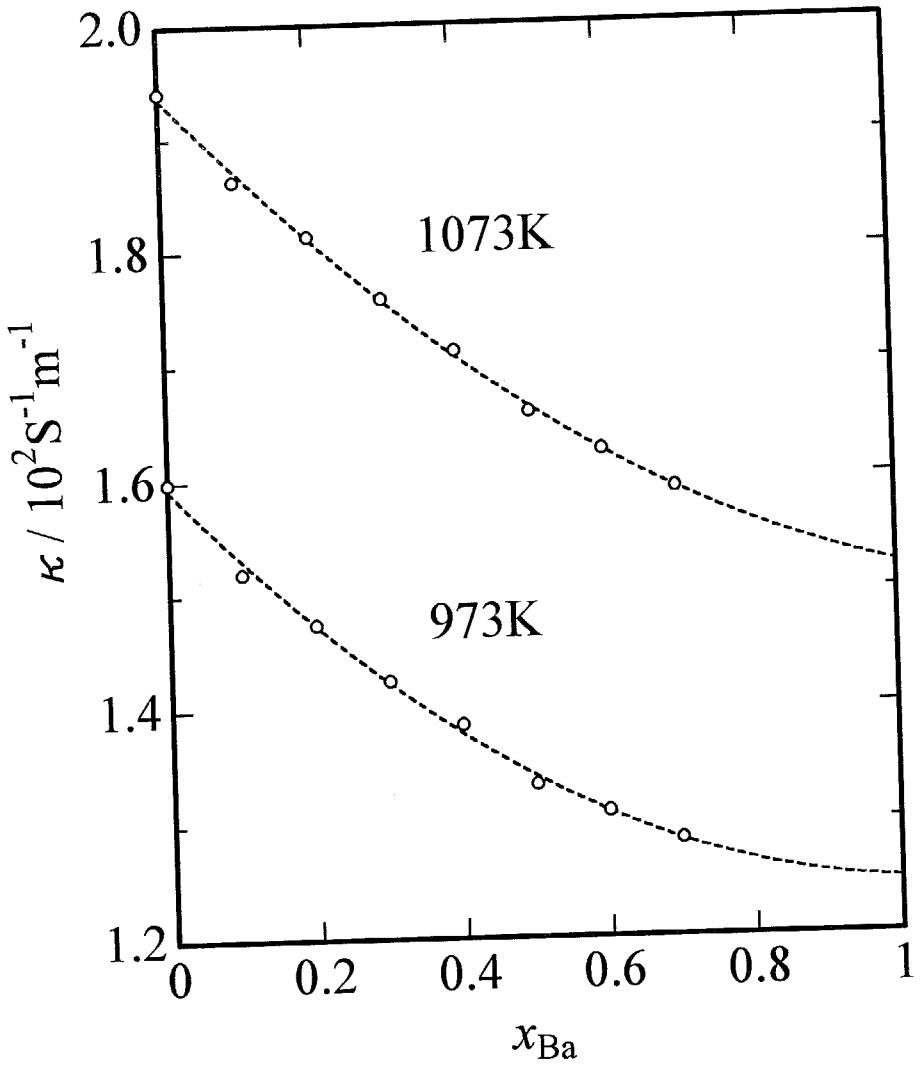

Fig. 3.10 Isotherm of the electric conductivity at 973 K and at 1073 K in the molten system (Ca, Ba)$_{(1/2)}$Cl[31]. The dashed line is drawn by a least squares fit:

$\kappa / \mathrm{S\ m^{-1}} = 159 - 66.7x_{\mathrm{Ba}} + 32.0x_{\mathrm{Ba}}^2$.(973 K)

$\kappa / \mathrm{S\ m^{-1}} = 194 - 68.2x_{\mathrm{Ba}} + 26.6x_{\mathrm{Ba}}^2$.(1073 K)

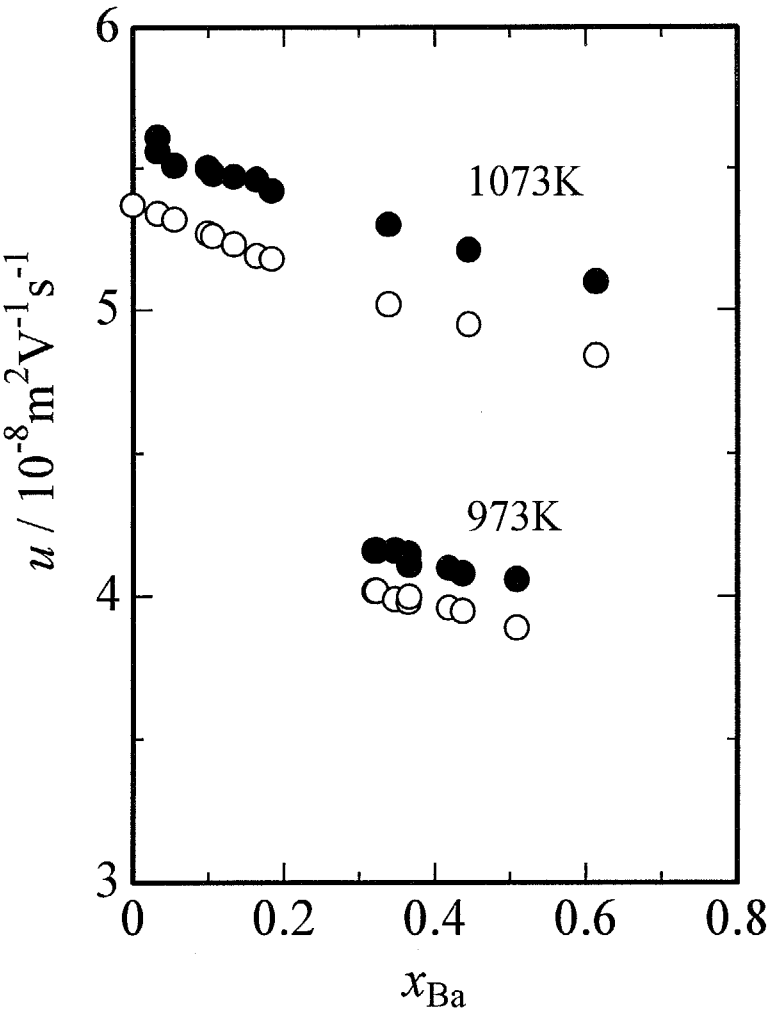

Fig. 3.11 Internal cation mobilities in the molten system (Ca, Ba)$_{(1/2)}$Cl at 973 K and 1073 K.

○:u_{Ca}; ●:u_{Ba}.

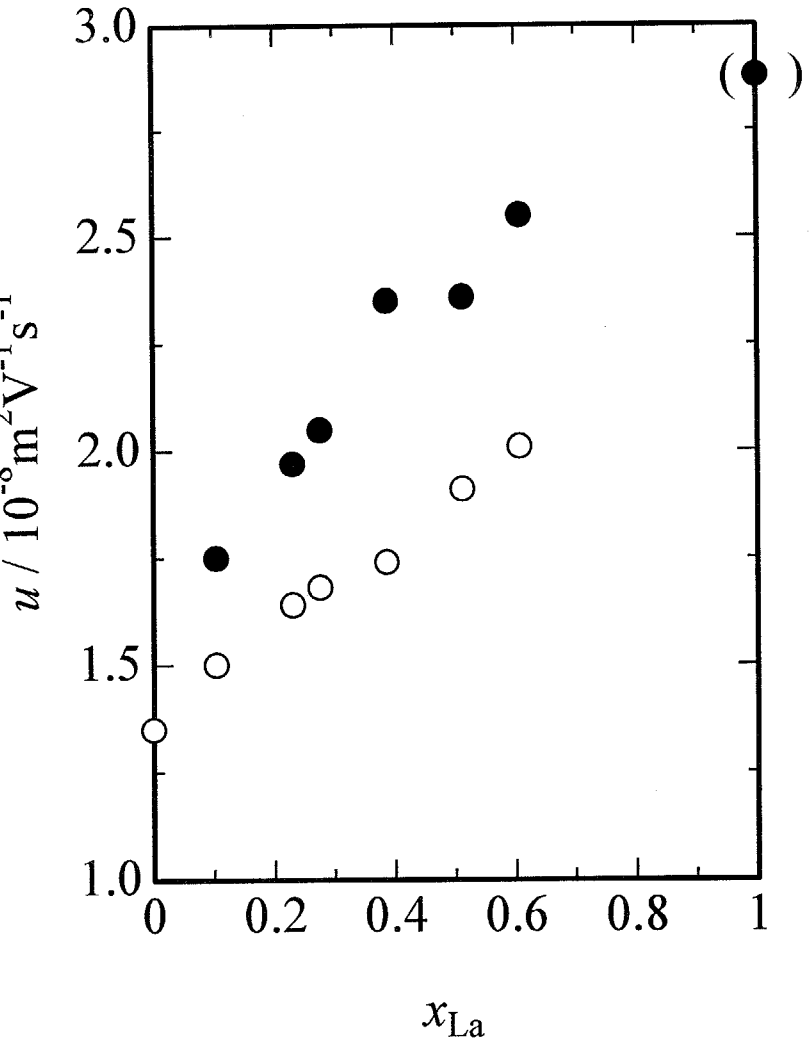

Fig. 3.12 Isotherms of u_Y and u_{La} in the molten system $(Y, La)_{(1/3)}Cl$ at 1073 K.

For pure $La_{(1/3)}Cl$, see the legend of Fig. 3.8.

○:u_Y, ●:u_{La}.

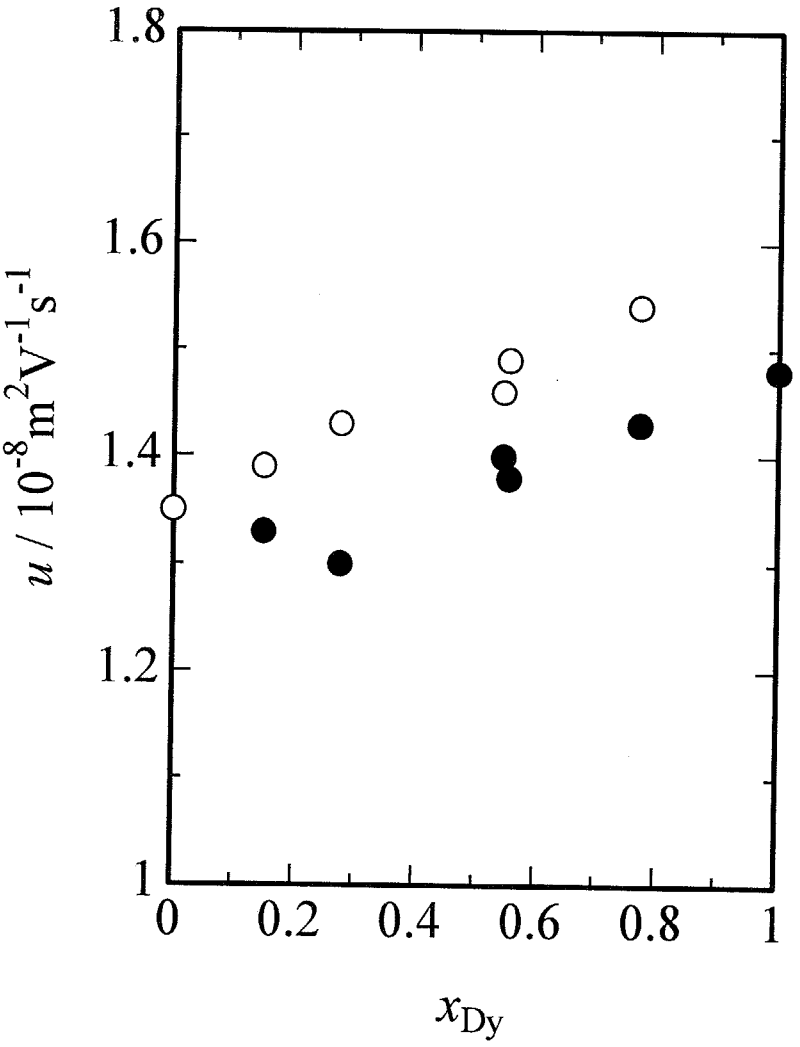

Fig. 3.13 Isotherms of u_Y and u_{Dy} in the molten system $(Y, Dy)_{(1/3)}Cl$ at 1073 K.

○:u_Y, ●:u_{Dy}.

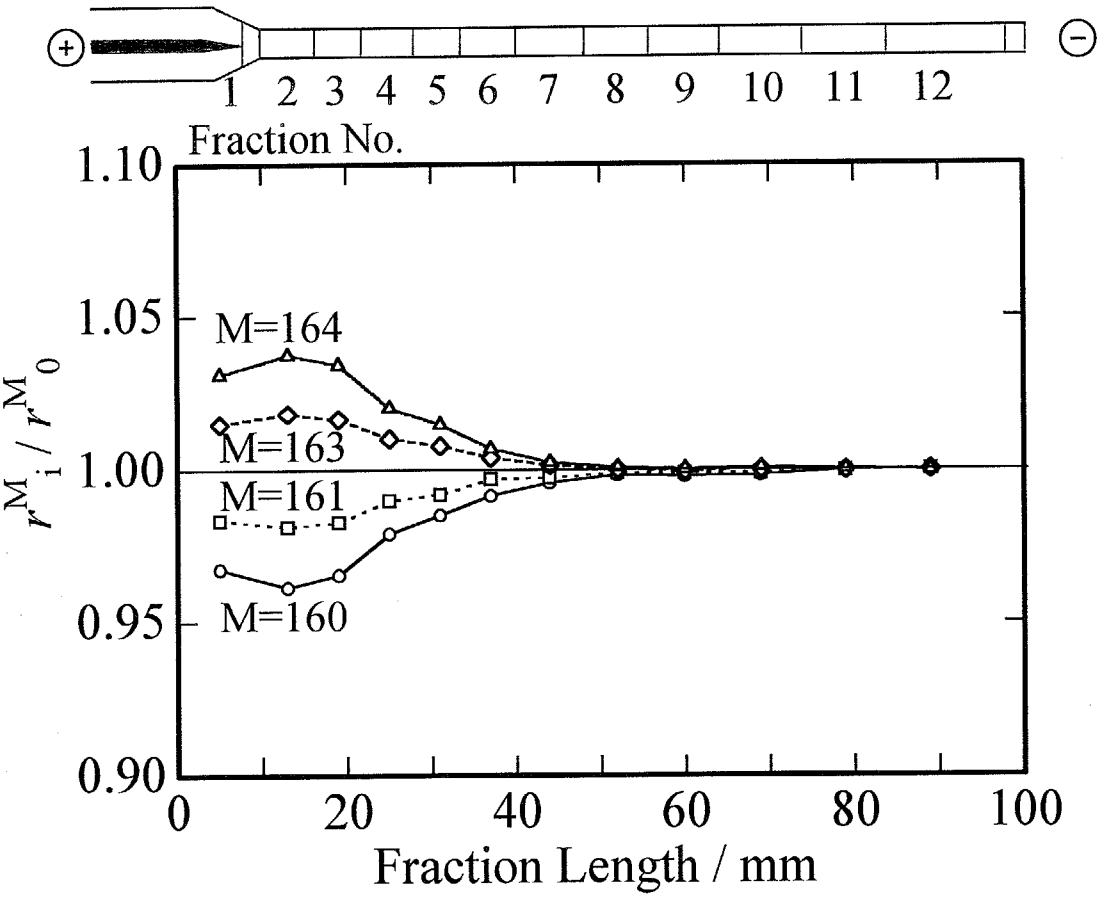

Fig. 3.14 Distribution of Dy isotopes in the separation tube (Run. No. 4)

$r_i^M = x_i^M / x_i^{162}$, $r_0^M = x_0^M / x_0^{162}$.

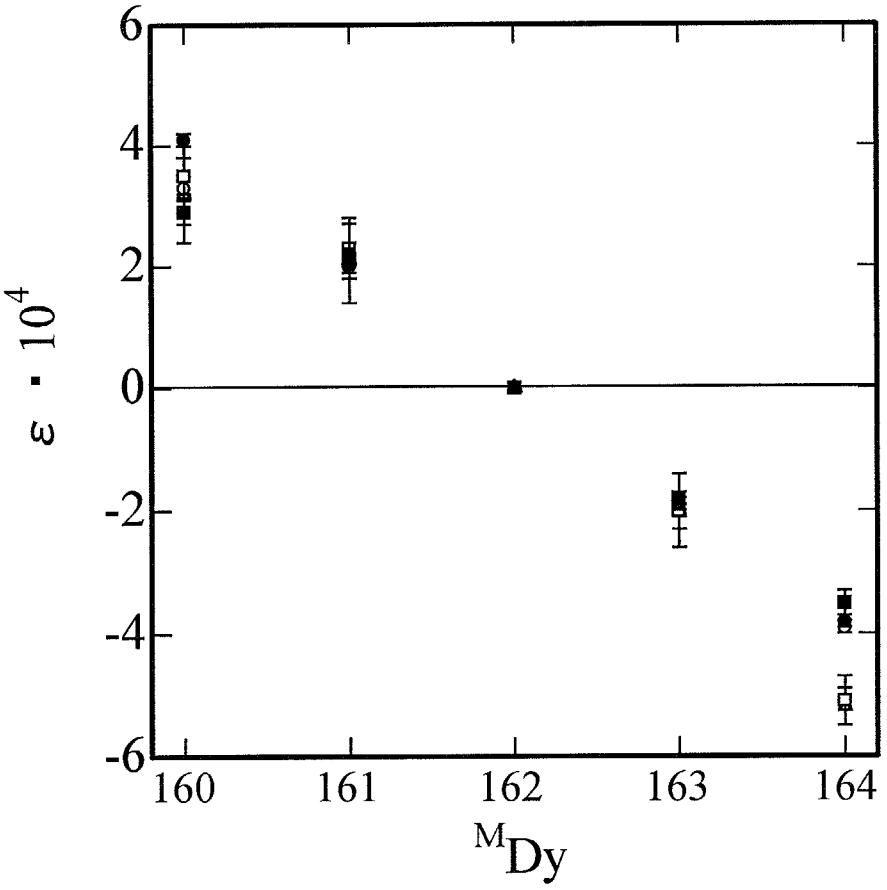

Fig. 3.15 The isotope effect of internal mobilities of Dy in molten $Dy_{(1/3)}Cl$

○: Run 1; □: Run 2; △: Run 3; ●: Run 4; ■: Run 5.

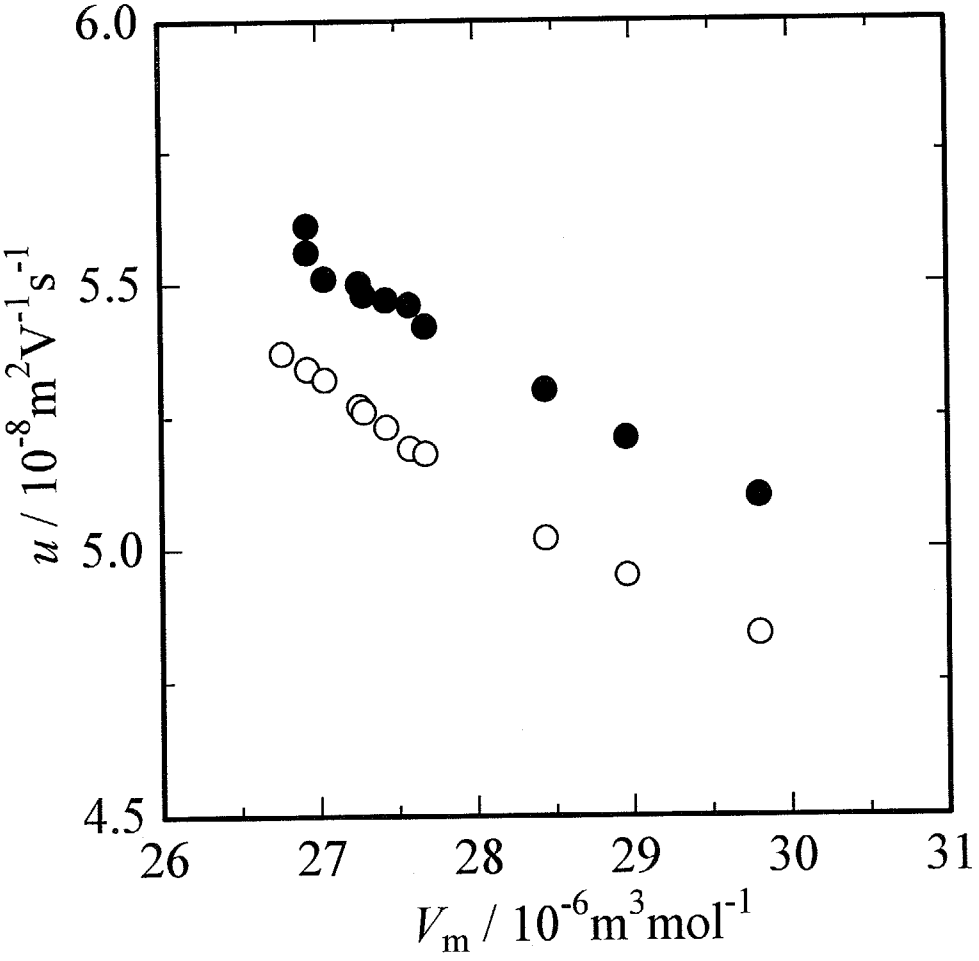

Fig. 3.16 u_{Ca} and u_{Ba} at 1073 K *vs.* molar volume.

○: u_{Ca}; ●:u_{Ba}

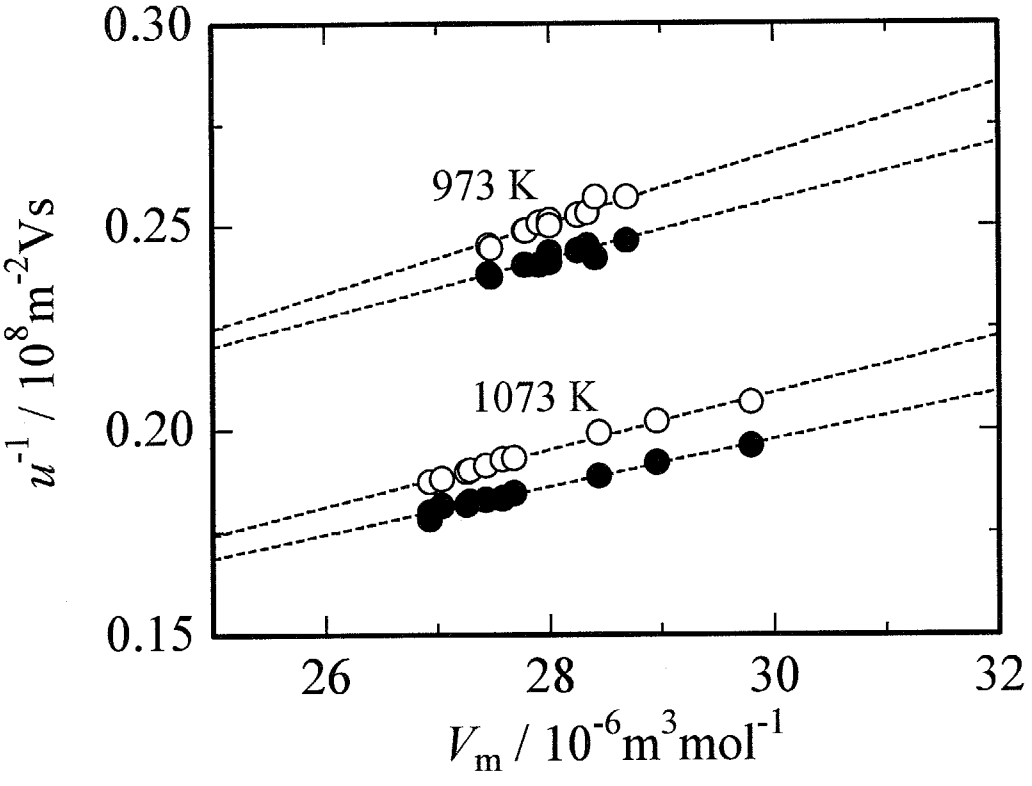

Fig. 3.17 The reciprocal of mobilities in the molten system $(Ca, Ba)_{(1/2)}Cl$ at 973 K and 1073 K.

○:u_{Ca}^{-1}; ●:u_{Ba}^{-1}.

The dashed lines are drawn according to (3.1) with the parameters in Table 3.8.

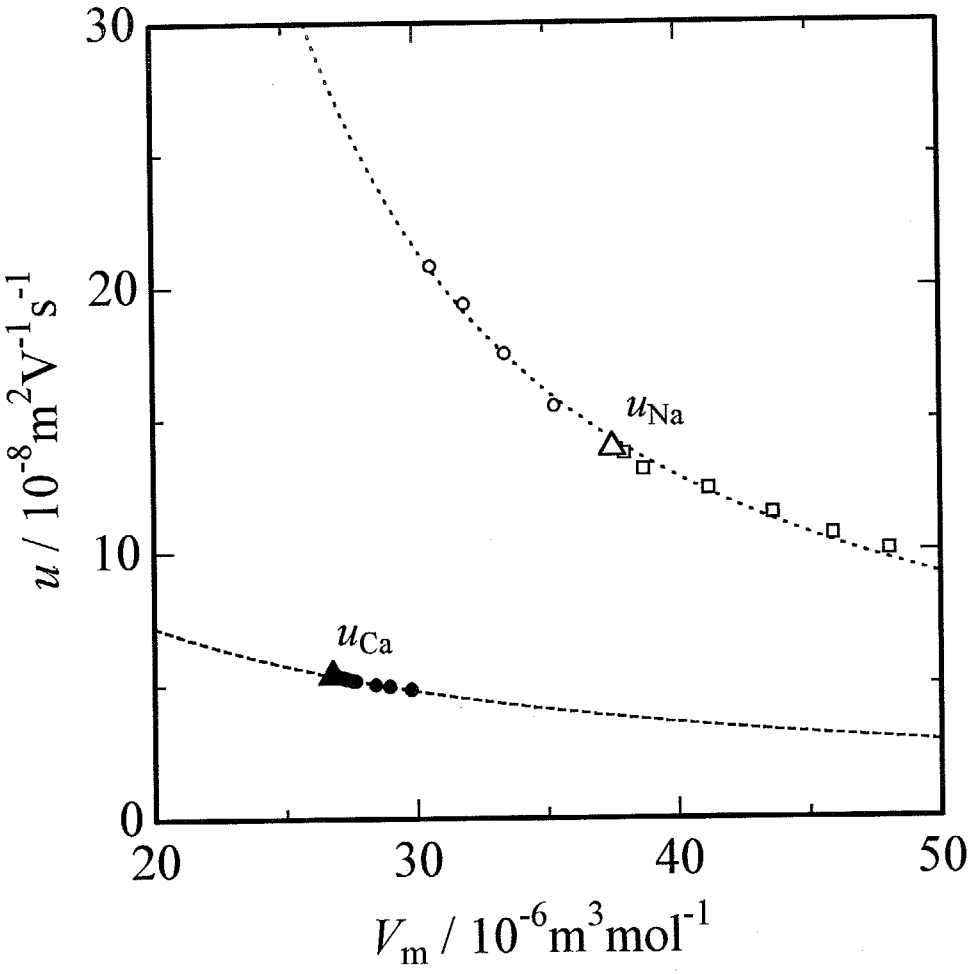

Fig. 3.18 Internal cation mobilities of Na^+ and Ca^{2+} at 1073 K *vs.* molar volume.

●: u_{Ca}(this work); ▲: pure u_{Ca}; ○, □: u_{Na} in the system (M, Na)Cl (M=Li and K)[2]; △: pure u_{Na}. The dotted lines are drawn by a least squares fit of the form of (3.1). As for the dashed line, see the legend of Fig. 3.17.

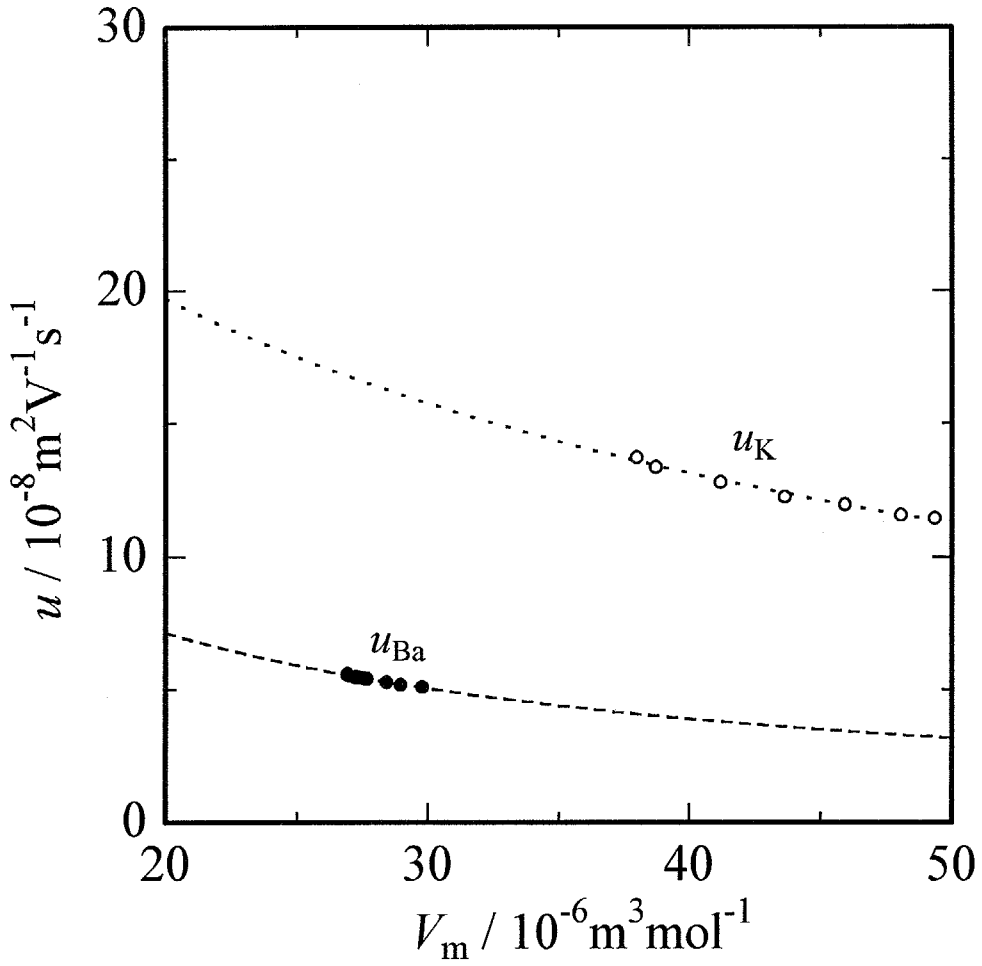

Fig. 3.19 Internal caiton mobilities of K^+ and Ba^{2+} at 1073 K *vs.* molar volume.

●: u_{Ba}(this work); ○: u_K in the system (Na, K)Cl[2]. As for the dotted and dashed lines, see the legend of Figure 3.18.

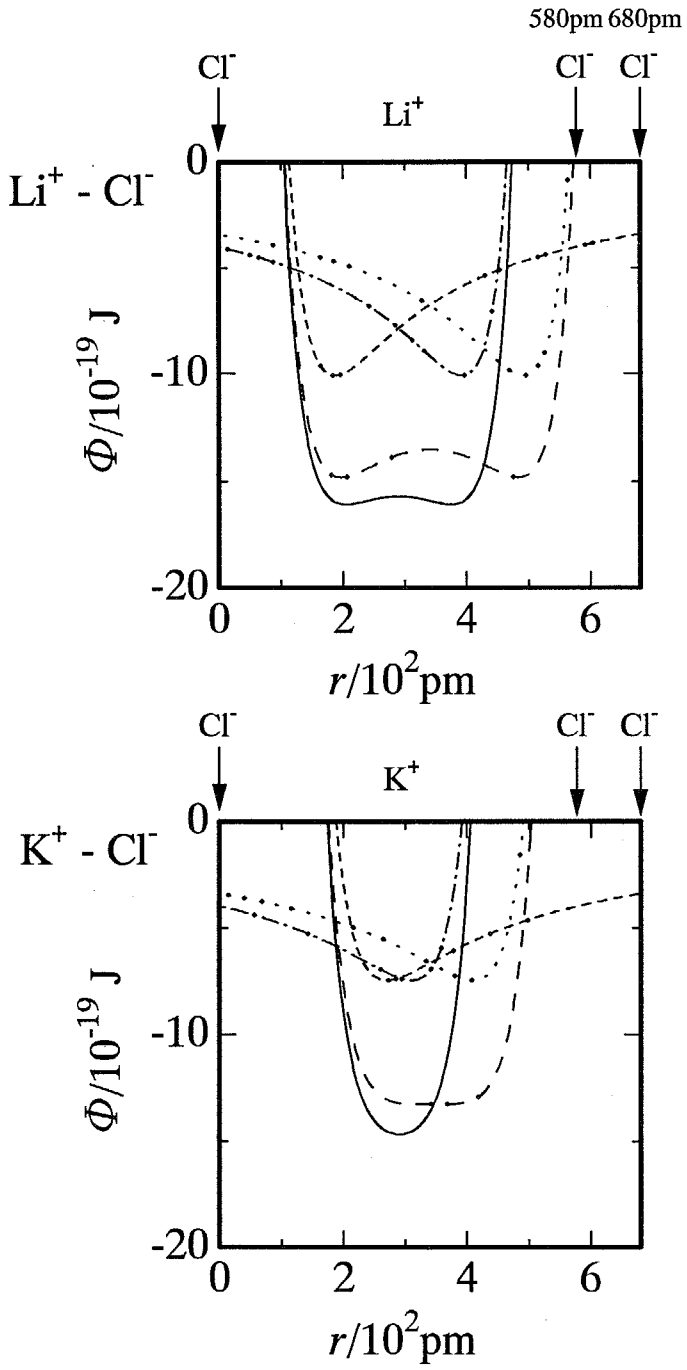

Fig. 3.20 Potentials felt by Li^+ and K^+ ions located collinearly between two Cl^- ions. These potentials are obtained by superposition of the pair potentials[42] shown here. The magnitude of one-dimensional kinetic energy at 1000 K is given for comparison. The separating motion of the cations located at the arrowed position from the referenced Cl^- ion (left-hand side one) during the process of the varying Cl^-—Cl^- distances is considered.

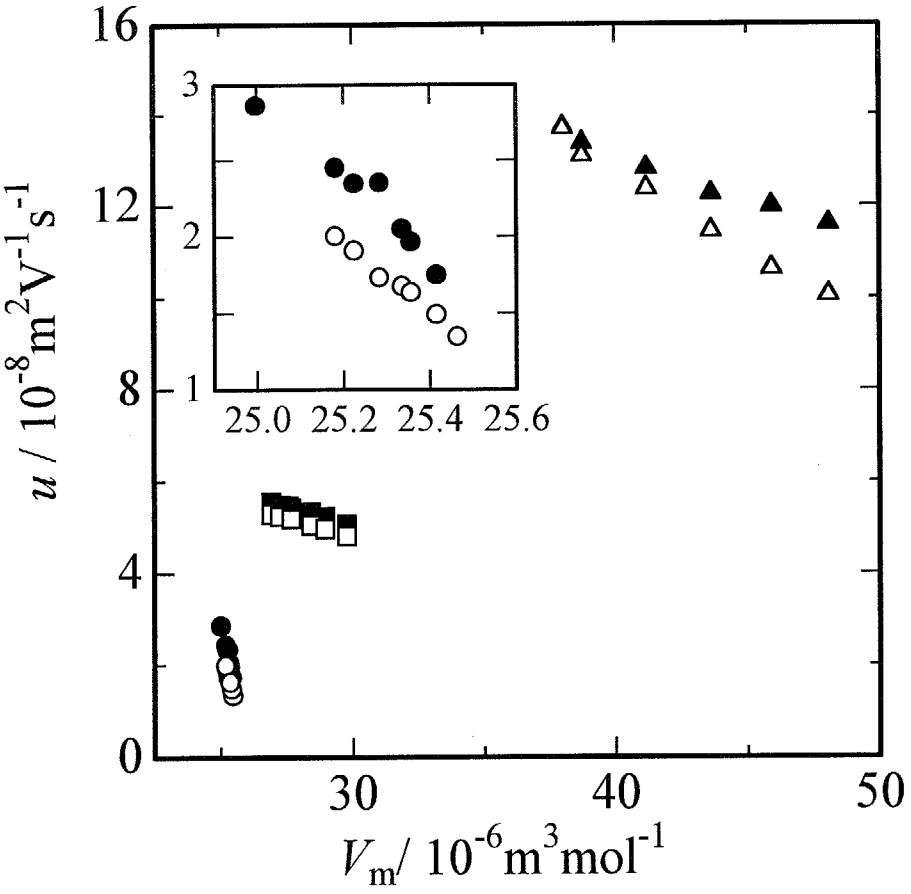

Fig. 3.21 Internal cation mobilities *vs.* molar volume at 1073 K in some molten binary systems. In the inset the values in the molten system $(Y, La)_{(1/3)}Cl$ are shown. △: u_{Na}, ▲: u_K in (Na, K)Cl[2]. □: u_{Ca}, ■: u_{Ba} in $(Ca, Ba)_{(1/2)}Cl$. ○: u_Y, ●: u_{La} in $(Y, La)_{(1/3)}Cl$.

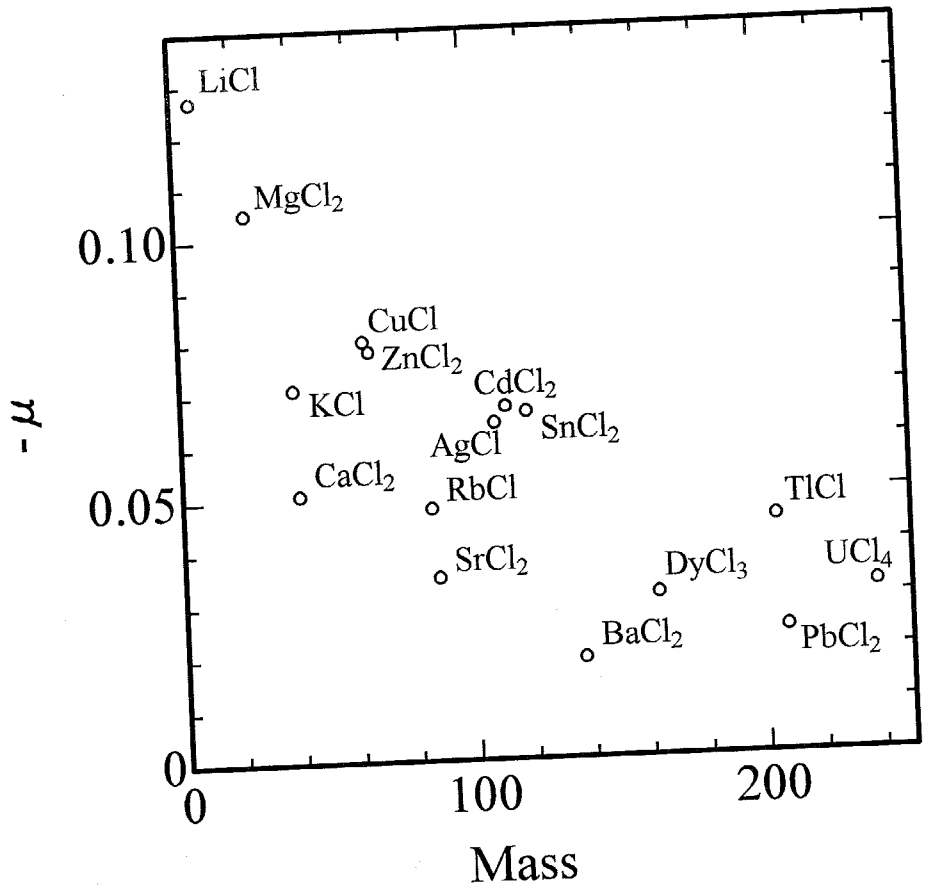

Fig. 3.22 The mass effect in molten chlorides plotted against the cation masses. Temperature dependence of the mass effect has been measured for some salts. However, the dependence is small enough for the present comparison.

References

[1] Ionic Mobilities of Monovalent Cations in Molten Salt Mixtures
M. Chemla and I. Okada, *Electrochim. Acta*, **35**, 1761-1776 (1990)
[2] Internal Cation Mobilities in the Molten Binary Systems (Li, Na)Cl and (Na, K)Cl
C. -C. Yang and B. -J. Lee, *Z. Naturforsch.*, **48a**, 1223-1228 (1993)
[3] H. Horinouchi and I. Okada, to be published
[4] The Chemla Effect in Molten (Li, Cs)Cl Electromigration and MD Simulation
I. Okada, S. Okazaki, H. Horinouchi and Y. Miyamoto, *Mat. Sci. Forum*, **73-75**, 175-182 (1991)
[5] The Chemla effect in the mobilities in the molten binary system of lithium chloride and caesium chloride
I. Okada and H. Horinouchi, *J. Electroanal. Chem.*, **396**, 547-552 (1995)
[6] MD-Simulation of Molten (Li, K)Cl at the Eutectic Composition. Self-Exchange Velocities of Li- and K-Isotopes near the Cl^--Ions
I. Okada, *Z. Naturforsch.* **42a**, 21-28 (1987).
[7] Internal Cation Mobilities in the Molten Binary System KNO_3-$Ca(NO_3)_2$
J. Habasaki, C. Yang and I. Okada, *Z. Naturforsch.*, **42a**, 695-699 (1987)
[8] Internal Cation Mobilities in the Molten Binary Systems KNO_3-$Sr(NO_3)_2$ and KNO_3-$Ba(NO_3)_2$
C. Yang, J. Habasaki, O. Odawara and I. Okada, *Z. Naturforsch.*, **42a**, 1021-1023 (1987)
[9] A Dynamic Dissociation Model for Internal Mobilities in Molten Alkali and Alkaline Earth Nitrate Mixtures
T. Koura, H. Matsuura and I. Okada, *J. Mol. Liquids*, **73/74**, 195-208 (1997)
[10] *Advances in Molten Salt Chemistry, Vol. 6*
A. Klemm, Ed. by G. Mamantov, C. B. Mamantov and J. Braunstein, p. 1. Elsevier, Amsterdam (1987)
[11] Internal Mobilities in Molten (Li, Pb(II))Cl as Remeasured by the Klemm Method
H. Haibara and I. Okada, *Z. Naturforsch.*, **45a**, 827-831 (1990)
[12] The Structure of Molten Barium Chloride
F. G. Edwards, R. A. Howe, J. E. Enderby and D. I. Page, *J. Phys. C: Solid State Phys.*, **11**, 1053-1057 (1978)
[13] The Structure of Molten Calcium Chloride
S. Biggin and J. E. Enderby, *J. Phys. C: Solid State Phys.*, **14**, 3577-3583 (1981)
[14] Structural Study of Molten $CaCl_2$-KCl System
K. Igarashi, K. Tajiri, T. Asahina and M. Kosaka, *Mat. Sci. Forum*, **73-75**, 79-84 (1991)
[15] Structural Investigation of the Molten System LiCl-$CaCl_2$ by X-ray Diffraction Method
N. Iwamoto, N. Umesaki, T. Asahina and M. Kosaka, *High Temp. Sci.* **23**, 1-15 (1987).
[16] Bounds of Complex Formation for Alkali-Earth Cation in Molten Alkali Chlorides
K. Sakai, T. Nakamura, N. Umesaki and N. Iwamoto, *Phys. Chem. Liq.*, **14**, 67-78 (1984)
[17] The electric conductance of simple molten electrolytes
J. O'M. Bockris, E. H. Crook, H. Bloom and N. E. Richards, *Proc. Roy. Soc. London* **A255**, 558-578 (1960).
[18] J. L. Copeland, "*Transport Properties of Ionic Liquids*", Gordon and Breach Science Publishers, London 1974, p.32.
[19] Melting in Trivalent Metal Chlorides
M. -L. Saboungi, D. L. Price, C. Scamehorn and M. P. Tosi, *Europhys. Lett.*, **15**, 283-288 (1991)
[20] Short Range Structures of Several Rare Earth Chloride Melts
J. Mochinaga, Y. Iwadate and K. Fukushima, *Mat. Sci. Forum*, **73-75**, 147-152 (1991)
[21] Structure of Molten $DyCl_3$ and Equimolecular $DyCl_3$-NaCl
J. Mochinaga, Y. Miyagi, K. Igarashi, K. Fukushima and Y. Iwadate, *Nippon Kagaku Kaishi*, **1993**,

459-464[in Japanese]
[22] Raman Spectrum of the $LaCl_6^{-3}$ Octahedron in Molten and Solid $Cs_2NaLaCl_6$, Cs_3LaCl_6 and K_3LaCl_6
G. N. Papatheodorou, *Inorg. Nucl. Chem. Letters*, **11**, 483-490 (1975)
[23] Raman Spectroscopic Studies of Yttrium (III) Chloride-Alkali Metal Chloride Melts and of Cs_2NaYCl_6 and YCl_3 Solid Compounds
G. N. Papatheodorou, *J. Chem. Phys.*, **66**, 2893-2900 (1977)
[24] Polarization Phenomenon in Molten $MgCl_2$-KCl and $MgCl_2$-NaCl
Y. Iwadate, J. Tominaga, K. Igarashi and J. Mochinaga, *Chem. Phys. Lett.*, **110**, 643-647 (1984)
[25] Molten Salts Data as Reference Standards for Density, Surface Tension Viscosity and Electrical Conductance: KNO_3 and NaCl
G. J. Janz, *J. Phys. Chem. Ref. Data*, **9**, 791-829 (1980).
[26] Electrical Conductivity of Molten $NdCl_3$-KCl, $NdCl_3$-NaCl and $NdCl_3$-$CaCl_2$ Solutions
J. Mochinaga, Y. Iwadate and K. Igarashi, *J. Electrochem. Soc.*, **138**, 3588-3592 (1991)
[27] G. J. Janz, F. W. Dampier, G. R. Lakshminarayanan, P. K. Lorenz and R. P. T. Tomkins, *Molten Salts: Volume 1, Electrical Conductance, Density and Viscosity Data.* NSRDS-NBS 15, New York 1968.
[28] Interaction of Lanthanum Chloride with Samarium(III) and Yttrium(III) Chlorides
B. G. Korshunov, D. V. Drobot and L. V. Durinina, *Russ. J. Inorg. Chem.*, **10**, 1154-1156 (1965)
[29] Electrical Conductivities of Binary and Ternary Melts between $MgCl_2$, $CaCl_2$, NaCl and KCl.
K. Grjotheim, R. Nikolic and H. A. Øye, *Acta Chem. Scand.* **24**, 489-509 (1970).
[30] The Polarization Correction in Conductance Measurements
R. P. T. Tomkins, G. J. Janz and E. Andalaft, *J. Electrochem. Soc.* **117**, 906-907 (1970).
[31] Electrical Conductance of Salts in the Fused State
V. A. Kochinashvili and V. P. Barzakovskii, *J. Appl. Chem. (USSR)*, **22**, 1824-1828 (1952)
[32] Die Phänomenologie zweier Verfahren zur Isotopentrennung
A. Klemm, *Z. Naturforsch.* **1**, 252-257 (1946).[in German]
[33] Electromigration in Molten and Solid Binary Sulfate Mixtures: Relative Cation Mobilities and Transport Numbers
V. Ljubimov and A. Lundén, *Z. Naturforsch.* **21a**, 1592-1600 (1966).
[34] Molten Salt Ionic Mobilities in Terms of Group Velocity Correlation Functions
A. Klemm. *Z. Naturforsch.* **32a**, 927-929 (1977)
[35] Revised Effective Ionic Radii and Systematic Studies of Interatomic Distances in Halides and Chalcogenides
R. D. Shannon, *Acta. Crystralogr.* **A32**, 751-767 (1976).
[36] Isotopenanreicherung bei Mg, Ca, Sr und Ba durch Ionenwanderung in geschmolzenen Halogeniden
A. Neubert and A. Klemm, *Z. Naturforsch.* **16a**, 685-692 (1961)[in German]
[37] A Molecular Dynamics Simulation of Molten (Li-Rb)Cl Implying the Chemla Effect of Mobilities
I. Okada, R. Takagi and K. Kawamura, *Z. Naturforsch.* **35a**, 493-499 (1980)
[38] Internal Cation Mobilities in the Binary System NaOH-KOH
C. C. Yang, O. Odawara and I. Okada, *J. Electrochem. Soc.* **136**, 120-125 (1989)
[39] The Maximum of the Conductivity of an Ionic Melt from MD Simulations at Various Temperatures
I. Okada and R. Takagi, *Z. Naturforsch.* **36a**, 378-380 (1981)
[40] Effect of Pressure on the Self-Exchange Velocities in MD Simulations of Molten LiCl and LiBr Reflecting the Anomaly in the Conductivities
I. Okada, A Endoh and S. Baluja, *Z. Naturforsch.* **46a**, 148-154 (1991)
[41] MD-Simulation of Molten LiCl; Self-Exchange Velocities of Li-Isotopes near Cl^--Ions
I. Okada, *Z. Naturforsch.* **39a**, 880-887 (1984)

[42] Ionic Sizes and Born Repulsive Parameters in the NaCl-Type Alkali Halides - II
M. P. Tosi and F. G. Fumi, *J. Phys. Chem. Solids*, **25**, 45-52 (1964)
[43] I. Okada, S. Okazaki and Y. Miyamoto, unpublished
[44] The Isotope Effect of Li^+ Ions in Electromigration of Molten $LiNO_3$
A. Endoh, I. Okada, M. Nomura and M. Okamoto, *Z. Naturforsch.*, **42a**, 700-704 (1987)
[45] The Isotope Effect of Li-Ions in Countercurrent Electromigration of Molten LiOH
C. -C. Yang, I. Okada, M. Nomura and M. Okamoto, *Z. Naturforsch.*, **43a**, 91-92 (1988)
[46] Ionenwanderung in Salzen und Geschmolzenen Metallen
A. Klemm. *J. Chim. Phys. Phys. Chem. Biol.* **60**, 237-244 (1963).[in German]
[47] X-ray-diffraction Analysis of the Molten $ZnCl_2$-KCl System
Y. Takagi and T. Nakamura, *J. Chem. Soc., Faraday Trans. I*, **81**, 1901-1912 (1985)
[48] The Structure of Molten Zinc Chloride
S. Biggin and J. E. Enderby, *J. Phys. C: Solid State Phys.*, **14**, 3129-3136 (1981)
[49] Anricherung der leichten Zinkisotope durch elektrolytische Überführung in geschmolzenem Zinkchlorid
A. Klemm, H. Hintenberger and A. Lundén, *Z. Naturforsch.*, **6a**, 489-494 (1951) [in German]
[50] Revised Effective Ionic Radii and Systematic Studies of Interatomic Distances in Halides and Chalcogenides
R. D. Shannon, *Acta. Crystralogr.* **A32**, 751-767 (1976).
[51] R. W. G. Wyckoff, *Crystal Structure, Vol. 2*, Interscience, pp.57, 78, New York (1964)
[52] Volume Changes on Melting for Several Rare Earth Chlorides
K. Igarashi and J. Mochinaga, *Z. Naturforsch.*, **42a**, 777-778 (1987)
[53] Electrical Conductivity of Molten $LaCl_3$-NaCl, $LaCl_3$-KCl and $LaCl_3$-$CaCl_2$
K. Fukushima, Y. Iwadate, Y. Andou, T. Kawashima and J. Mochinaga, *Z. Naturforsch.*, **46a**, 1055-1059 (1991)

Chapter 4.

Internal cation mobilities in molten monovalent-multivalent cation chloride systems

4.1 Background

In previous chapters, we have shown the internal mobilities, u, in various molten binary chloride systems containing multivalent cation measured by Klemm's countercurrent electromigration method. For example, the internal cation mobility isotherms at 673 K in $(M_1, M_{2(1/2)})NO_3$ (M_1=Li, Na, K; M_2=Ca, Sr, Ba) are plotted against x_2 in Fig. 4.1. In the molten binary system $(K, M_{(1/2)})NO_3$ (M=Ca, Sr and Ba)[1],[2], u_K decreases with increasing x_M; x is mole fraction. This tendency could be interpreted in terms of the tranquilization effect by M^{2+} ions. Meanwhile, u_M increases with increasing x_K; this trend may be attributed to the agitation effect by K^+ ions. However, the conductance mechanism of the alkaline earth cation in its higher concentration range cannot be discussed, since these alkaline earth nitrates are not stable in molten state. Thus, in this chapter the mechanism of the ionic conductance in molten binary monovalent-multivalent cation chloride systems will be discussed partly in comparison with the nitrate systems. For this purpose the system $(K, Ca_{(1/2)})Cl$ and $(K, Dy_{(1/3)})Cl$ were chosen. Internal mobilities of the $(K, Ca_{(1/2)})Cl$ system have so far been measured by the EMF mothod[3]; however, since the EMF method is inherently inferior to the Klemm method[4], we have remeasured the internal transport numbers in the present system by the Klemm method. Internal mobilities in I-III cation systems were not previously measured, whereas electric conductivities of such systems have been measured in some chlorides[5],[6],[7],[8].

4.2 Experimental

The chemicals KCl and $CaCl_2$ (Kanto Chemical Co. Inc.,) used were of regent grade. These salts were vacuum dried at ca. 400 K for several hours. $DyCl_3$ was prepared by the same procedure as stated in chapter 3. After mixing in a chosen ratio, they were put in a small quartz vessel and melted. The apparatus and procedures used were also similar to those described in previous chapters. With a temperature controller, during electromigration, temperature was kept at 1073 K within $\pm$2K and 1093 K within $\pm$2K on molten system (K, $Ca_{(1/2)}$)Cl, and (K, $Dy_{(1/3)}$)Cl, respectively. After electromigration for several hours, the separation tube was taken out of the large container and cut into several pieces for determining the K^+ and Ca^{2+} with emission spectrometry, the Dy^{3+} with ICP spectrometry.

4.3 Results

Both of the phase diagrams in the present systems are available[9),(10)], which are shown in Figs. 4.2 and 4.3. Especially, the mixture of the composition K_3DyCl_6 has a congruent melting point at 1078 K, which is higher than those of pure KCl (1048 K) and pure $DyCl_3$ (928 K). Thus, electromigration was performed in the (K, $Dy_{(1/3)}$)Cl at 1093 K, whereas we performed electromigration in the (K, $Ca_{(1/2)}$)Cl system at 1073 K.

In the present study $Ca_{(1/2)}Cl$ and $Dy_{(1/3)}Cl$ is regarded as a molar unit, unless otherwise stated.

ε is defined by

$$\varepsilon = (u_1 - u_2) / u_c \qquad (4.1)$$

where $u_c = x_1 u_1 + x_2 u_2$ (u_i is the internal cation mobility of i and x_i is the mole fraction: $x_1 + x_2 = 1$).

The ε values were calculated by an equation as shown in chapter 2

$$\varepsilon = -(F / Q)(N_1 / x_1 - N_2 / x_2) \qquad (4.2)$$

Since the difference in the mobilities of K^+ and Ca^{2+}, K^+ and Dy^{3+} are large, these ions were easily separated each other by electromigration. Therefore, much electric current could not be transported for the measurement of ε, which, in turn, inevitably involved relatively large errors of ε. The ε values in the molten (K, $Ca_{(1/2)}$)Cl and the molten (K, $Dy_{(1/3)}$)Cl are given in Tables 4.1 and 4.2, respectively, together with the main experimental conditions.

The u values are calculated from the ε values and data available on the electrical conductivities κ [9),(11)] and molar volumes V_m [9),(12)] of the mixtures.

$$u_1 = (\kappa V_m / F)(1 + x_2 \varepsilon) \qquad (4.3)$$

$$u_2 = (\kappa V_m / F)(1 - x_1 \varepsilon) \qquad (4.4)$$

It should be mentioned that in the present case ε is not the relative difference in

the internal mobilities, since u_c is not the average cation mobility[13]. The average cation mobility u_{ac} may be expressed by

$$u_{ac} = y_1 u_1 + y_2 u_2 \tag{4.5}$$

where y_i is the mole fraction of i when $CaCl_2$ instead of $Ca_{(1/2)}Cl$ is regarded as a molar unit; y is related with x by

$$y_K = 2x_K / (1 + x_K) \tag{4.6}$$

$$y_{Ca} = x_{Ca} / (2 - x_{Ca}) \tag{4.7}$$

and when $DyCl_3$ instead of $Dy_{(1/3)}Cl$ is regarded as a molar unit;

$$y_K = 3x_K / (1 + 2x_K) \tag{4.6'}$$

$$y_{Dy} = x_{Dy} / (3 - 2x_{Dy}) \tag{4.7'}$$

4.4 Discussion

4.4.1 Internal mobility of monovalent cation

The isotherms of u_K and u_{Ca} at 1073 K are shown in Fig. 4.4. u_K is much greater than u_{Ca} over the whole concentration, as expected from the results on the molten systems (K, $M_{(1/2)}$)NO_3[1),(2)]. u_K decreases with increasing x_{Ca}.

The isotherms of u_K and u_{Dy} at 1093 K are shown in Fig. 4.5. u_K is much greater than u_{Dy} over the whole concentration, as also expected. u_K decreases with increasing x_{Dy}.

It has previously been found that in molten binary alkali nitrates, the internal mobilities, u_1 of cation 1 are well expressed by an empirical equation:

$$u_1 = (A / (V_m - V_0)) \exp(-E / RT) \qquad (4.8)$$

where A, E and V_0 are constants nearly independent of the kind of coexisting cations; R is the gas constant, T the temperature. u_K's in the present systems are plotted against the molar volume together with those in molten system (Na, K)Cl[14] in Fig. 4.6.

The dotted line is drawn assuming a type of Eq. (4.8) for u_K in (Na, K)Cl. The u_K in (Na, K)Cl increases with decreasing molar volume, which is the normal case, as expected from Eq. (4.8). On the other hand, u_K in (K, $Ca_{(1/2)}$)Cl and (K, $Dy_{(1/3)}$)Cl decreases. In other words, u_K in (K, $Ca_{(1/2)}$)Cl and (K, $Dy_{(1/3)}$)Cl decreases with increasing mole fraction of Ca^{2+} and Dy^{3+}, respectively. This may be accounted for in terms of the tranquilization effect[1] by these cations on u_K. The tranquilization effect is assumed to occur by a strong Coulombic interaction of cations with a common anion, that is Cl^- ion in the present case. Figure 4.6 shows that at a given molar volume the tranquilization effect by Ca^{2+} is stronger than that by Dy^{3+}, although the interaction of Ca^{2+}-Cl^- is presumably weaker than that of Dy^{3+}-Cl^-. This apparent contradiction may be explained in terms of the difference in the number of these cations per Cl^- ion. The

ratio of the numbers of Ca^{2+}/Cl^- is considerably greater than that of Dy^{3+}/Cl^-; for example, at $V_m=35\times10^{-6}m^3mol^{-1}$, $x_{Ca}=0.643$ and $x_{Dy}=0.681$, that is $Ca^{2+}/Cl^-=0.322$ and $Dy^{3+}/Cl^-=0.227$. Thus, the apparently more effective tranquilization effect by Ca^{2+} than by Dy^{3+} is due to the more condensed number density of the multivalent cation.

4.4.2 Internal mobility of multivalent cation

Figure 4.4 shows that u_{Ca} increases with increasing x_K. The u_{Ca} measured in the present study is plotted against the molar volume V_m in Fig. 4.7, where u_{Ca}'s in the system $(Ca, Ba)_{(1/2)}Cl$ previously measured at 1073 K are also shown for comparison. u_{Ca} in the present system is larger than the extrapolated value of u_{Ca} in the molten system $(Ca, Ba)_{(1/2)}Cl$. This may be attributed to the agitation effect by K^+ ions; the separating motion of Ca^{2+} ions from the neighboring Cl^- ions are agitated by the more active motion of the coexisting K^+ ions, since the Coulombic interaction of the monovalent cation with the Cl^- ion is considerably weaker than that of the divalent cation.

Figure 4.5 shows that u_{Dy} decreases with increasing x_K. The u_{Dy} measured in the present study is plotted against the molar volume V_m in Fig. 4.8, where u_{Dy}'s in the system $(Y, Dy)_{(1/3)}Cl$ previously measured at 1073 K are also shown for comparison. Although u_{Dy} in the present system seems to decrease with increasing molar volume, the profile of u_{Dy} in the present system as a function of molar volume is clearly different from that in $(Y, Dy)_{(1/3)}Cl$. As molar volume increases, Dy^{3+} ion will be more associated with the neighboring Cl^- ions. Raman spectroscopic studies suggest that there exist such species as $[LnCl_6]^{3-}$ in the mixture system $(KCl\text{-}LnCl_3)$(Ln: La[15),(16)], Y[17], Gd[18]). Neutron and X-ray diffraction studies of pure $LnCl_3$ melts also suggest that even in the pure melts the octahetral unit exist, which is connected to other units by edge- or corner-sharing (Ln: Y(neutron)[19], Nd(X-ray)[20], La, Ce, Pr, Nd, Gd, Dy and Sm (X-ray)[21]). X-ray diffraction has been performed also for a mixture melt of the composition K_3DyCl_6[22].

Figure 4.5 suggests that at $x_K>0.5$(a concentration of $x_K=0.5$ equal to $y_K=0.75$ corresponds to K_3DyCl_6) u_{Dy} seems to become particularly small. This is presumably because an isolated species of $[LnCl_6]^{3-}$ is formed. This would not necessarily lead to a

conclusion, however, that in this concentration range such anionic species as $[DyCl_6]^{3-}$ is also electrically-conducting species. It would be presumably impossible that such a large species becomes an electrically-conducting species. This could be examined by studying the isotope effect of Dy in electromigration. We have not yet succeeded in measuring the isotope effect of Dy in the mixtures rich in K^+ by electromigration, because in such mixture systems K^+ and Dy^{3+} were separated each other before electric current enough for the isotope effect measurement was passed. On the other hand, measurement of the isotope effect of Dy in pure molten $Dy_{(1/3)}Cl$ suggests that the electrically-conducting species containing Dy is Dy^{3+} [23].

The formation of such species as $[DyCl_6]^{3-}$ with increasing x_K could be explained based on the Coulombic interaction.

Figure 4.5 also shows that, while x_K increases, u_{Dy} seems to be nearly constant at least in the range x_K=0~0.3. This demonstrates that in this range the electrically-conducting species of Dy does not change much, and is therefore assumed to be mainly Dy^{3+}, although such species as $[DyCl_6]^{3-}$ is expected to exist partially.

Figure 4.8 shows that, as molar volume increases, u_{Dy} in the present system does not decrease so much as that in $(Y, Dy)_{(1/3)}Cl$. With increasing molar volume, that is with increasing x_K, the number of more free Cl^- ions will increase. This in turn will make separating motion of Dy^{3+} from Cl^- favorable to some extent, which is called the agitation effect on u_{Dy} by K^+. In the system $(K, Ca_{(1/2)})Cl$, with increasing molar volume, that is with increasing x_K, u_{Ca}'s do not vary much. In both cases the two opposite effects mentioned above, that is the association and the agitation, are assumed to be superimposed on u_{Dy} and u_{Ca}. In the former case, however, the association may be more pronounced than in the latter case.

Table 4.1 Main experimental conditions and the internal mobilities in the molten system (K, $Ca_{(1/2)}$)Cl at 1073 K.

x_{Ca}[a]	Q (C)	ε[a]	κ (S m^{-1})	V_m ($10^{-6}m^3mol^{-1}$)	u_K[a]	u_{Ca}[a] ($10^{-8}m^2V^{-1}s^{-1}$)
0			223	49.23	11.37	
0.067±0.004	982	0.499±0.038	207	47.75	10.57±0.13	5.47±0.19
0.333±0.007	2005	0.344±0.014	167	41.83	8.09±0.28	5.59±0.56
0.487±0.005	1970	0.210±0.017	152	38.45	6.67±0.13	5.40±0.07
0.658±0.004	1076	0.036±0.004	141	34.66	5.20±0.21	5.02±0.11
0.669±0.006	2013	0.085±0.004	141	34.41	5.32±0.20	4.89±0.10
0.675±0.001	1529	0.061±0.001	141	34.30	5.23±0.11	4.92±0.05
0.693±0.003	2120	0.062±0.001	141	33.89	5.17±0.13	4.86±0.06
0.698±0.008	1588	0.121±0.004	141	33.77	5.36±0.21	4.76±0.09
0.802±0.004	1670	0.068±0.002	147	31.56	5.12±0.17	4.78±0.04
1			209	27.09		5.86

Table 4.2 Main experimental conditions and the internal mobilities in the molten system (K, $Dy_{(1/3)}$)Cl at 1093 K.

x_{Dy}[a]	Q (C)	ε[a]	κ (S m^{-1})	V_m ($10^{-6}m^3mol^{-1}$)	u_K[a]	u_{Dy}[a] ($10^{-8}m^2V^{-1}s^{-1}$)
0.241±0.005	1411	1.20±0.02	174	44.38	10.28±0.00	0.69±0.12
0.420±0.002	610	1.56±0.02	141	40.38	9.79±0.05	0.54±0.06
0.532±0.035	617	1.40±0.06	123	38.06	8.45±0.28	1.68±0.27
0.670±0.012	536	2.10±0.03	103	35.22	9.05±0.13	1.15±0.20
0.760±0.002	2089	1.38±0.00	91.4	33.37	6.48±0.01	2.11±0.00
0.836±0.000	684	1.80±0.01	82.8	31.80	6.84±0.03	1.92±0.01
0.913±0.004	649	1.95±0.02	74.7	30.20	6.51±0.05	1.94±0.02
0.945±0.002	1184	1.58±0.02	71.8	29.55	5.49±0.04	2.01±0.01
1			67.0	28.41		1.97

[a]The sign ± for x_{Dy}, ε and u indicates the errors due to the chemical analysis.

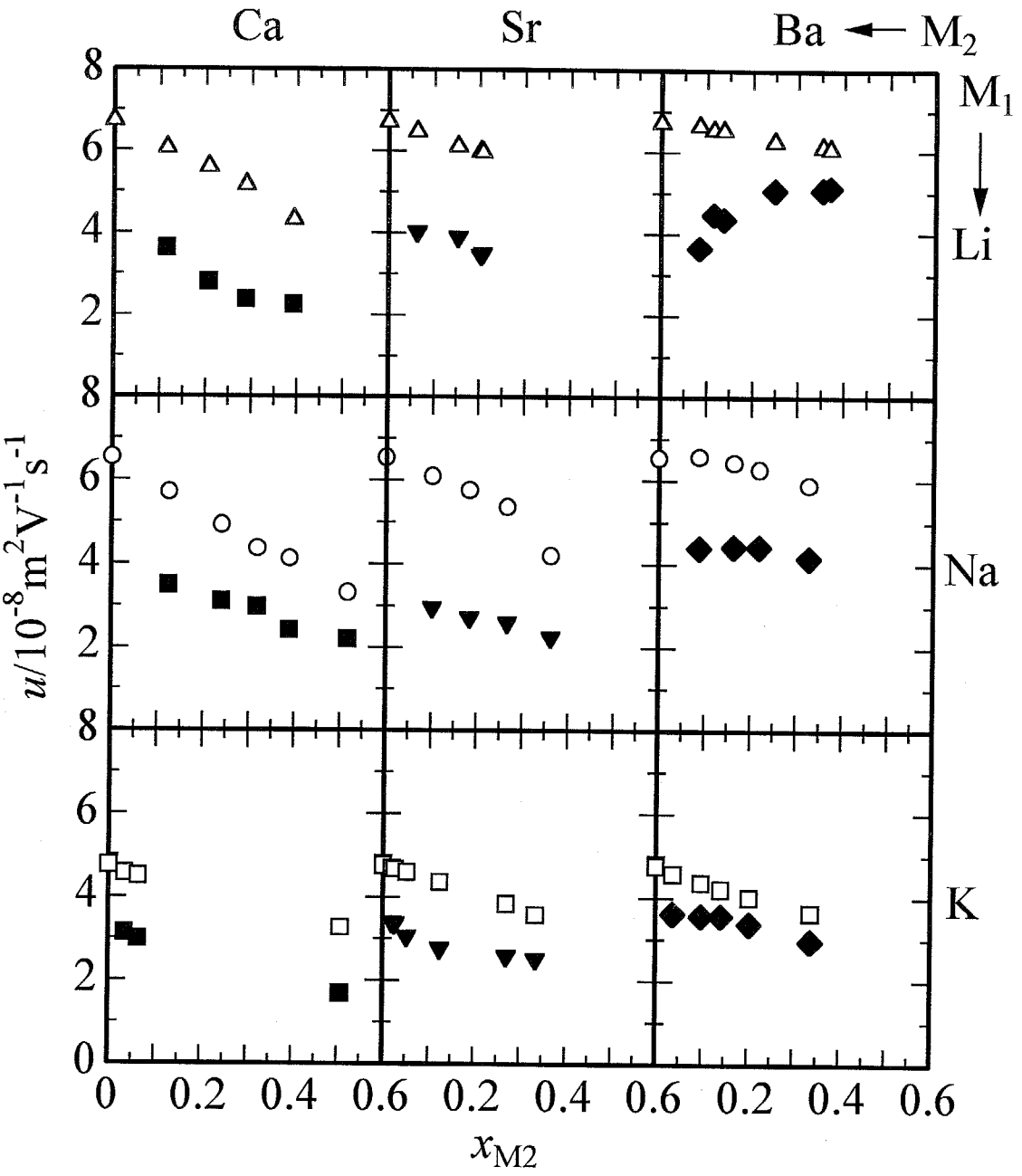

Fig. 4.1 Isotherms of the internal mobilities in the molten mono-divalent nitrate systems

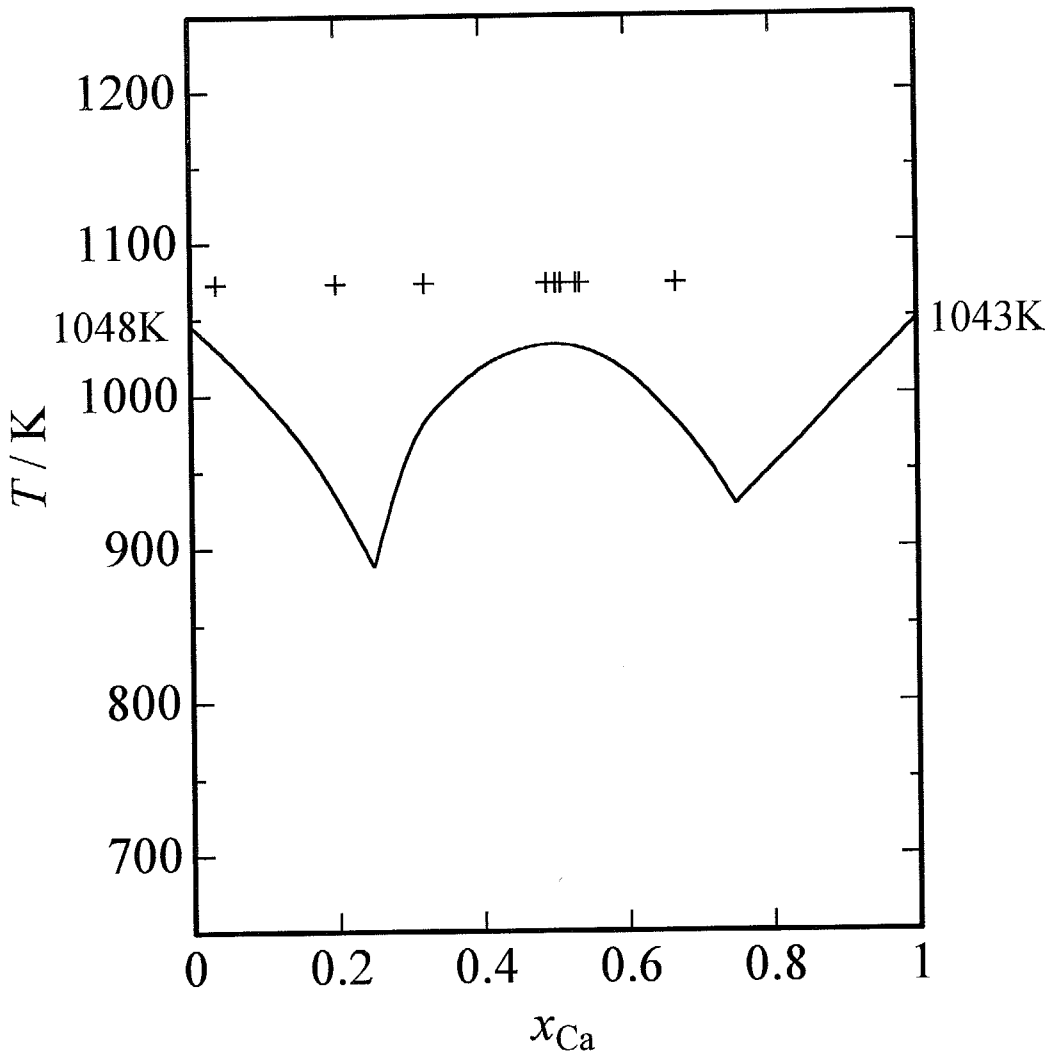

Fig. 4.2 Phase diagram of the system KCl-$Ca_{(1/2)}Cl$

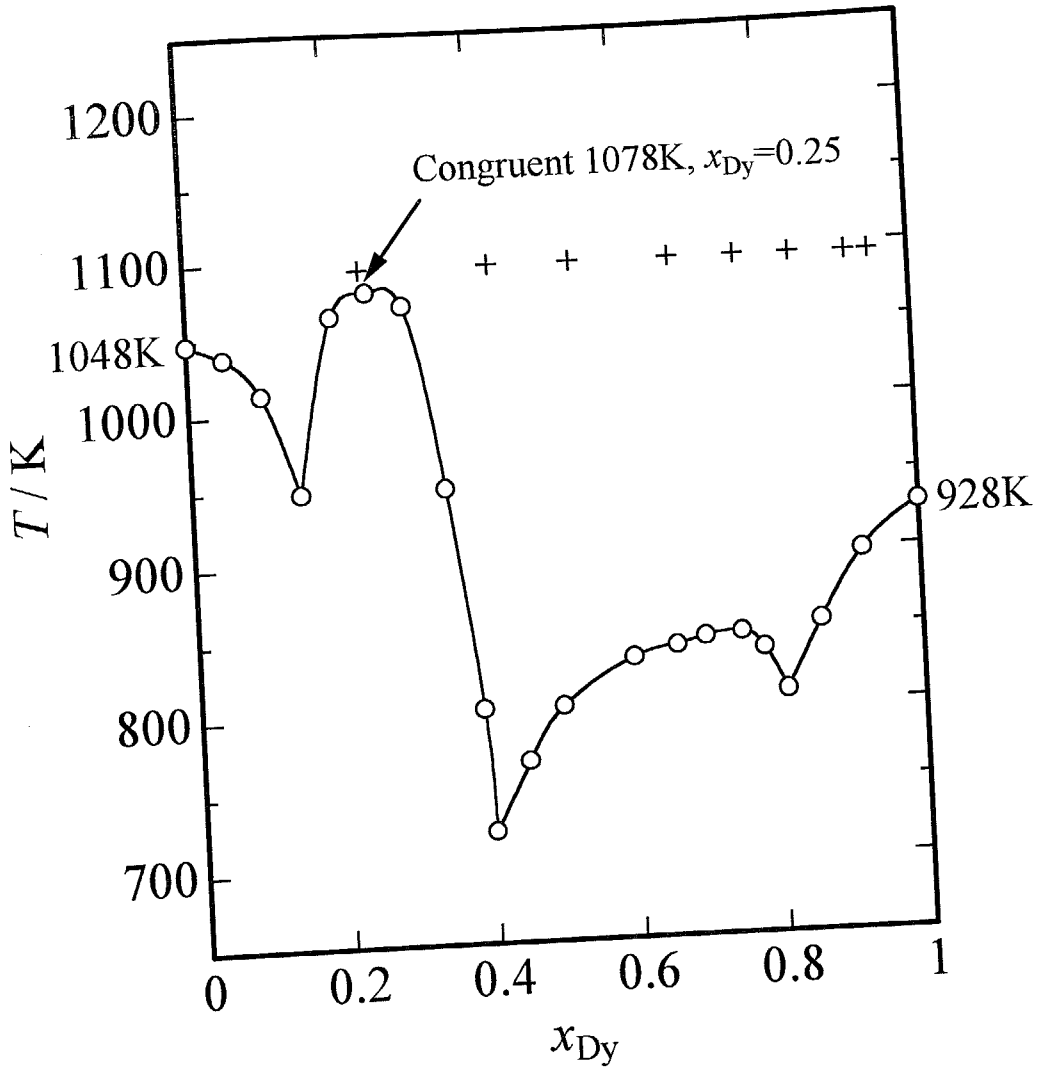

Fig. 4.3 Phase diagram of the system KCl-$Dy_{(1/3)}Cl$

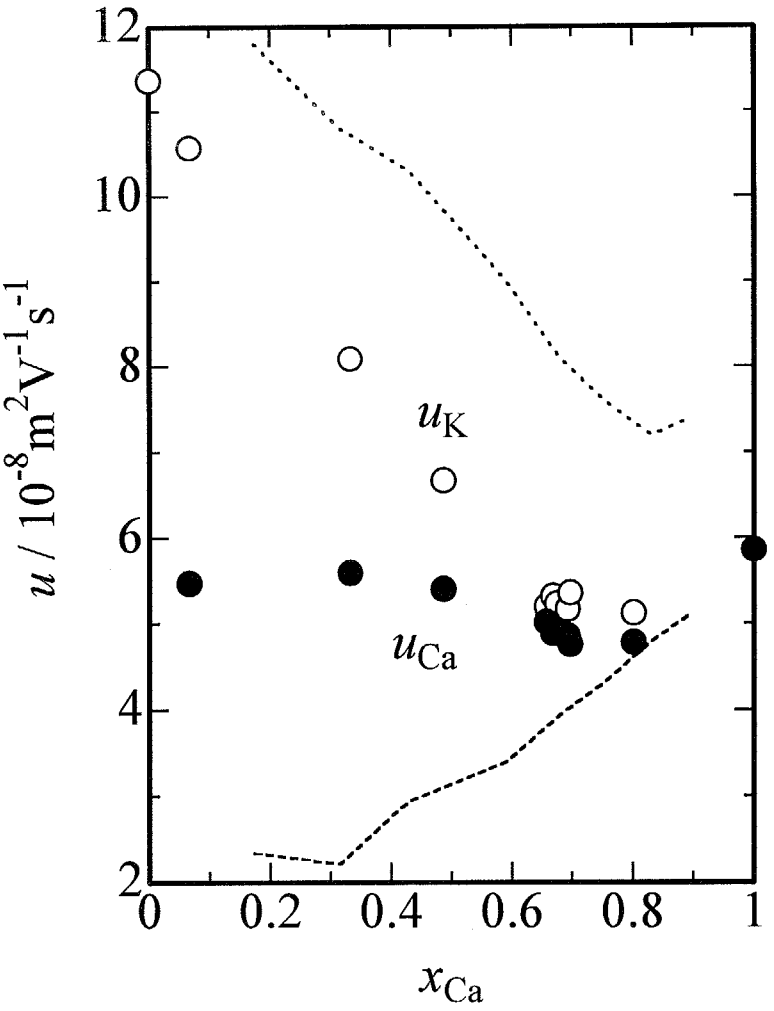

Fig. 4.4 Isotherms of u_K and u_{Ca} in the molten system KCl-$Ca_{(1/2)}Cl$ at 1073 K.

○: u_K, ●: u_{Ca}. The dashed line is drawn by ref [3]; dotted line: u_K, dashed line: u_{Ca}

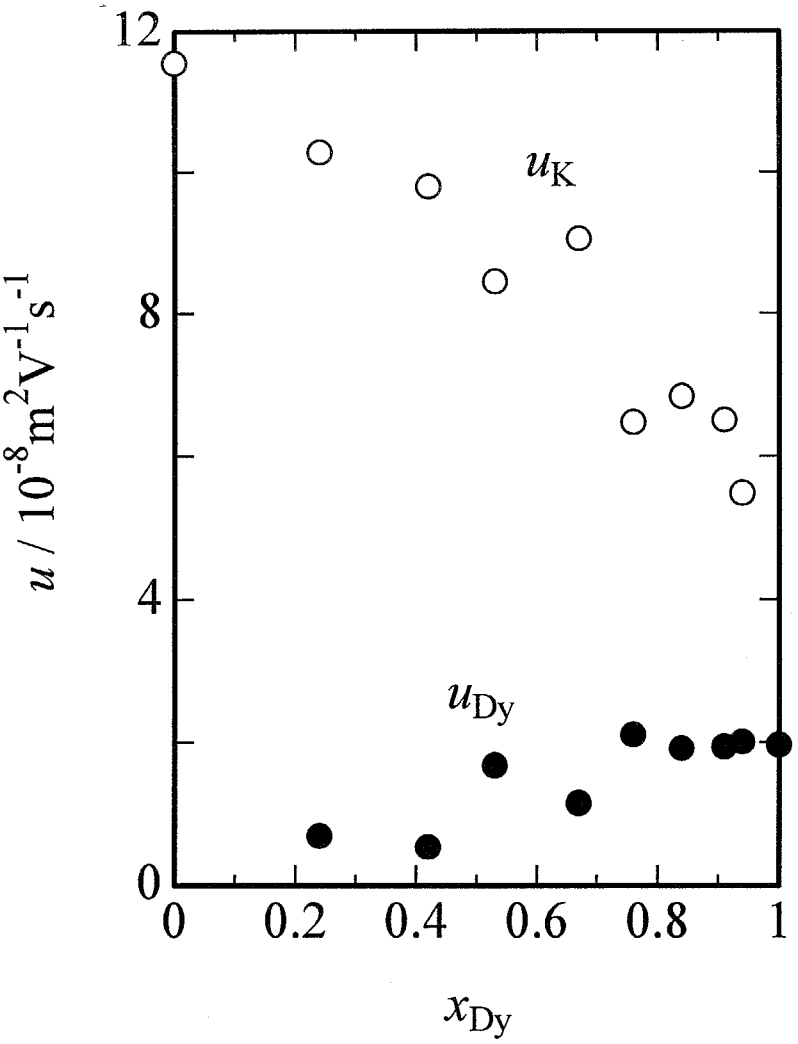

Fig. 4.5 Isotherms of u_K and u_{Dy} in the molten system KCl-$Dy_{(1/3)}Cl$ at 1093 K.

○: u_K, ●: u_{Dy}.

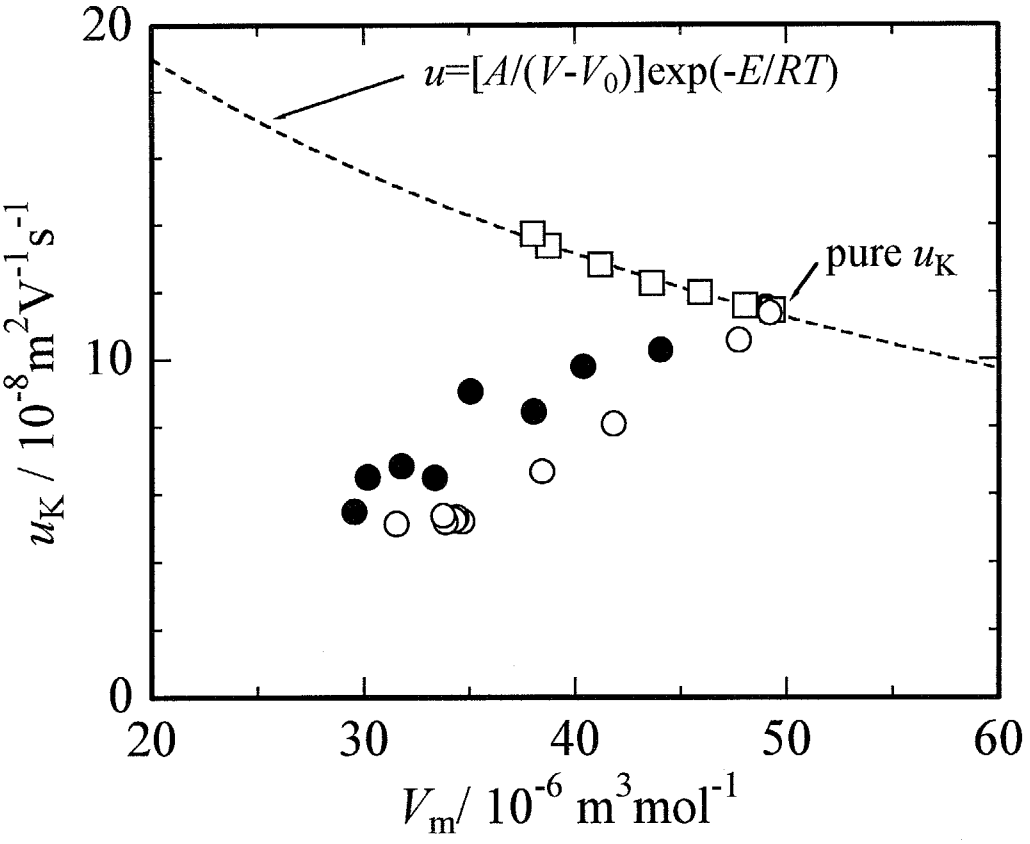

Fig. 4.6 Internal cation mobilities of K *vs.* molar volume in some molten binary systems.

□: u_K in (Na, K)Cl[14], ○: u_K in (K, $Ca_{(1/2)}$)Cl, ●: u_K in (K, $Dy_{(1/3)}$)Cl

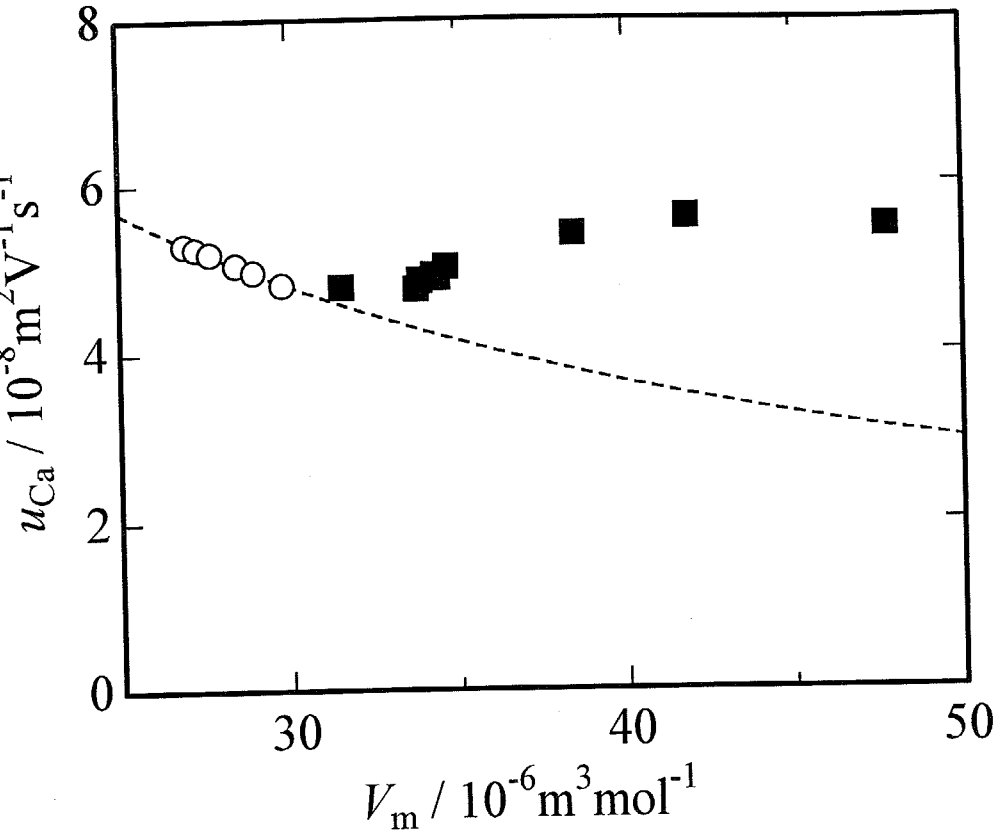

Fig. 4.7 Internal cation mobilities of Ca *vs.* molar volume in some molten binary systems.

○: u_{Ca} in $(Ca, Ba)_{(1/2)}Cl$, ■: u_{Ca} in $(K, Ca_{(1/2)})Cl$.

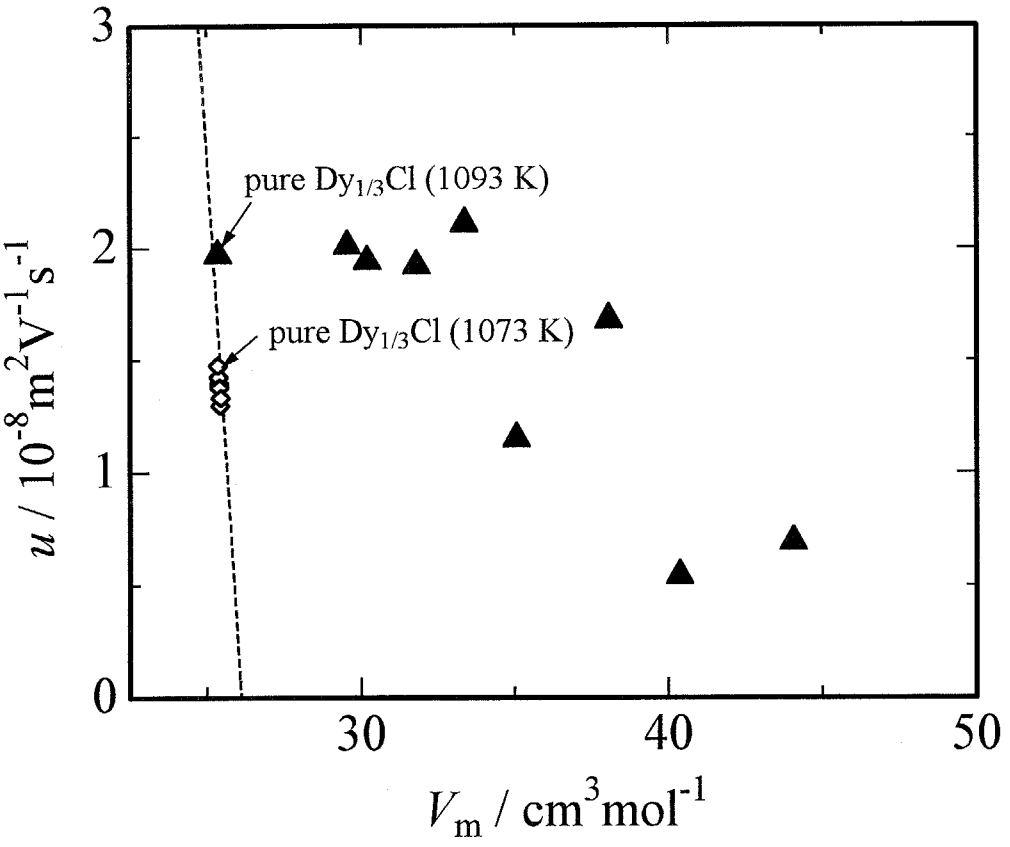

Fig. 4.8 Internal cation mobilities of Dy *vs.* molar volume in some molten binary systems. The molar volume of pure $Dy_{(1/3)}Cl$ appears to be slightly smaller at 1093 K[24] than at 1073 K[25]. This inconsistency comes from the different origins of the cited references.

◇: u_{Dy} in $(Y, Dy)_{(1/3)}Cl$, ▲: u_{Dy} in $(K, Dy_{(1/3)})Cl$.

References

[1] Internal Cation Mobilities in the Molten Binary System KNO_3-$Ca(NO_3)_2$
J. Habasaki, C. Yang and I. Okada, *Z. Naturforsch.*, **42a**, 695-699 (1987)
[2] Internal Cation Mobilities in the Molten Binary Systems KNO_3-$Sr(NO_3)_2$ and KNO_3-$Ba(NO_3)_2$
C. Yang, J. Habasaki, O. Odawara and I. Okada, *Z. Naturforsch.*, **42a**, 1021-1023 (1987)
[3] On the structure of charge-unsymmetrical salt melts of alkaline earth and alkali metal chlorides
H. -H. Emons, G. Bräutigam and H. Vogt, *Z. anorg. allg. Chem.* **394**, 279-289 (1972) [in German];
EMK-Messungen in geschmolzenen Mischungen von Calciumchlorid mit Alkalimetallchloriden
G. Roewer and H. -H. Emons, *Z. anorg. allg. Chem.*, **370**, 119-127(1969)[in Greman]
[4] Internal Cation Mobilities in Molten (Li, Ag)NO_3 and (K, Ag)NO_3 Remeasured by the Klemm Method
I. Okada and K. Ichioka, *Z. Naturforsch.*, **47a**, 781-787 (1992)
[5] Electrical Conductivity of Molten Charge-Asymmetric Salts---$PrCl_3$-NaCl, $PrCl_3$-KCl and $PrCl_3$-$CaCl_2$ Systems
Y. Iwadate, K. Igarashi, J. Mochinaga and T. Adachi, *J. Electrochem. Soc.*, **133**, 1162-1166 (1986)
[6] Electrical Conductivity of Molten $NdCl_3$-KCl, $NdCl_3$-NaCl and $NdCl_3$-$CaCl_2$ Solutions
J. Mochinaga, Y. Iwadate and K. Igarashi, *J. Electrochem. Soc.*, **138**, 3588-3592 (1991)
[7] Molar Volume Variation and Ionic Conduction in Molten $ErCl_3$-NaCl and $ErCl_3$-KCl systems
K. Fukushima, T. Ikumi, J. Mochinaga, R. Takagi, M. Gaune-Escard and Y. Iwadate, *J. Alloy. Comp.*, **229**, 274-279 (1995)
[8] Electrical Conductivity of Molten $LnCl_3$ and M_3LnCl_6 Compounds (Ln=La, Ce, Pr, Nd; M=K, Rb, Cs)
P. Gaune, M. Gaune-Escard, L. Rycerz and A. Bogacz, *J. Alloy. Comp.*, **235**, 143-149 (1996)
[9] Molten Salts: Volume 4, Part 2, Chlorides and Mixtures, Electrical Conductance, Density, Viscosity, and Surface Tension Data
G. J. Janz, R. P. T. Tomkins, C. B. Allen, J. R. Downey, Jr., G. L. Gardner, U. Krebs and S. K. Singer, *J. Phys. Chem. Ref. Data*, **4**, 871-1178 (1975)
[10] Phase Diagram of Ternary $DyCl_3$-KCl-NaCl System
J. Mochinaga, H. Ohtani and K. Igarashi, *Denki Kagaku*, **49**, 19-21 (1981)
[11] K. Fukushima, J. Mochinaga and Y. Iwadate private communication
[12] K. Fukushima, J. Mochinaga and Y. Iwadate private communication
[13] Internal Mobilities in Molten (Li, Pb(II))Cl as Remeasured by the Klemm Method
H. Haibara and I. Okada, *Z. Naturforsch.*, **45a**, 827-831 (1990)
[14] Internal Cation Mobilities in the Molten Binary Systems (Li, Na)Cl and (Na, K)Cl
C. -C. Yang and B. -J. Lee, *Z. Naturforsch.*, **48a**, 1223-1228 (1993)
[15] On the Existence of Associated Species in Lanthanum (III) Chloride-Potassium Chloride Melts
V. A. Maroni, E. J. Hathaway and G. N. Papatheodorou, *J. Phys. Chem.*, **78**, 1134-1135 (1974)
[16] Raman Spectrum of the $LaCl_6^{-3}$ Octahedron in Molten and Solid $Cs_2NaLaCl_6$, Cs_3LaCl_6 and K_3LaCl_6
G. N. Papatheodorou, *Inorg. Nucl. Chem. Letters*, **11**, 483-490 (1975)
[17] Raman Spectroscopic Studies of Yttrium (III) Chloride-Alkali Metal Chloride Melts and of Cs_2NaYCl_6 and YCl_3 Solid Compounds
G. N. Papatheodorou, *J. Chem. Phys.*, **66**, 2893-2900 (1977)
[18] Raman Spectra of Molten $GdCl_3$-KCl and $GdCl_3$-NaCl
A. Matsuoka, K. Fukushima, K. Igarashi, Y. Iwadate and J. Mochinaga, *Nippon Kagaku Kaishi*, **1993**, 471-474[in Japanese]
[19] Melting in Trivalent Metal Chlorides

M. -L. Saboungi, D. L. Price, C. Scamehorn and M. P. Tosi, *Europhys. Lett.*, **15**, 283-288 (1991)
[20] X-ray Diffraction Analysis of $NdCl_3$ Melt
K. Igarashi, M. Kosaka, M. Ikeda and J. Mochinaga, *Z. Naturforsch.* **45a**, 623-626 (1990)
[21] Short Range Structures of Several Rare Earth Chloride Melts
J. Mochinaga, Y. Iwadate and K. Fukushima, *Mat. Sci. Forum*, **73-75**, 147-152 (1991)
[22] Y. Iwadate, Y. Miyagi, M. Oowaki, K, Tanaka and K. Fukushima, unpublished
[23] The Isotope Effect on the Internal Cation Mobility of Molten Dysprosium Chloride
H. Matsuura, I. Okada, M. Nomura, M. Okamoto and Y. Iwadate, *J. Electrochem. Soc.* **143**, 3380-3382 (1996)
[24] K. Fukushima, J. Mochinaga, T. Sekino and Y. Iwadate, to be pubilished
[25] Volume Changes on Melting for Several Rare Earth Chlorides
K. Igarashi and J. Mochinaga, *Z. Naturforsch.*, **42a**, 777-778 (1987)

Chapter 5.

High enrichment of uranium and fission products in ionic salt bath by countercurrent electromigration

5.1 Background

The PUREX method was originally planned for separation of U and Pu. Many investigators have proposed several nuclear fuel cycle concepts by modifying the PUREX method, in most of which radioactive materials are to be vitrified to inorganic matrix and stored in the underground. The Integral Fast Reactor (IFR) concept proposed by Argonne National Laboratory[1] contains a sophisticated idea of pyrochemical treatment in the nuclear fuel cycle. After electrowinning U as well as transuranium elements (TRU), a small amount of the fuel elements and a large amount of fission products are left in the melt bath. In the IFR concept, after removal of the fuel materials, the salt bath containing fission products will be occluded into the zeolites and stocked as the deposits. However, from a standpoint of the harmonization of nuclear systems with global environment,

①we should remove the residue of U and TRU completely for minimization of nuclear waste and utilization of rare fuel elements,

②we should also make an effort to separate the fission products each other for incineration or utilization of medical tracers, rare materials and so on.

Thus, Shimizu and Fujii-e have proposed Self-Consistent Nuclear Energy System (SCNES)[2], which aims at zero release of radioactive materials out of the fuel cycle[3], as shown in Fig. 5.1. In the SCNES we need to separate fuel elements and fission products into the following groups;

1) U and TRU should be recycled as fuel elements,

2) a series of fission products whose half-lives are more than 1 year should be returned back to the reactor core for their incineration, and the other should be cooled down and released from the fuel cycle.

As one of the most feasible candidates for the SCNES is a metallic fuel fast breeder reactor (FBR), we have adopted pyrochemical treatment of metallic fuel as a chemical separation process. One of concepts using molten chlorides as solvent is shown in Fig. 5.2. After the electrorefining and drawdown process, all alkali halides, alkaline-earth halides and some amounts of rare earth halides from fission products still remain in the salt bath. Thus, in order to use the salt bath repeatedly, we have applied a countercurrent electromigration method which originated from isotope separation(e.g. enrichment of ^{6}Li[4],[5],[6]).

As mentioned in Chapter 4, from data on internal mobilities in the molten KCl-$Dy_{(1/3)}Cl$ mixture[7] and the molten KCl-$Ca_{(1/2)}Cl$ mixture[8], Dy and Ca are assumed to be much enriched from their low concentration melts. Horinouchi and Okada have measured the internal mobilities in the molten LiCl-CsCl mixture[9], where Cs was enriched at the anode at $x_{Cs} < 0.2$. Then, we have proposed to apply the electromigration method to chemical separation process to remove fission products.

There are two methods proposed for separation of alkali metals and alkaline-earth metals from the mixture solution. One of them is to use crown ethers[10],[11],[12],[13],[14],[15],[16],[17],[18],[19]. Crown ethers have excellent selectivity for each alkali metal and alkaline-earth metal by trapping into different sizes of cages. These, which are polymerized or kept in resin, may be used as ligands for extractor or separation columns. Fission products can be absorbed and eluted by selecting the ligands, solvents and eluents. These properties lead to a complicated separation process, which cannot be performed in the molten state.

The other process is concerned with inorganic ion exchangers[20),(21),(22)]. For example, some series of zeolites can adsorb alkali metals and alkaline-earth metals into different sizes of holes according to the ionic radii. We can trap most of all the elements into the holes if we can select several species of zeolites. This technique can also be applied to the pyrochemical treatment of the molten salt containing fission products as described in the IFR concept[(23)]. However, if we want to keep the adsorbed molecules in the matrix firmly, we should make calcination over 973 K. Then, this absorbed molecules cannot be readily taken out again. This character plays a merit for deposition but a demerit for utilization of the radioisotopes.

The electromigration method has an advantage for the pyrochemical treatment due to its simple construction for being able to use the same container with the conductive melt bath. Iwasaki and Takagi have already demonstrated enrichment of La in the NaCl-KCl equimolar mixture bath[(24)]. In the present work, we have employed two series of experiments;

①molten $NdCl_3$, UCl_3 and UCl_4 in the LiCl-KCl eutectic mixture as examples of fuel elements,

②molten CsCl, $SrCl_2$ and $GdCl_3$ in the LiCl-KCl eutectic mixture as examples of fission products.

5.2 Experimental

In a series of experiments ①, high grade chemical $NdCl_3$ was prepared from Nd_2O_3(University of Marie Curie, Lublin, Poland). Oxide was dissolved in concentrated HCl. $Nd_2O_3 \cdot H_2O$ was crystallized from solution. Anhydrous Nd_2O_3 was prepared by dehydration of $Nd_2O_3 \cdot H_2O$ and NH_4Cl mixtures under reduced pressure followed by distillation of product under vacuum. The details of preparation procedure were described by Gaune-Escard *et al.*[25]. UCl_4 was prepared from U_3O_8(Merck) by hydrogen reduction to UO_2, and then chlorination with CCl_4 vapors[26]. UCl_3 was prepared by reduction of sublimated UCl_4 with Zn[27]. Completeness of the synthesis was verified by DTA. LiCl (B.D.H. Ltd.)and KCl(PPOCH) were dehydrated by heating under gaseous HCl to melting. Excess of HCl was removed by dry Ar. All reagents were stored in sealed glass ampoules under dry Ar.

In a series of experiments ②, high grade chemicals LiCl-KCl of the eutecitic composition (59mol%LiCl + 41mol%KCl) and $SrCl_2$ (both were supplied by APL Engineered materials, INC.), CsCl and $GdCl_3$ (both were provided by Rare Metallic Co., Ltd.) were used without further purification. All reagents were kept in sealed ampoules filled with dry Ar before use.

Especially, the cell for electromigration was revised in ① as shown in Fig. 5.3. The cell was considered to be divided into the main part for anode (migration tube) and the substitute part for cathode. The melt bath, which contained a mixture of solvent salt LiCl-KCl eutectic composition and fuel component (UCl_3, UCl_4, $NdCl_3$), was kept in the main container. In the sub container, $PbCl_2$ was melted for reduction to Pb metal instead of the reduction of ionic bath elements. The main container and the sub container were connected by two branch pipes. One of them was gas bypass and the other was ion bypass through quartz wool. Both cathode and anode were made of

super fine graphite rods (5mm ϕ). The upper part of migration tubes had an outlet for Cl_2 gas. The lower part of migration tubes were packed with alumina powder (100 μ m ϕ) in order to prevent the melt from convection in the migration tubes (4mm ϕ). Temperature was kept at 873 K with a temperature controller(Eurotherm Ltd.) and measured by a Pt-PtRh10 thermocouple during migration.

Since all equipments needed to be kept under Ar gas to prevent $NdCl_3$, UCl_3 and UCl_4 from oxidation, we constructed Ar flow system, which is shown in Fig. 5.4. Ar gas line of vinyl pipe was connected by sticking with epoxide polymer. Ar gas was purified by the purifier(Unigaz) during experiments. During migration, Cl_2 gas was trapped by NaOHaq. solution. Before electromigration, migration tubes were preheated and saturated by Ar and then moved into the main cell. The sample melt containing $NdCl_3$, UCl_3 and UCl_4 with desired compositions was well mixed by Ar gas bubbling. The melt was introduced into the migration tubes by suction through a T-type stopcock. Constant current supplier(Unitra - Unima, Poland) fed electric currents of 20mA and 50mA. Transported charge was measured by a Cu coulometer. After about 1000C was transported, the migration tubes were removed from the bath and the salt was quenched quickly. The edge of the migration tubes were covered by epoxide polymer immediately and cleaned outside and cut into several pieces with 7~8 mm length in a glove box. The salt in each fraction was weighed for estimating the amount of solvent salt and dissolved in hydrochloric acid. The amount of Nd was analyzed by the Arcenazo III method (colorimetry: λ = 650nm)[28] by a colorimeter(Carl Zeiss, Jena). The amount of U was analyzed also by the Arcenazo III method after reduction by Zn metal(λ = 665nm)[28]. The amount of Li and K was determined by ICP spectrophotometry(Perkin-Elmer).

In the series of experiments ②, the cell used for electromigration was of the

similar type shown in Chapter 2. Especially, the melt bath contained a mixture of LiCl-KCl of the eutectic composition as well as sample salts(CsCl, $SrCl_2$ and $GdCl_3$). The melt was well mixed and was introduced directly from the salt bath into the migration tube through the bottom by sucking with a handy pump. Temperature was kept at 873 K $\pm$ 2 K during migration. Since the melts should be kept under Ar gas atmosphere for preventing $GdCl_3$ from oxidation and LiCl from hydration, we have performed all migration in an Ar-flow glove-box(Vacuum Atmosphere Corp. MO40-2) with purification columns. The amount of Sr, Li and K in each fraction was determined by flame spectrophotometry and Cs was determined by absorption spectrometry(Hitachi Corp. Z-6100). The amount of Gd was analyzed by ICP spectrometry(Seiko Denshi Kogyo SPS-7000).

We have performed a series of experiments of CsCl (x_{Cs}=0.0042～0.0891) in the LiCl-KCl eutectic melt at first and then a few experiments of $SrCl_2$ (x_{Sr}=0.0013～0.0120) in the LiCl-KCl eutectic melt. Then, we have employed all the reagents (CsCl, $SrCl_2$ and $GdCl_3$) (x_{Cs}=0.0048～0.115, x_{Sr}=0.0013～0.0217, x_{Gd}=0.0001～0.0034) in the LiCl-KCl eutectic melt.

5.3 Results

ε was defined as,

$$\varepsilon = (u_1 - u_2) / \bar{u} \qquad (5.1)$$

where u_1 was the internal mobility of 1, that is, Nd, U, Cs, Sr, Gd, u_2 was the average internal mobility of the solvent, that is the LiCl-KCl mixture of the eutectic composition, $\bar{u}$ was the average cation mobility of all the cations concerned. The ε values were calculated by Eq.(5.2) based on the material balance,

$$\varepsilon = -(F / Q)(N_1 / x_1 - N_2 / x_2) \qquad (5.2)$$

where Q was the transported charge, N_M the total quantities in mole of $(1/Z)M^{Z+}$ in the separation tube from the anode to the position where the chemical composition remained unchanged during electromigration and x_M the mole fractions before electromigration. The LiCl-KCl mixture has a Chemla crossing point at $x_{Li} \approx 0.78$ at 873 K[29]. However, for a conventional calculation, LiCl-KCl eutectic was considered to be a quasi-one component system, because the mobilities of Li and K are very similar at the eutectic composition[30]. The $\varepsilon < 0$ means that Nd, U, Cs, Sr or Gd migrates slower than Li and K. The values of ε are given in Tables 5.1 and 5.2 together with the main experimental conditions.

One of the results of the salt distribution along the tubes in each fraction in the system of $NdCl_3$ in the LiCl-KCl eutectic melt and one of the results in the system of UCl_3 and UCl_4 in the LiCl-KCl eutectic melt are shown in Figs. 5.5 and 5.6, respectively. One of the results of the salt distribution along the tubes in each fraction in the system of CsCl in the LiCl-KCl eutectic melt and another result in the system of CsCl, $SrCl_2$ and $GdCl_3$ in the LiCl-KCl eutectic melt are shown in Fig. 5.7. In Fig. 5.7, the upper abscissa indicates the distance from the anode.

5.4 Discussion

5.4.1. System of $NdCl_3$, UCl_3 or UCl_4 in the LiCl-KCl eutectic melt

Figures 5.5 and 5.6 show that the electromigration method can concentrate Nd or U near the anode area on the condition of the initial concentration more than $x_M = 10^{-4}$. Table 5.1 shows that even though ε's are much scattered, U and Nd migrates much slower than Li and K. As $\varepsilon_{U^{3+}}$'s and $\varepsilon_{U^{4+}}$'s are smaller than $\varepsilon_{Nd^{3+}}$'s, Uranium is more concentrated from the same initial concentration. Calorimetric investigations[31] suggest that anionic species *e.g.* $[NdCl_6]^{3-}$ are stable, especially in lower concentration of rare earth cations. It is assumed that most of Nd ions and U ions are made complex ions with chloride. On comparison between UCl_3 and UCl_4 systems, the $\varepsilon_{U^{4+}}$'s are nearly equal to $\varepsilon_{U^{3+}}$'s. $\varepsilon_{U^{3+}}$'s and $\varepsilon_{U^{4+}}$'s are calculated on the average to be -0.95 and -0.914, respectively. In previous works[7],[8], internal moblilities were much influenced by the difference of the cationic charge. However, in UCl_3 system, the color of solidified salt in the migration tubes in the area near the anode changed from red to yellow-green. It is supposed that this change of color is caused by oxidation of U^{3+} by chlorine gas. The relative difference of internal cation mobilities is calculated by the material and charge balances through an arbitrary plane where the concentration unchange. As some amount of U^{3+} was oxidized to U^{4+} in the area near the anode, it is supposed that U^{4+} migrated through the plane in the UCl_3 system.

5.4.2. System of CsCl in the LiCl-KCl eutectic melt

Figure 5.7 shows the electromigration method can concentrate Cs near the anode area on the condition of the initial concentration $x_{Cs} > 4 \times 10^{-3}$. The values of $-\varepsilon_{Cs}$ in this system are plotted against x_{Cs} in Fig. 5.8. The values of $-\varepsilon_{Cs}$ seem to be almost constant at $x_{Cs} < 0.09$. Though the data on $-\varepsilon_{Cs}$ are scattered at $x_{Cs} < 10^{-2}$, Cs migrates more slowly than Li and K.

As we mentioned before, the Chemla crossing point exists in the isotherms in the molten LiCl-CsCl mixture[9]. Although the mobility isotherms have not yet been measured in the molten KCl-CsCl, there must also exist a Chemla crossing point. In the molten binary[32] and ternary alkali nitrates[33], we have found that the internal mobilities of alkali ions are approximately expressed by an empirical equation:

$$u = \{A / (V_m - V_0)\} \exp(-E / RT) \qquad (5.3)$$

where V_m is the molar volume and A, V_0 and E are constants characteristic of the cation of interest and nearly independent of the coexisting cations. Also in the chloride systems, such an equation is assumed to exist. In the LiCl-KCl system and the LiCl-CsCl system, V_m's at the Chemla crossing point are $\sim 32 \times 10^{-6} m^3 mol^{-1}$ [9], and $\sim 35 \times 10^{-6} m^3 mol^{-1}$ [29] respectively, at 873 K, while the KCl-CsCl system has not been studied yet. Therefore, in the ternary mixture of LiCl-KCl-CsCl, there will not exist a molar volume (and therefore a composition) where the mobilities of these 3 cations are equal. Thus, the sequence of u_{Li}, u_K and u_{Cs} is dependent on the composition. As far as concentration of CsCl is low, there must be a concentration range where $u_{Cs} < u_{Li} \approx u_K$.

5.4.3. System of CsCl, $SrCl_2$ and $GdCl_3$ in the LiCl-KCl eutectic melt

In the mixture of CsCl, $SrCl_2$ and $GdCl_3$, Cs, Sr and Gd can be enriched near the anode, as shown in Fig. 5.7. Figure 5.7 shows these are more enriched in the 2nd fraction than in the 1st one, because the salt in the 1st fraction happened to contain salt unelectromigrated to some extent. Although such a case often occurs, this does not affect the calculation of the ε value by Eq. (5.2)[34]. Figure 5.7 shows also that, $-\varepsilon_{Gd}$ and $-\varepsilon_{Sr}$ are clearly larger than $-\varepsilon_{Cs}$. The coulombic interaction between Gd^{3+} and Cl^- and between Sr^{2+} and Cl^- is much stronger than that between Cs^+ and Cl^-. In the molten KCl-$Dy_{(1/3)}Cl$[7]and KCl-$Ca_{(1/2)}Cl$ [8], Dy and Ca were well enriched from their low concentrations, respectively, as mentioned previously. Thus, this electromigration method could be effectively used for separation of multivalent cations from monovalent cations.

The values of $-\varepsilon_{Cs}$ in the mixture system are plotted also in Fig. 5.8. In this system, $-\varepsilon_{Cs}$ decreases with increasing x_{Cs}. At higher x_{Cs}, the Chemla crossing point, where $\varepsilon_{Cs} = 0$, is expected to be observed. $-\varepsilon_{Cs}$ in the mixture system is less than those of the system containing mainly Cs. This may be accounted for in terms of the tranquilization effect[35] by Gd^{3+} and Sr^{2+} on internal mobilities of Cs^+. The tranquilization effect occurs by the strong coulombic interaction of cations with the common anion Cl^-. In the molten KCl-$Dy_{(1/3)}Cl$[7] and KCl-$Ca_{(1/2)}Cl$[8] mixtures, internal mobilities of K^+ decrease with increasing mole fractions of Dy^{3+} and Ca^{2+}, respectively, owing to the tranquilization effect. The tranquilization effect becomes more effective for the second monovalent cation of a larger ionic radius, because Cl^- ions are more attracted to multivalent cations in the large-monovalent cation neighbors than in the small-monovalent ones[36]. When Cl^- ions are associated by multivalent cations, the tranquilization effect of these cations on the internal mobility of the monovalent cation

will occur. Thus, the electromigration method will be used as a powerful tool to separate multivalent materials from coexisting Cs^+.

On the other hand, Gd was more concentrated at its lower concentration as seen from Table 5.2. Raman spectroscopic studies suggest that there exist anionic complexes such as $[GdCl_6]^{3-}$ in the mixture with the alkali metal chlorides[37]. Thermodynamic studies of mixing enthalpy[38] also suggest that these anionic complexes are stable, especially at lower concentration of rare earth cations. Thus, in lower concentration of Gd, this associated species is conjectured to be the main electrically-conductive species.

For the future R&D, we should estimate the energy required for the electromigration process by using data available for the fission yields at the equilibrium state as well as the data on ε_M's for each element. We should check the limit of maximum concentration in the migration column, because the salt containing concentrated elements will be solidified near the anode if its melting point is high. Furthermore, for application of the electromigration method to the practical plant, we should arrange the column so as to take out the concentrated fission products continuously.

Table 5.1 Experimental conditions and relative difference in internal mobilities at 873 K.

(1a) *$NdCl_3$ system*

Run No.	current(mA)	Q(C)	$x_{Nd^{3+}}$	$\varepsilon_{Nd^{3+}}$
a-1	50	905	8.35×10^{-4}	-0.198
a-2	20	998	1.31×10^{-3}	-0.133
a-3	50	1040	2.60×10^{-3}	-0.238
a-4	20	965	4.45×10^{-3}	-0.274
a-5	50	1068	5.45×10^{-3}	-0.535
a-6	20	1260	7.22×10^{-3}	-0.286
a-7	50	805	1.19×10^{-2}	-0.503
a-8	20	1144	1.28×10^{-2}	-0.613
a-9	50	1003	2.51×10^{-2}	-0.704
a-10	20	1063	2.34×10^{-2}	-0.734

(1b) *UCl_3 system*

Run No.	current(mA)	Q(C)	$x_{U^{3+}}$	$\varepsilon_{U^{3+}}$
b-1	50	978	4.75×10^{-5}	-1.12
b-2	20	934	2.94×10^{-5}	-1.39
b-3	50	1074	1.48×10^{-4}	-0.848
b-4	20	925	1.31×10^{-4}	-0.377
b-5	50	994	9.05×10^{-4}	-0.782
b-6	20	957	8.77×10^{-4}	-0.970

(Table 5.1 continued)

b-7	50	987	2.63×10^{-3}	-0.873
b-8	20	951	1.64×10^{-3}	-1.24

(1c) *UCl_4 system*

Run No.	current(mA)	Q(C)	$x_{U^{4+}}$	$\varepsilon_{U^{4+}}$
c-1	50	1009	2.91×10^{-5}	-1.39
c-2	20	835	7.04×10^{-5}	-1.59
c-3	20	955	1.24×10^{-4}	-0.652
c-4	50	983	1.04×10^{-3}	-0.733
c-5	20	943	1.06×10^{-3}	-0.777
c-6	50	908	2.11×10^{-3}	-0.693
c-7	20	908	2.11×10^{-3}	-0.563

Table 5.2 Experimental conditions and relative differences in internal mobilities at 873 K.

(2a) *system of CsCl in the LiCl-KCl eutectic melt*

Run No.	current (A)×(h)	Q (C)	Voltage (V)	x_{Cs}	ε_{Cs}
a-1	0.06×11	2436	15	0.0042±0.0002	-0.067±0.019
a-2	0.1×12	4379	25	0.0043±0.0002	-0.123±0.010
a-3	0.1×6	2237	25	0.0049±0.0003	-0.060±0.007
a-4	0.2×6	4485	45	0.0090±0.0007	-0.085±0.011
a-5	0.1×14	5026	25	0.0125±0.0004	-0.099±0.007
a-6	0.1×19	6902	25	0.0146±0.0005	-0.145±0.008
a-7	0.2×6.5	4716	45	0.0374±0.0021	-0.091±0.010
a-8	0.1×12	4643	20	0.0418±0.0054	-0.065±0.016
a-9	0.2×7	5053	50	0.0679±0.0037	-0.086±0.008
a-10	0.1×10	3647	30	0.0836±0.0184	-0.089±0.040
a-11	0.1×16	6001	25	0.0891±0.0039	-0.078±0.006

(2b) *system of $SrCl_2$ in the LiCl-KCl eutectic melt*

Run No.	current (A)×(h)	Q (C)	Voltage (V)	x_{Sr}	ε_{Sr}
b-1	0.2×3	2222	50	0.0013±0.0006	-0.33±0.21
b-2	0.1×1.5+0.2×2	1237	60	0.0026±0.0002	-0.26±0.03
b-3	0.2×1.5	1220	60	0.0120±0.0009	-0.63±0.10

(Table 5.2 continued)

(2c) *system of CsCl, $SrCl_2$ and $GdCl_3$ in the LiCl-KCl eutectic melt*

Run FP	current (A)×(h)	Q (C)	Voltage (V)	x_M	ε_M
c-1-Cs	0.1×15	5450	25	0.0048±0.0005	-0.053±0.016
-Sr				0.0013±0.0000	-0.36±0.02
-Gd				0.0001±0.0000	-14.4±1.1
c-2-Cs	0.2×12	8550	50	0.115±0.018	-0.045±0.010
-Sr				0.0021±0.0003	-6.39±1.02
-Gd				0.0034±0.0003	-0.49±0.05
c-3-Cs	0.2×3	2259	50	0.0695±0.0024	-0.061±0.010
-Sr				0.0217±0.0010	-0.39±0.03
-Gd				0.0034±0.0002	-0.67±0.06
c-4-Cs	0.2×6	4556	50	0.0645±0.0014	-0.073±0.005
Sr				0.0241±0.0043	-0.38±0.08
-Gd				0.0006±0.0002	-3.28±1.36
c-5-Cs	0.2×16	11760	45	0.0651±0.0029	-0.061±0.004
-Sr				0.0015±0.0004	-3.83±1.10
-Gd				0.0007±0.0002	-0.99±0.22
c-6-Cs	0.05×15	3323	20	0.0118±0.0006	-0.075±0.011
-Sr				0.0044±0.0001	-0.32±0.01
-Gd				0.0028±0.0002	-0.23±0.02

(Table 5.2 continued)

The sign ± refers to the errors of chemical analyses.

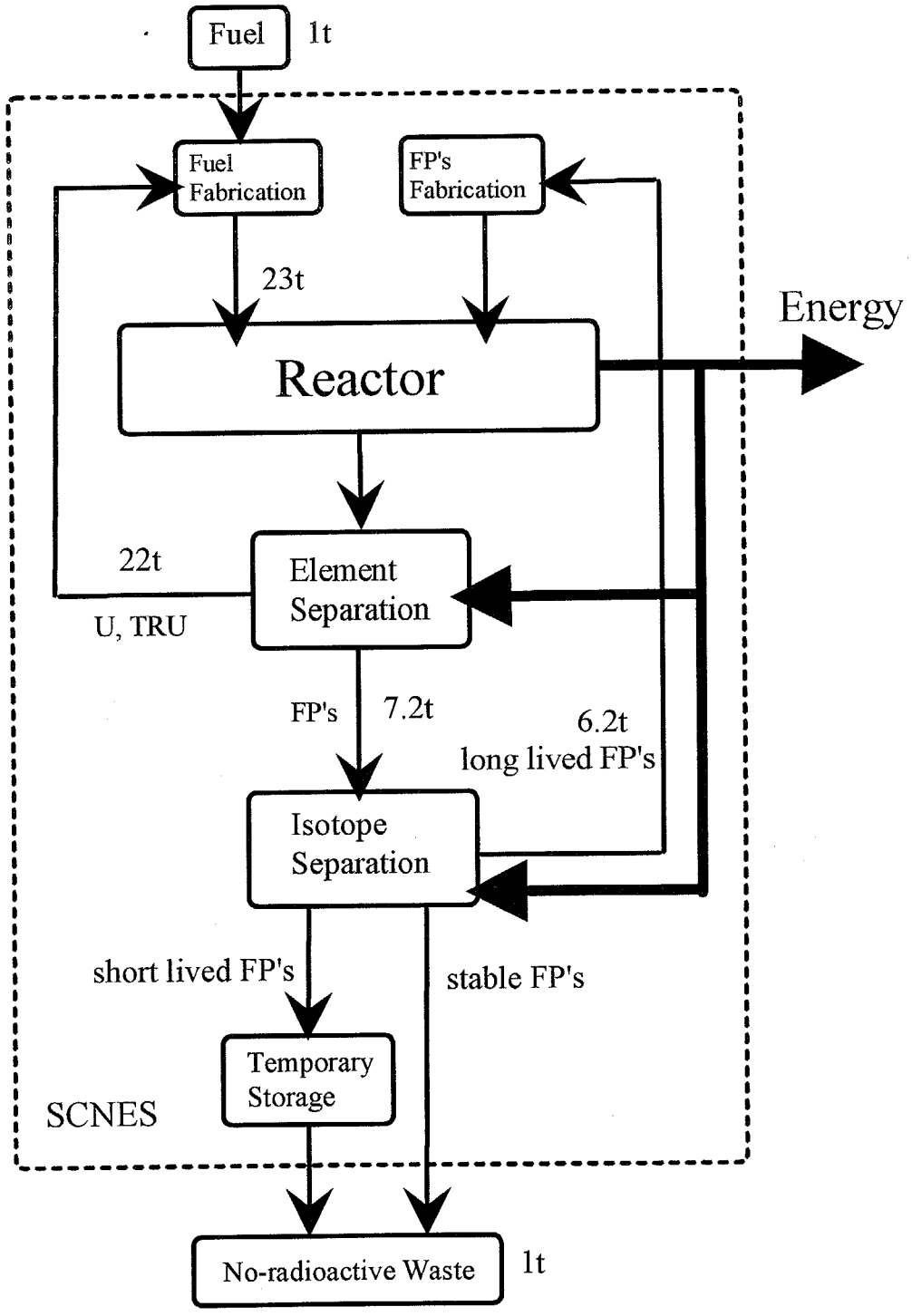

Fig. 5.1 Self-consistent nuclear energy system

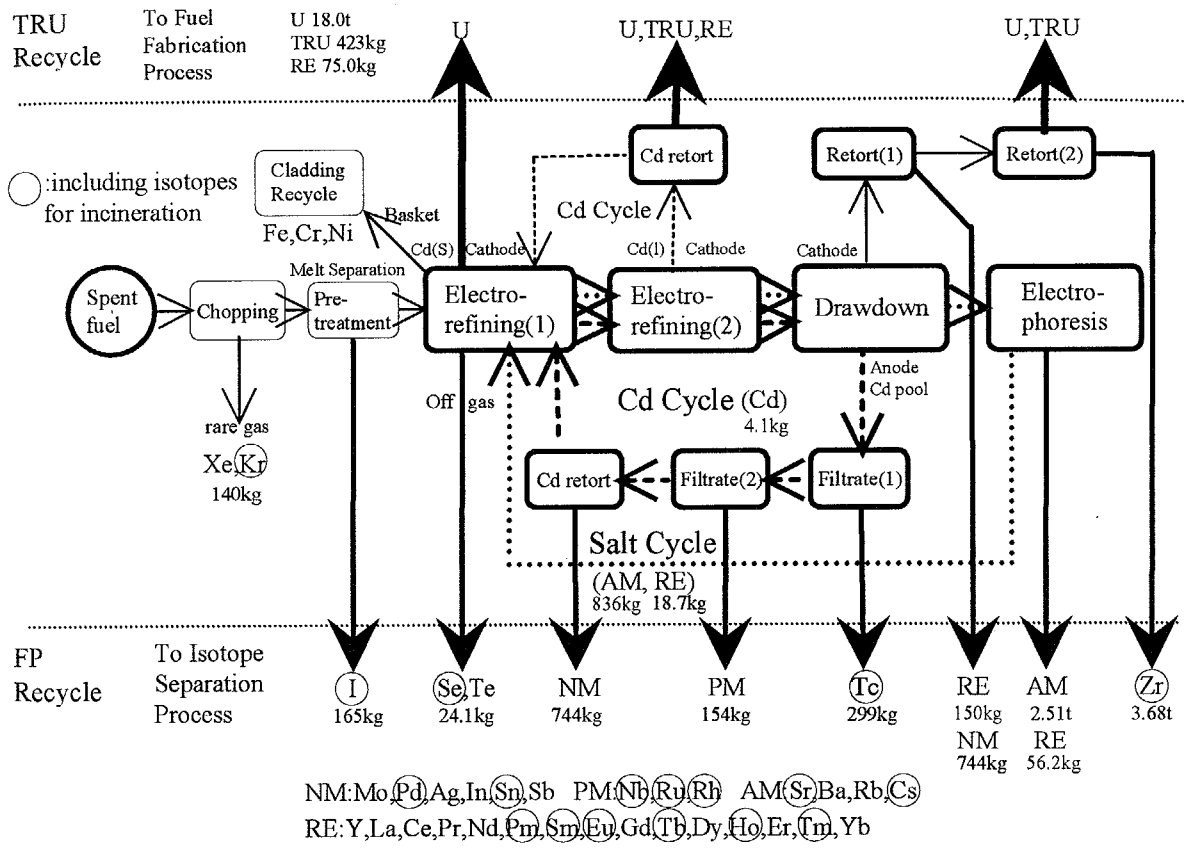

Fig. 5.2 One of the concepts for pyrochemical process using molten chlorides (mass balance)

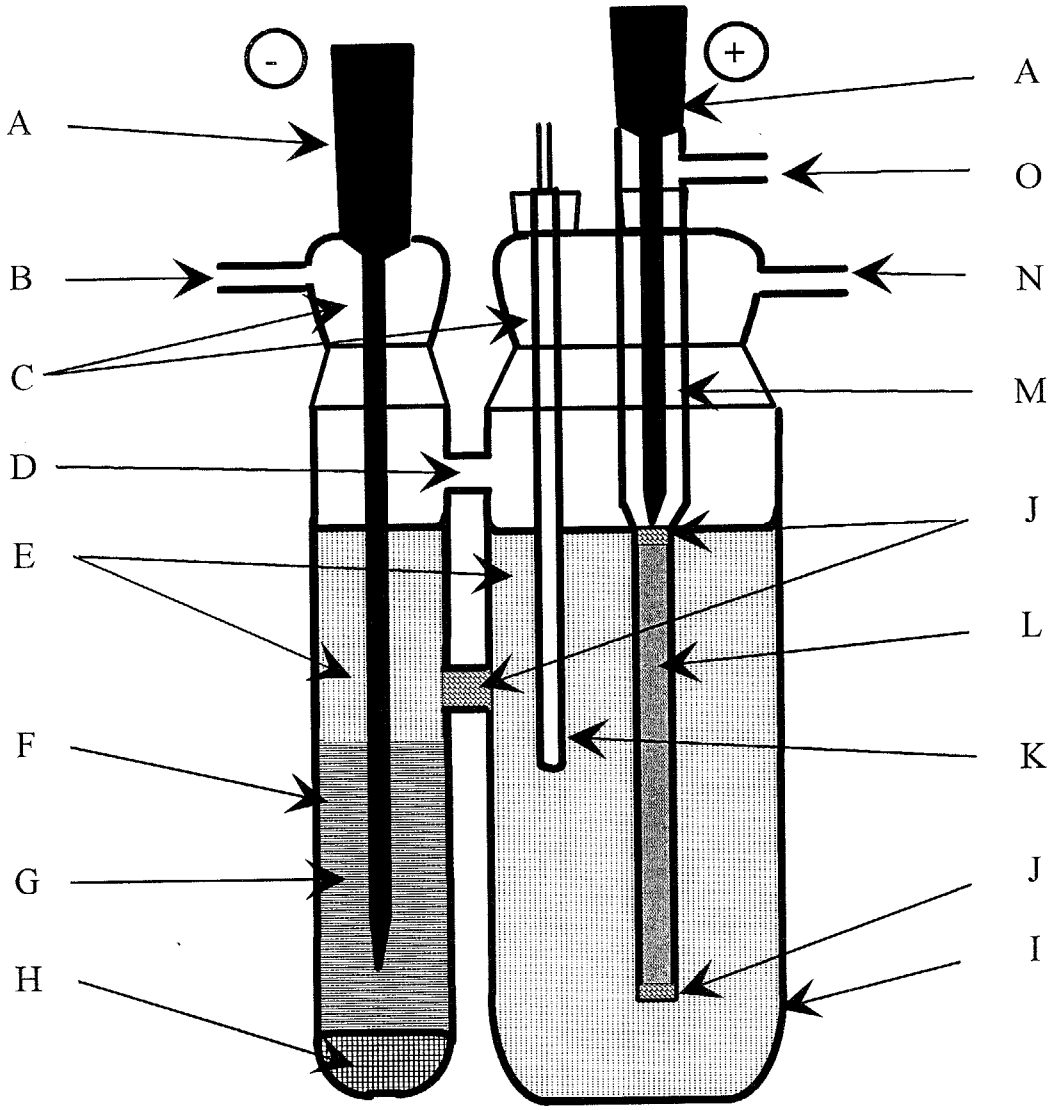

Fig. 5.3 Electromigration cell.

A: graphite electrode; B: Ar gas inlet; C: covers; D: gas bypass; E: molten LiCl-KCl (eutectic) + sample salt ($NdCl_3$, UCl_3, UCl_4); F: sub-container; G: molten $PbCl_2$; H: molten Pb metal; I: main-container; J: quartz wool; K: thermocouple; L: alumina powder; M: migration tube; N: Ar gas outlet; O: Cl_2 gas outlet.

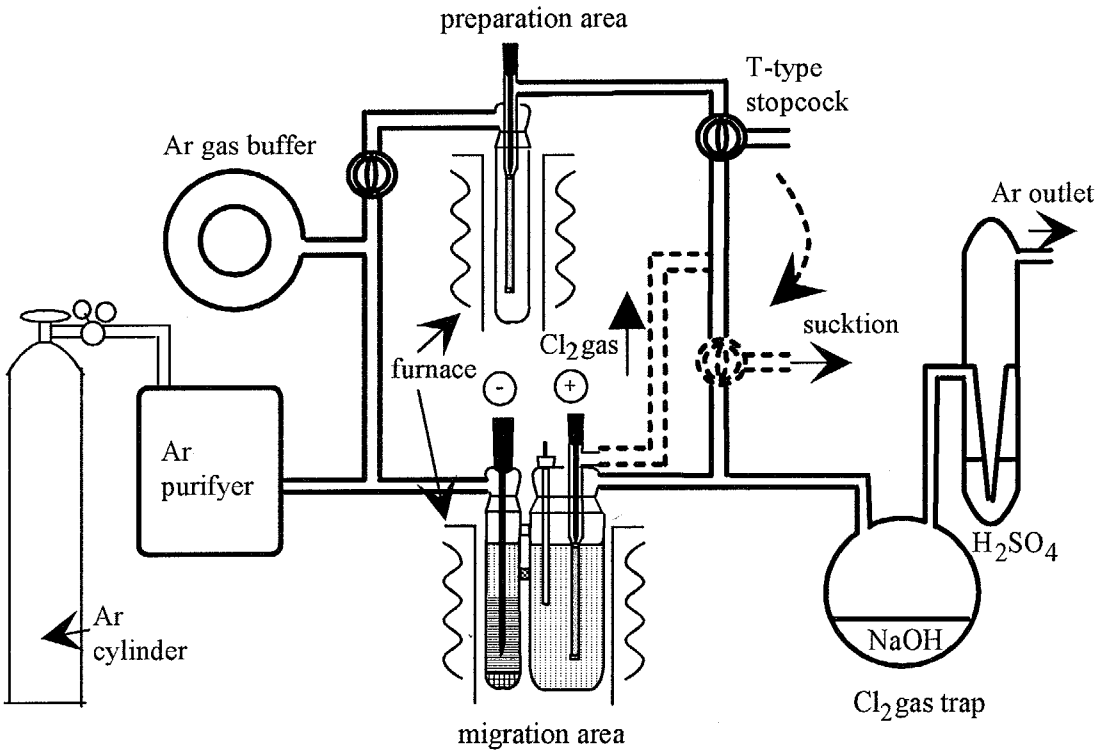

Fig. 5.4 Ar circulating system for electromigration.

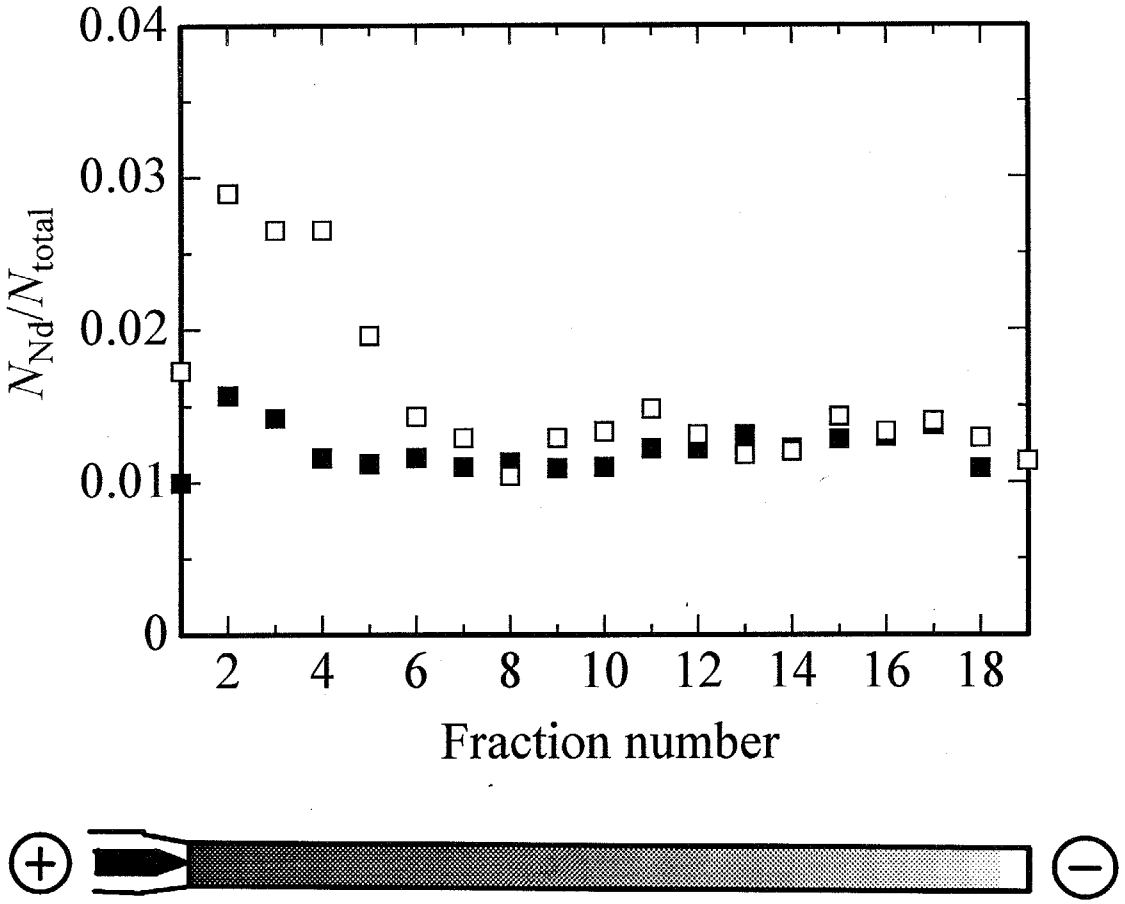

Fig. 5.5 One of the concentration profile in the migration tube of $NdCl_3$ system (Run No. a-7 and a-8). ■: $N_{Nd^{3+}}/N_{total}$ on Run a-7; □: $N_{Nd^{3+}}/N_{total}$ on Run a-8.

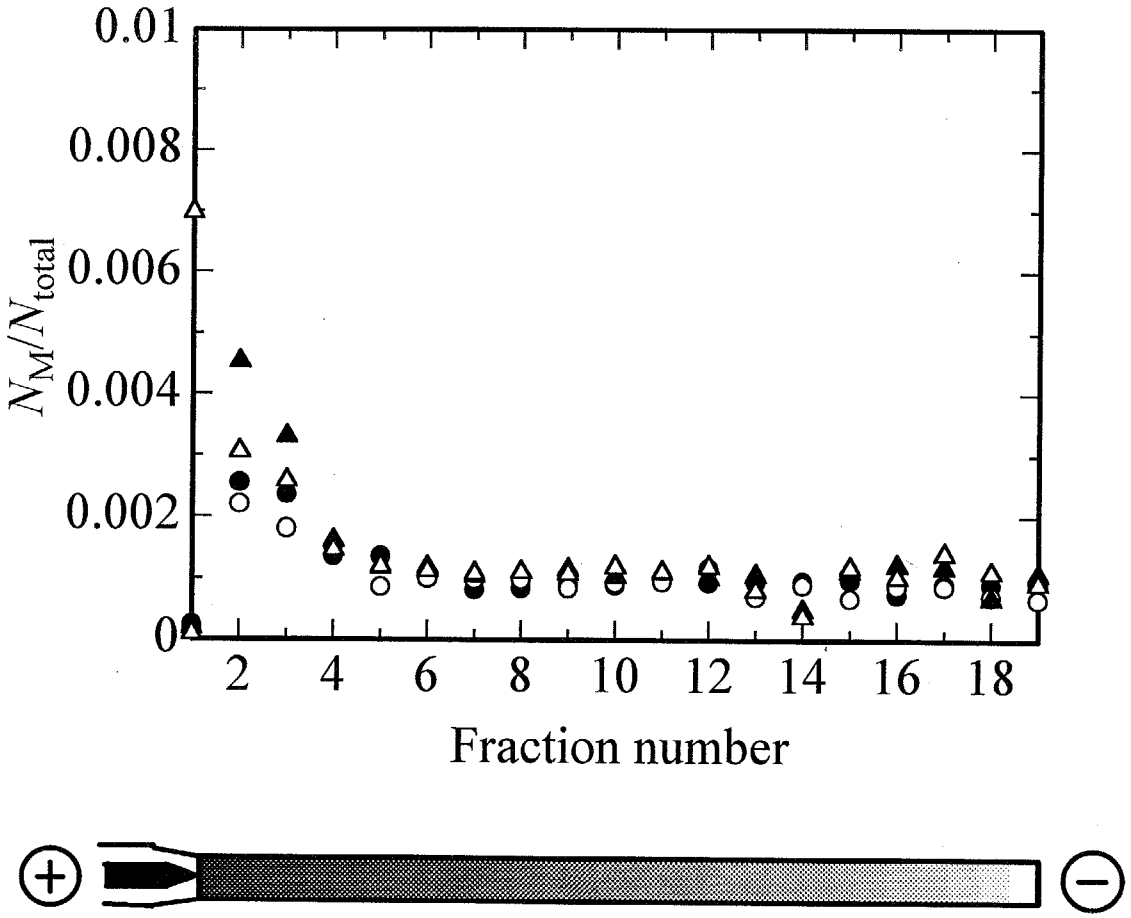

Fig. 5.6 One of the concentration profile in the migration tube of UCl_3 and UCl_4 system (Run No. b-5, b-6, c-4 and c-5). ●: $N_{U^{3+}}/N_{total}$ on Run b-5; ○: $N_{U^{3+}}/N_{total}$ on Run b-6; ▲: $N_{U^{4+}}/N_{total}$ on Run c-4; △: $N_{U^{4+}}/N_{total}$ on Run c-5.

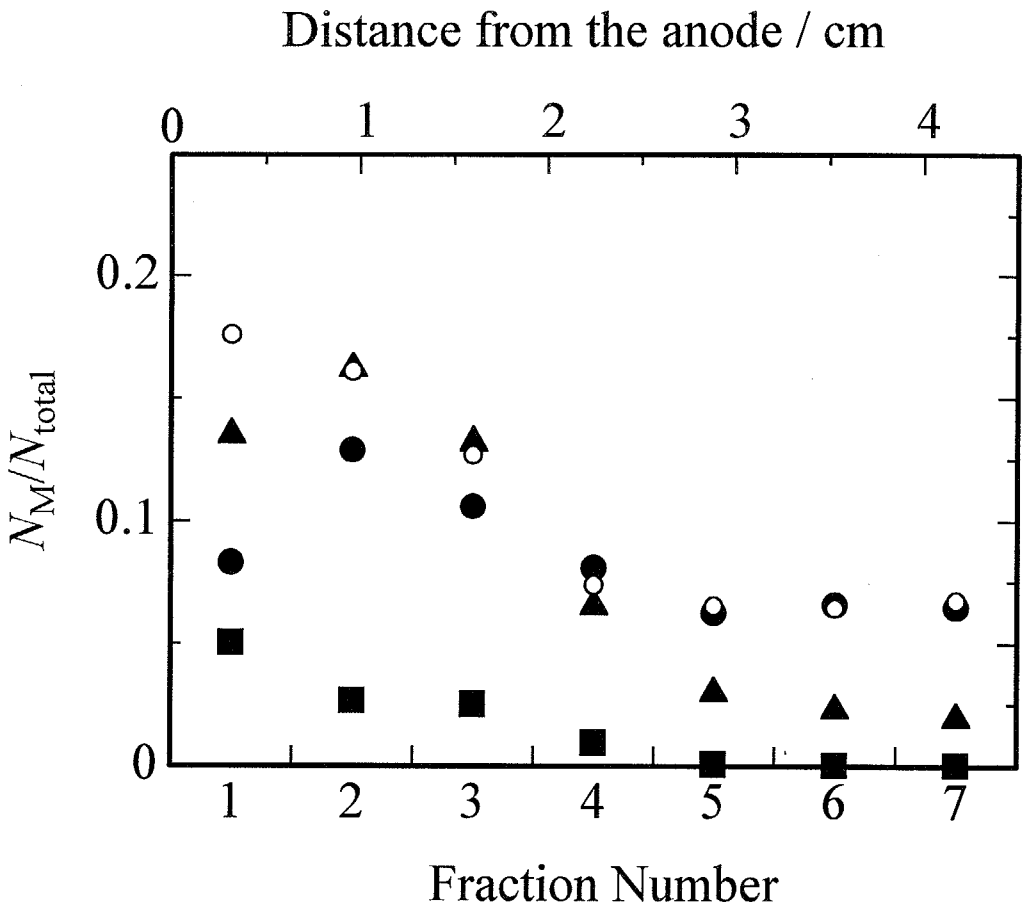

Fig. 5.7 One of the concentration profiles in the migration tubes(Run No.a-9 and c-4). Molar ratio in each fraction, N_M/N_{total};

○:N_{Cs}/N_{total} on Run a-9; ●:N_{Cs}/N_{total} on Run c-4; ▲:N_{Sr}/N_{total} on Run c-4; ■:N_{Gd}/N_{total} on Run c-4.

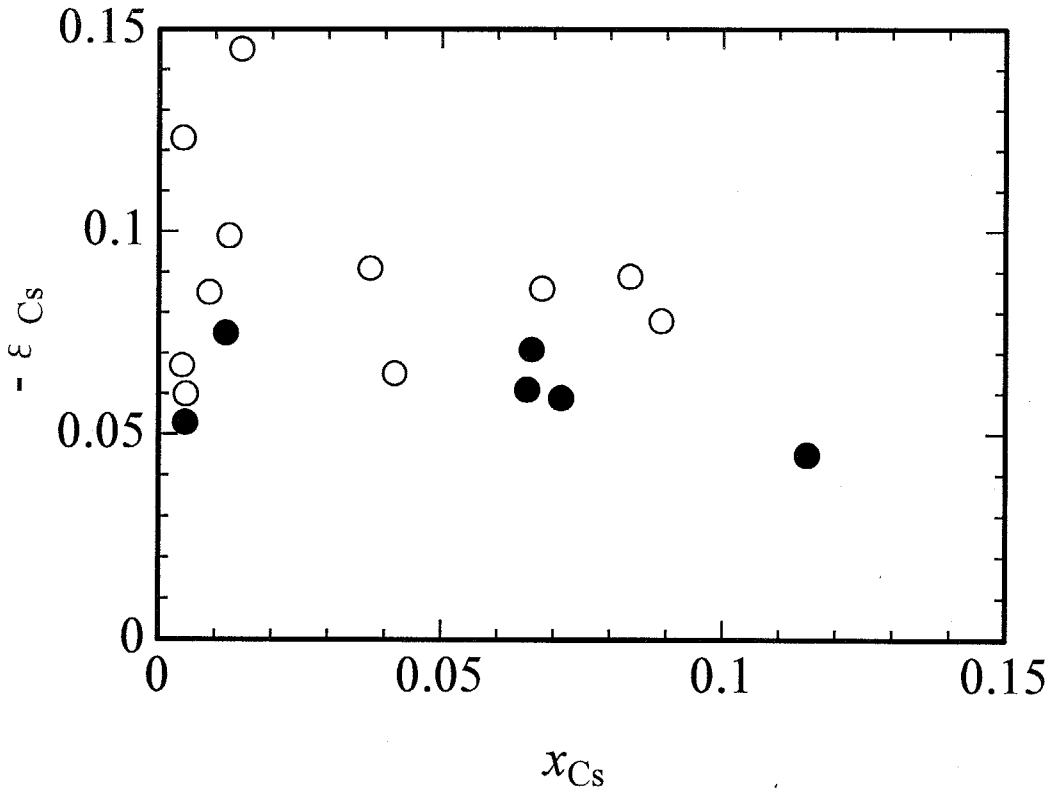

Fig. 5.8 - ε_{Cs} *vs.* x_{Cs} .○:in the system of CsCl in the LiCl-KCl eutectic melt;

●:in the system of CsCl, $SrCl_2$ and $GdCl_3$ in the LiCl-KCl eutectic melt.

References

[1] Integral Fast Reactor Program Summary Progress Report FY 1985 - FY 1989
Y. I. Chang, L. C. Walters, J. E. Battles, D. R. Pedersen, D. C. Wade and M. J. Lineberry, *ANL-IFR-125* (1990).

[2] Self-Consistent Nuclear Energy Systems
A. Shimizu and Y. Fujii-e, *Prog, Nucl. Energy*, **29**, (*Suppl.*) 25-32 (1995).

[3] A Fuel Cycle Concept for Self-Consistent Nuclear Energy System
R. Takagi, H. Matsuura, Y. Fujii-e, R. Fujita and M. Kawashima, *Prog. Nucl. Energy*, **29**, (*Suppl.*) 471-476 (1995).

[4] Anreichrung des shweren Silberisotops durch Ionenwanderung in Silberjodid
A. Klemm, *Naturwissenshaften*, **32**, 69-70 (1944).[in German]

[5] Anreicherung der schweren Isotope von Li und K durch elcktrolytische Ionenwanderung in geschmolzenen Chloriden
A. Klemm, H. Hintenberger and P. Hoernes, *Z. Naturforsch.*, **2a**, 245-249 (1947) [in German].

[6] Enrichment of Li-6 by Countercurrent Electromigration in Molten $LiNO_3$
T. Haibara, O. Odawara, I. Okada, M. Nomura and M. Okamoto, *J. Electrochem. Soc.*, **136**, 1059-1063 (1989).

[7] Internal Cation Mobilities in Molten (K, $Dy_{1/3}$)Cl
H. Matsuura, I. Okada, R. Takagi and Y. Iwadate, *Z. Naturforsch.*, **53a**, 45-50 (1997).

[8] Internal Cation Mobilities in the Molten Binary System (K, $Ca_{0.5}$)Cl
H. Matsuura and I. Okada, *Denki Kagaku*, **61**, 732-733 (1993).

[9] The Chemla effect in the mobilities in the molten binary system of lithium chloride and caesium chloride
I. Okada and H. Horinouchi, *J. Electroanal. Chem.*, **396**, 547-552 (1995)

[10] Effects of Structural Variation within Proton-Ionizable Crown Ethers upon the Selectivity and Efficiency of Solvent Extraction of Alkali Metal and Alkaline Earth Cations
R. A. Bartsch, *Solv. Extr. and Ion Exch.*, **7**, 829-854 (1989).

[11] Selectivity in Stripping of Alkali-Metal Cations from Crown Ether Carboxylate Complexes
R. A. Bartsch, W. Walkowiak and T. W. Robinson, *Separation Sci. and Tech.*, **27**, 989-993 (1992).

[12] Correlation of the Extraction of Strontium Nitrate by a Crown Ether with the Water Content of the Organic Phase
E. P. Horwitz, M. L. Dietz and D. E. Fisher, *Solv. Extr. and Ion Exch.*, **8**, 199-208 (1990).

[13] Extraction of Strontium from Nitric Acid Solutions Using Dicyclohexano-18-Crown-6 and its Derivatives
E. P. Horwitz, M. L. Dietz and D. E. Fisher, *Solv. Extr. and Ion Exch.*, **8**, 557-572 (1990).

[14] SREX: A New Process for the Extraction and Recovery of Strontium from Acidic Nuclear Waste Streams
E. P. Horwitz, M. L. Dietz and D. E. Fisher, *Solv. Extr. and Ion Exch.*, **9**, 1-25 (1990).

[15] Complexing properties of poly-dibenzo-crown ether resins towards inorganic cations. Case of poly-DB18-C6
J. Rault-Berthelot and L. Angély, *Synth. Metals*, **58**, 51-62 (1993).

[16] Adsorption Properties of Crown-16 in Halogenide Melts and Alkali Metal Thiocyanates
N. Kh. Tumanova, G. I. Mironyuk, L. V. Bogdanovich and V. F. Lapshin, *Ukr. Khim. Zhurn.(English Transl.)*, **59**, 576-580 (1993).

[17] Strontium Extraction with a Polymer-Bound 18-Crown-6 Polyether
G. Zirnhelt, M. J. F. Leroy, J. P. Brunette, Y. Ferre and Ph. Gramain, *Separation Sci. and Tech.*, **28**, 2419-2429 (1993).

[18] Influence of the Extractant on Strontium Transport from Reprocessing Concentrate Solutions through Flat-Sheet Supported Liquid Membranes

J. F. Dozol, J. Casas and A. M. Sastre, *Separation Sci. and Tech.*, **29**, 1999-2018 (1994).
[19] Transport of Cesium from Reprocessing Concentrate Solutions through Flat-Sheet-Supported Liquid Membranes: Influence of the Extractant
J. F. Dozol, J. Casas and A. M. Sastre, *Separation Sci. and Tech.*, **30**, 435-448 (1995).
[20] Development of Partitioning Method: Developments of Processing Method of Liquid Waste containing ^{90}Sr and ^{137}Cs with Inorganic Ion Exchanger Column
M. Kubota, I. Yamaguchi, H. Nakamura, K. Okada, F. Mizuno and T. Sato, *JAERI-M* 82-144 (1982), [in Japanese].
[21] Development of Partitioning Method: Dynamic Adsorption Characteristics of Titanic Acid and Zeolite mixed Column for Sr and Cs Ions
R. Mori, I. Yamaguchi and M. Kubota, *JAERI-M* 86-013 (1986), [in Japanese].
[22] Separation of Heat-Generating Nuclides from High-Level Liquid Wastes through Zeolite Columns
H. Mimura, K. Akiba and K. Kawamura, *J. Nucl. Sci. Technol.*, **31**, 463-469 (1994).
[23] Salt-Occluded Zeolites as an Immobilization Matrix for Chloride Waste Salt
M. A. Lewis, D. F. Fischer and L. J. Smith, *J. Am. Ceram. Soc.*, **76**, 2826-2832 (1993)
[24] Enrichment of Lanthanum in Its Dilute Molten Salt Solution
M. Iwasaki and R. Takagi, *J. Nucl. Sci. Technol.*, **31**, 751-753 (1994).
[25] Calorimetric investigation of $NdCl_3$-MCl liquid mixtures (where M is Na, K, Rb, Cs)
M. Gaune-Escard, A. Bogacz, L. Rycerz and W. Szczepaniak, *Thermochim. Acta.*, **236**, 67-80 (1994).
[26] Electrical Conductivities, Densities, and Surface Tensions of Molten Salts in the System LiCl-UCl_4
A. Bogacz and B. Ziólek, *Roczniki Chemii Ann. Soc. Chim. Polonorum*, **14**, 857-870 (1970)
[27] D. Brown, "*Halides of the Lanthanides and Actinides*", p. 757 (1958), [in Russian].
[28] Z. Marczenko, "*Spektrofotometryczne oznaczanie pierwiastkow*" 3rd. ed., PWN, Warszawa, (1979), [in Polish].
[29] Internal Cation Mobilities and their Isotope Effects in the Molten System (Li, K)Cl
A. Lundén and I. Okada, *Z. Naturforsch.*, **41a**,1034-1040 (1986)
[30] Relative Cation Mobilities in Potassium Chloride-Lithium Chloride Melts
C. T. Moynihan and R. W. Laity, *J. Phys. Chem.* **68**, 3312-3317 (1964)
[31] $NdCl_3$ and Alkali Chlorides Mixtures: Calorimetric Investigation and Modeling
M. Gaune-Escard, A. Bogacz, L. Rycerz and W. Szczepaniak, *Mat. Sci. Forum*, **73-75**, 61-70 (1991)
[32] Internal Cation Mobilities in the Molten Systems (Li-Na)NO_3 and (Na-Cs)NO_3
C. -C. Yang, R. Takagi and I. Okada, *Z. Naturforsch.*, **35a**, 1186-1191 (1980).
[33] Internal Cation Mobilities in the Ternary Molten System (Li, Na, K)NO_3 of the Eutectic Composition
J. Habasaki and I. Okada, *Z. Naturforsch.*, **40a**, 906-908 (1987).
[34] Electromigration in Molten and Solid Binary Sulfate Mixtures: Relative Cation Mobilities and Transport Numbers
V. Ljubimov and A. Lundén, *Z. Naturforsch.*, **21a**, 1592-1600 (1966).
[35] Internal Cation Mobilities in the Molten Binary System KNO_3-$Ca(NO_3)_2$
J. Habasaki, C. Yang and I. Okada, *Z. Naturforsch.*, **42a**, 695-699 (1987)
[36] A Dynamic Dissociation Model for Internal Mobilities in Molten Alkali and Alkaline Earth Nitrate Mixtures
T. Koura, H. Matsuura and I. Okada, *J. Mol. Liquids.*, **73/74**, 195-208 (1997)
[37] Raman Spectra of Molten $GdCl_3$-KCl and $GdCl_3$-NaCl
A. Matsuoka, K. Fukushima, K. Igarashi, Y. Iwadate and J. Mochinaga, *Nippon Kagaku Kaishi*, **1993**, 471-474[in Japanese]
[38] Mixing Enthalpy and Structure of the Molten NaCl-$DyCl_3$ System
R. Takagi, L. Rycerz and M. Gaune-Escard, *Denki Kagaku*, **62**, 240-245 (1994)

Chapter 6.

Conclusion

The profiles of the isotherms of the internal cation moblities in $(Ca, Ba)_{(1/2)}Cl$ system are similar to those in alkali chlorides, although the values of u_{Ca} and u_{Ba} are smaller than those of u_{Na} and u_K, respectively, by a factor of 2~3. The present results suggest that the general rules so far found for the internal mobilities in the binary alkali chlorides hold also for those for binary alkaline-earth chlorides. The main electrically-conducting species in alkaline-earth chloride melts are conjectured to be monoatomic ions.

In $(Y, La)_{(1/3)}Cl$, u_{La} is greater than u_Y over all the range investigated. The larger cation, La^{3+}, is more mobile than the smaller one, Y^{3+}, probably because the cation-anion interaction is weaker for the former than for the latter. The isotherms of u as a function of the molar volume are quite similar to those observed generally for binary monovalent and binary divalent cation systems in that the mobilities increase with decreasing molar volume, but are different in that the increasing magnitude is greater for the larger cation (La^{3+}) than for the smaller one (Y^{3+}). This difference may be ascribed to the difference in the coordination structures of the two cations in the molten state.

In $(Y, Dy)_{(1/3)}Cl$ u_Y is slightly greater than u_{Dy}. Since the difference in the cationic radii is very small, the difference in the masses is probably the dominant factor in the mobilities.

The main cationic electrically conducting species are conjectured to be the nonassociated trivalent cations in all the rare earth chloride melts, although their lifetime is presumably very short.

The isotope effect on internal mobilities of Dy has been measured in molten $Dy_{(1/3)}Cl$ by countercurrent electromigration. The lighter Dy isotopes migrate faster

toward the cathode. If the mass ratio of the cation to the anion is taken into account, the isotope effect of Dy is large as compared with those of monovalent and divalent cations. Thus, the main electrically conducting species in molten dysprosium chloride are conjectured to be nonassociated Dy^{3+} and therefore also Cl^- ions.

Internal cation mobilities in the molten binary systems (K, $Ca_{(1/2)}$)Cl and (K, $Dy_{(1/3)}$)Cl have been measured by Klemm's countercurrent electromigration at 1073 K and at 1093 K, respectively. Especially, this was the first trial of this method applied to a molten (alkali metal-rare earth metal) cation mixture system with a common anion. u_K is greater than u_{Ca} in the whole concentration range, as previously observed in the systems of nitrates. u_K is much (ca. 3~10 times) greater than u_{Dy} in the whole concentration range, as expected. Thus, this method may be used for effective separation of monovalent ions and multivalent ions.

As concentration of multivalent cations increases, u_K considerably decreases. This decrease is ascribed to the tranquilization effect by multivalent cations which strongly interacts with Cl^- ions.

As concentration of K^+ increases, u_{Ca} gradually increases. This increase may be attributed to the agitation effect by active monovalent cations. Meanwhile, as concentration of K^+ increases, u_{Dy} gradually decreases and becomes considerably small in the concentration range rich in KCl. This decrease may be attributed to a promoted association of species containing Dy^{3+} and generation of the isolated species $[DyCl_6]^{3-}$. It could not be concluded by the present experiment, however, whether the electrically conducting species containing Dy is cationic or anionic in the concentration range rich in KCl.

We have carried out two series of experiments of countercurrent electromigration using the LiCl-KCl eutectic melt solvent: the solutes were①$NdCl_3$, UCl_3 or UCl_4, ②

$CsCl$, $SrCl_2$ or the mixture of $CsCl$, $SrCl_2$ and $GdCl_3$. We have measured the relative differences in internal mobilities, ε_M's for each experiment with respect to that of the solvent salt, where the mobilities of Li and K are regarded as practically equal. In the system of $NdCl_3$, UCl_3 or UCl_4 in the LiCl-KCl eutectic melt, Nd and U were concentrated. As U is better enriched than Nd, we can show also the applicability of the electromigation method for separation between U and rare earth elements. In the system of CsCl in the LiCl-KCl eutectic melt, Cs was also concentrated. As Gd and Sr were enriched better than Cs, we can propose applicability of the electromigation method for separation between multivalent materials and monovalent materials. If we apply the electromigration method to remove the fission products from the ionic bath, we should pass a little electric charge to the cell at first in order to remove U, Gd and Sr, and then, continuously we should transfer more charge to the cell for removing Cs. If we can find the column arrangement in order to take out the concentrated fission products continuously, the electromigration method may be applied to the salt bath cleaning process as well as to treatment of high-level radioactive wastes.

Acknowledgments

The work presented in this thesis has been performed mainly at Department of Electronic Chemistry (chapter 3 and 4), and Research Laboratory for Nuclear Reactors (chapter 5) , Tokyo Institute of Technology.

The work (chapter 3) was partly performed at Department of Materials Science, Faculty of Engineering, Chiba University.

The work (chapter 5) was, in part, performed for cooperative research between Institute of Inorganic Chemistry and Metallurgy, Technical University of Wroclaw, Poland and Research Laboratory for Nuclear Reactors, Tokyo Institute of Technology, Japan.

I am deeply indebted to Professor I. Okada for his continuing guidance and valuable discussion during the present work.

I am grateful to Professor R. Takagi for his guiding my work and arranging my visit to Poland.

I am also grateful to Professor S. Okazaki, Professor Y. Fujii, Professor K. Tokuda and Professor A. Morikawa for their useful suggestions and encouragement.

I am grateful to Professor M. Okamoto and Dr. M. Nomura of Tokyo Institute of Technology for making the ICP spectrometer and the mass spectrometer available for me.

I gratefully acknowledge Professor J. Mochinaga, Professor Y. Iwadate and Ms. K. Fukushima of Chiba University for assistance in preparing the chemicals and measuring the conductivities and providing me with many valuable data. I express appreciation to Mitsui Mining Smelting Company, Ltd., for providing rare earth oxides.

I also gratefully acknowledge Professor W. Szczepaniak, Dr. L. Rycerz and Ms. M. Zablocka for assistance in arrangement of the cell and many interesting experience in

Poland. Especially, I express appreciation to Mr. E. Czermak for glass-blowing complicated quartz cells. I am grateful to PROXIMA Laboratory in Wroclaw for ICP analyses. The financial support of this trip, in part, by Tokyo Electric Power Co. is gratefully acknowledged.

Further, I also express appreciation to the members of SCNES group, Professor Y. Fujii-e, Professor A. Shimizu, Professor H. Sekimoto, Professor H. Tomiyasu, Professor M. Saito, Professor H. Ninokata, Professor M. Suzuki, Professor M. Igashira, Professor H. Akatsuka, Dr. T. Sawada, Dr. T. Obara and Dr. T. Ohsaki of Research Laboratory for Nuclear Reactors, Tokyo Institute of Technology, for valuable discussions in making the flowsheet of SCNES and for a lot of encouragement. Especially, I am grateful to Dr. R. Fujita of Toshiba Co. for many critical discussions and providing me with chemicals.

Lastly, I would like to express my gratitude to Professor O. Odawara, Dr. A. Akiyama and Dr. J. Habasaki and all of the colleagues of Professor Okada's laboratory, Professor Odawara's laboratory, Professor Takagi's laboratory, Professor Mochinaga's laboratory and Professor Szczepaniak's laboratory.

松浦治明

List of Publications

1) Internal Cation Mobilities in the Molten Binary System (K, $Ca_{0.5}$)Cl

Haruaki MATSUURA and Isao OKADA,

DENKI KAGAKU, **61**, 732-733 (1993).

2) Internal Cation Mobilities in Molten (Ca, Ba)Cl_2

Haruaki MATSUURA and Isao OKADA,

Z. Naturforsch., **49a**, 690-694 (1994).

3) A Fuel Cycle Concept for Self-Consistent Nuclear Energy System

Ryuzo TAKAGI, Haruaki MATSUURA, Yoichi FUJII-E, Reiko FUJITA and

Masatoshi KAWASHIMA,

Prog. Nucl. Energy, **29** (Suppl.), Edited by A. Shimizu, Elsevier, Oxford, p. 471-476 (1995).

4) Internal Cation Mobilities in the Molten Binary Systems (Y, La)Cl_3 and (Y, Dy)Cl_3

Haruaki MATSUURA, Isao OKADA, Yasuhiko IWADATE

and Junichi MOCHINAGA,

J. Electrochem. Soc. **143**, 334-339 (1996).

5) The Isotope Effect on the Internal Cation Mobility of Molten Dysprosium Chloride

Haruaki MATSUURA, Isao OKADA, Masao NOMURA, Makoto OKAMOTO and

Yasuhiko IWADATE,

J. Electrochem. Soc., **143**, 3830-3832 (1996).

6) High Enrichment of Uranium and Rare Earth Elements in Ionic Salt Bath by Countercurrent Electromigration

Haruaki MATSUURA, Ryuzo TAKAGI, Monika ZABLOCKA-MALICKA,

Leszek RYCERZ and Wlodzimierz SZCZEPANIAK,

J. Nucl. Sci. Technol., **33**, 895-897 (1996).

7) Enrichment of Fission Products in Ionic Salt Bath by Countercurrent Electromigration

Haruaki MATSUURA, Ryuzo TAKAGI, Isao OKADA and Reiko FUJITA,

J. Nucl. Sci. Technol., **34**, 304-309 (1997).

8) Internal Cation Mobilities in Molten (K, $Dy_{1/3}$)Cl

Haruaki MATSUURA, Isao OKADA, Ryuzo TAKAGI and Yasuhiko IWADATE,

Z. Naturforsch., **53a**, 45-50 (1998).

References

1) Solvent Extraction of p-Nitrophenol into Cyclohexane with Phoshines and Their Derivatives

Hirochica NAGANAWA, Haruaki MATSUURA, Yasushi OGIHARA,

Satoshi KUSAKABE and Tatsuya SEKINE,

Anal. Sci., 287-289 (1990)

2) Internal Cation Mobilities in the Molten Systems (Ag, Rb)NO_3 and (Ag, Cs)NO_3 Remeasured by the Klemm Method,

Pao-hwa CHOU, Haruaki MATSUURA and Isao OKADA,

Z. Naturforsch., **48a**, 1207-1213 (1993).

3) Activity Coefficients of Component Ions in LiF-SrF_2 and NaF-SrF_2 Systems

Kazuyoshi NAGAKUBO, Haruaki MATSUURA and Ryuzo TAKAGI,

DENKI KAGAKU, **63**, 938-940 (1995).

4) A Dynamic Dissociation Model for Internal Mobilities in Molten Alkali and Alkaline Earth Nitrate Mixtures,

Tsuneo KOURA, Haruaki MATSUURA and Isao OKADA,

J. Mol. Liquids, **73/74**, 195-208 (1997).

5) A Feasibility Study on FP Incineration for Self-Consistent Nuclear Energy System(SCNES),

Reiko FUJITA, Masatoshi KAWASHIMA, Hiroaki UEDA, Ryuzo TAKAGI, Haruaki MATSUURA and Yoichi FUJII-E,

Proceedings of Grobal Enviroment & Nuclear Energy System, to be published.

List of Presentations

1) Haruaki MATSUURA and Isao OKADA,

Internal Cation Mobilities in the Molten System (Ca, Ba)Cl_2,

Proc. of 59th Conference of The Electrochem. Soc. of Japan, 2C09, Hachioji, p. ?

(1992) [in Japanese].

2) Haruaki MATSUURA and Isao OKADA,

Internal Cation Mobilities in the Molten System (K, $Ca_{0.5}$)Cl,

Proc. of 24th Symposium on Molten Salt Chemistry, B-7, Kyoto, p. 39-40 (1992)

[in Japanese].

3) Haruaki MATSUURA, Isao OKADA, Yasuhiko IWADATE and Junichi MOCHINAGA,

Internal Cation Mobilities in the Molten Binary System (Y, La)Cl_3,

Proc. of the 4th Japan-China Bilateral Conference on Molten Salt Chemistry and Technology, Kyoto, p. 71-74 (1992).

4) Haruaki MATSUURA, Isao OKADA, Yasuhiko IWADATE and Junichi MOCHINAGA,

Internal Cation Mobilities in the Molten Binary System (Y, Dy)Cl_3,

Proc. of 60th Conference of The Electrochem. Soc. of Japan, 1E17, Tokyo, p. '113

(1993)[in Japanese].

5) Internal Cation Mobilities in the Molten Binary System (Y, La)Cl_3,

Haruaki MATSUURA, Isao OKADA, Yasuhiko IWADATE

and Junichi MOCHINAGA,

Proc. of the International Symposium on Molten Salt Chemistry and Technology 1993, Honolulu, Hawaii, p. 155-160 (1993).

6)Haruaki MATSUURA, Isao OKADA, Yasuhiko IWADATE, Masao NOMURA and

Makoto OKAMOTO,
Isotope Effect in the Internal Cation Mobility in Molten Dysprosium Chloride,
Proc. of 25th Symposium on Molten Salt Chemistry, 1A03, Kobe, p. 5-6 (1993)
[in Japanese].

7) Haruaki MATSUURA, Ryuzo TAKAGI, Yasuhiko IWADATE and Isao OKADA,
Internal Cation Mobilities in the Molten Binary System KCl-$DyCl_3$,
Proc. of 26th Symposium on Molten Salt Chemistry, 1B08, Sapporo, p. 73-74 (1994)
[in Japanese].

8) Haruaki MATSUURA, Ryuzo TAKAGI, Isao OKADA and Reiko FUJITA,
Waste Treatment of Molten Salts Including Fission Products by Electrophoresis,
Proc. of 1995 Annual Meeting of the Atomic Energy Society of Japan, J52, Tokyo,
p.488 (1995)[in Japanese].

9) Haruaki MATSUURA, Hiroshi AKATSUKA, Masaaki SUZUKI, Ryuzo TAKAGI
and Yoichi FUJII-E,
Element Separation for Isotope Separation of FP's and Energy Balance in SCNES,
Proc. of 1995 Fall Meeting of the Atomic Energy Society of Japan, G40, Ibaraki, p.528
(1995)[in Japanese].

10) Haruaki MATSUURA, Ryuzo TAKAGI, Isao OKADA and Reiko FUJITA,
Waste Treatment of Molten Salts Including Fission Products by Electrophoresis,
Proc. of 27th Symposium on Molten Salt Chemistry, 1B02, Yokohama, p. 74-75 (1995)
[in Japanese].

11) Haruaki MATSUURA, Ryuzo TAKAGI, Isao OKADA and Reiko FUJITA,
Waste Treatment of Molten Salts Including Fission Products by Electrophoresis,
Proc. of 1996 Annual Meeting of the Atomic Energy Society of Japan, N23, Suita,
p.687 (1996)[in Japanese].

12) Haruaki MATSUURA, Ryuzo TAKAGI, Monika ZABLOCKA-MALICKA, Leszek RYCERZ and Wlodzimierz SZCZEPANIAK,
High Enrichment of Uranium and Rare Earth Elements in Ionic Salt Bath by Countercurrent Electromigration,
Proc. of 28th Symposium on Molten Salt Chemistry, 2B12, Kofu, p. 257-258 (1996) [in Japanese].

13)Haruaki MATSUURA, Ryuzo TAKAGI, Monika ZABLOCKA-MALICKA, Leszek RYCERZ and Wlodzimierz SZCZEPANIAK,
High Enrichment of Uranium and Rare Earth Elements in Ionic Salt Bath by Countercurrent Electromigration,
Proc. of 5th International Symposium on Molten Salt Chemistry and Technology, Dresden, Germany (1997).